Gully Mapping using Remote Sensing: Case Study in KwaZulu-Natal, South Africa

by

Kanyadzo Taruvinga

A thesis
presented to the University of Waterloo
in fulfillment of the
thesis requirement for the degree of
Master of Environmental Studies
in
Geography

Waterloo, Ontario, Canada, 2008

AUTHOR'S DECLARATION

I hereby declare that I am the sole author of this thesis. This is a true copy of the thesis, including any required final revisions, as accepted by my examiners. I understand that my thesis may be made electronically available to the public.

Abstract

At present one of the challenges of soil erosion research in South Africa is the limited information on the location of gullies. This is because traditional techniques for mapping erosion which consists of the manual digitization of gullies from air photos or satellite imagery, is limited to expert knowledge and is very time consuming and costly at a regional scale (50-10000km²). Developing a robust, reliable and accurate means of mapping gullies is a current focus for the Institute for Soil, Climate and Water Conservation (ISCW) of the Agricultural Research Council (ARC) of South Africa. The following thesis attempted to answer the question whether "medium resolution multi-spectral satellite observations, such as Landsat TM, combined with information extraction techniques, such as Vegetation Indices and multispectral classification algorithms, can provide a semi-automatic method of mapping gullies and to what level of accuracy?".

More specifically, this thesis investigated the utility of three Landsat TM-derived Vegetation Index (VI) techniques and three classification techniques based on their level of accuracy compared to traditional gully mapping methods applied to SPOT 5 panchromatic imagery at selected scales. The chosen study area was located in the province of KwaZulu-Natal (KZN) South Africa, which is considered to be the province most vulnerable to considerable levels of water erosion, mainly gully erosion. Analysis of the vegetation indices found that Normalized Difference Vegetation Index (NDVI) produced the highest accuracy for mapping gullies at the sub-catchment level while Transformed Soil Adjusted Vegetation Index (TSAVI) was successful at mapping gullies at the continuous gully level. Mapping of gullies using classification algorithms highlighted the spectral complexity of gullies and the challenges faced when trying to identify them from the surrounding areas. The Support Vector Machine (SVM) classification algorithm produced the highest accuracy for mapping gullies in all the tested scales and was the recommended approach to gully mapping using remote sensing.

Acknowledgements

The successful completion of this thesis is due to all the help and support I have received from many different people, both in the collection and processing of all the data used in this thesis and in the writing and editing of the final product. I would like to first express my sincerest appreciation to the people at the Agricultural Research Council (ARC), Mr. and Mrs. Grundling and Mr. Jay Le Roux, for creating this wonderful research opportunity, supporting me in every way during my time in South Africa and assisting in my field work. I would also like to thank my colleague Miss Holly Waite for her amazing support in brainstorming ideas, staying up with me all those late nights, proof reading my material and being the strongest shoulder to cry on. Another special thanks is given to my family and friends for being so supportive through the duration of my thesis. Last but defiantly not least I would also like to thank Dr. Richard Kelly and Dr. Jonathan Price from the University of Waterloo for their help and guidance in my research, and providing me with exceptional advice.

Table of Contents

List of Figures

List of Tables

List of Equations

List of Abbreviations

ARC	-	Agricultural Research Council
AVIRIS	-	Airborne Visible and Infrared Imaging
DN	–	Digital number
DWAF	-	Department of Water, Agriculture and Forestry
EM	–	Electromagnetic
ERU	–	Erosion Response Unit
ESM	-	Erosion Susceptibility Map
ETM+	-	Enhanced Thematic Mapper
GIS	-	Geographic Information System
HRVIR	-	High Resolution Visible Infrared
HRV	-	High Resolution Visible
IR	–	Infrared
ISCW	-	Soil, Climate and Water Conservation
KZN	-	KwaZulu-Natal
MDC	-	Mahalanobis Distance Classifier
MLC	-	Maximum Likelihood Classifier
MSS	–	Multi-spectral Scanner
NDVI	-	Normalized Vegetation Index
NIR	–	Near infrared
PCA	–	Principle Component Analysis
PWEM	-	Predicted Water Erosion Map
RUSLE	-	RevisedUniversal Soil Loss Equation
SAVI	–	Soil Adjusted Vegetation Index
SLEMSA		Soil Loss Estimator for Southern Africa
SPOT	-	Systeme Pour l'Observation de la
SVM	-	Support Vector Machine
TM	-	Thematic Mapper
TSAVI	-	Transformed Soil Adjusted Vegetation Index
USLE	-	Universal Soil Loss Equation

Chapter 1
Introduction

Soil erosion by water, particularly gully erosion, is regarded as a serious environmental problem in South Africa where there is need for semi-automatic gully mapping methods (Le Roux *et al.*, 2007)**.**

1.1 Overview

Soil erosion is a natural process caused by water, wind and ice, and is a serious land degradation problem globally (Ritchie, 2000). Soil erosion by water is one of the most important global land degradation problems mainly because of its negative on-site landscape effects such as loss of soil productivity and quality (Dwivedi *et al.*, 1997; Eswaran *et al.*, 2001), and off-site effects such as sedimentation of rivers, lakes and estuaries. Erosion decreases organic matter, fine grained soil particles, water holding capacity and depth of the top soil (rooting depth) (Ritchie, 2000) and is accelerated through anthropogenic stresses, particularly agriculture (Lal, 2001).

Soil erosion by water occurs if the combined power of the rainfall energy and overland flow exceeds the resistance of soil to point of detachment (Hadley *et al.*, 1985). The process involves (1) detachment, with rainfall being the most important force of detachment (de Jong, 1994) (2) transportation of sediment (redistribution over the landscape) by surface runoff and (3) deposition (in depressional sites and aquatic ecosystems) of soil (Lal, 2001). The three main forms of soil erosion by water are sheet erosion, rill erosion and gully erosion – gully erosion being the most severe. Sheet erosion is the detachment and transportation of soil particles that occurs as a result of rainsplash and overland flow (Garland *et al.*, 2000). Rill erosion is the removal of soil in small channels and gully erosion, by contrast, is the removal of soil in large channels (gullies) by concentrated runoff either on the surface or subsurface level. From an agricultural perspective, gullies are defined as erosion features that are too deep to be ploughed with ordinary farm equipment; although there has not been a specific upper limit to the size of gullies, they typically range in size from 0.5m to as much as 30m deep (Soil Science Society of America, 1996).

Improved mapping capabilities of gully distribution and magnitude could lead to enhancements in agricultural production and water resource management, as well as provide more accurate hazard maps through accurately locating severely eroded areas. Changes in the distribution and extent of gullies play an important role in determining the location and resources required for erosion control mitigation projects. Gully erosion maps, produced quickly and cheaply from readily-accessible information, are a useful tool in regional planning for erosion control. Therefore, developing a robust, reliable and accurate means of mapping gullies is a current focus for the Institute for Soil, Climate and Water Conservation (ISCW) of the Agricultural Research Council (ARC) of South Africa (Le Roux *et al.*, 2007).

The gully erosion problem in South Africa is largely a product of several unfavorable natural conditions that are characteristic of the region, primarily the low and unreliable amounts of rainfall and soil type. The high temperatures cause rapid decomposition of organic matter which leads to a reduction in the soils' structural support (Laker, 2000). This is accelerated when there are episodes of prolonged droughts followed by torrential rains because the soils are vulnerable to erosion due to lack of vegetation cover. South Africa is characterized by highly erodible solonetzic soils (Fox and Rowntree, 2001). These soils have very low infiltration rates. However, once saturated soil cohesion and stability is lost leading to increased erosion (Jones and Keech, 1966). The province of KwaZulu-Natal (KZN), with its fine-grained soils, torrential rainfall and sparse vegetation, is considered to be the province most vulnerable to considerable levels of water erosion (Hoffman and Ashwell, 2001), mainly gully erosion.

At present one of the challenges of soil erosion research in South Africa is the limited information on the location of gullies (Le Roux *et al.*, 2007; Mpumalanga, 2002). Most of the land degradation mapping projects were conducted by recognized experts at a national scale, with little or no focus on mapping gullies (Garland *et al.*, 2000; Pretorius and Bezuidenhout, 1994; Pretorius, 1995). The Bare Soil Index (BSI) map developed with Landsat TM focuses on the status of eroded areas, not specifically delineating individual gullies (Pretorius and Bezuidenhout, 1994). The Erosion Susceptibility Map (ESM) and Predicted Water Erosion Map (PWEM) of South Africa were produced using an erosion model that identified areas under severe threat by water erosion but not gully erosion specifically (Pretorius, 1995). In some areas these erosion hazard maps inaccurately mapped the current extent of soil loss (Le Roux *et al.*, 2007). The most recent approach was a more

qualitative assessment of land degradation which mapped the type and severity of soil degradation for different land use types. This map was compiled with information gathered from 34 workshops throughout South Africa (Garland *et al.*, 2000; Le Roux *et al.*, 2007) and is therefore subject to the perspectives of the participants.

As stated by Le Roux (2007), "there exists no methodological framework, or 'blueprint,' to assess the spatial distribution of soil erosion types at different regional scales in South Africa." This is because traditional techniques for mapping erosion which consists of the manual digitization of gullies from air photos or satellite imagery, is limited to expert knowledge and is very time consuming and costly at a regional scale (50-10000km²). However, multi-spectral remote sensing methods offer the possibility of using semi-automatic mapping techniques to consistently map gullies. The following thesis is a stepping stone for the incorporation of satellite remote sensing for mapping gullies at the sub-catchment level in KZN, South Africa. It explores and demonstrates a standard approach for gully mapping through addressing key issues such as expert knowledge required, time, cost and accuracy of different remote sensing techniques.

Improving gully mapping methods by applying remote sensing is important and beneficial for erosion control, not only in South Africa, but other regions around the world. The efficacy of efforts to mitigate against damage caused by gully erosion rests in understanding gully erosion processes. A robust semi-automatic procedure using remote sensing imagery to map gullies means that geomorphologists with limited background knowledge about the location can easily and economically create a map displaying the extent of a gully network. Furthermore, stakeholders in erosion management require spatially explicit erosion feature maps with documented level of accuracy for decision-making processes. The spatial and spectral resolutions of Landsat TM could be beneficial for mapping gullies using semi-automatic methods and higher spatial resolution SPOT 5 imagery could be used to delineate gullies using traditional methods. Therefore, the overall aim of this thesis is to investigate the utility of Landsat TM-derived Vegetation Index (VI) techniques and three classification techniques based on their level of accuracy compared to traditional gully mapping methods applied to SPOT 5 panchromatic imagery in KZN. More specifically this thesis will:

1. Evaluate three vegetation indices: Normalized Difference Vegetation Index (NDVI), Soil Adjusted Vegetation Index (SAVI) and Transformed Soil Adjusted Vegetation Index (TSAVI) for accuracy in gully mapping;

2. Evaluate three supervised classification techniques: Maximum Likelihood Classifier (MLC), Mahalanobis Distance Classifier (MDC) and Support Vector Machine (SVM) for accuracy in gully mapping and determine if a higher spatial resolution (SPOT 5) is required to map gullies;
3. Link traditional gully mapping techniques carried out in South Africa to current remote sensing techniques of today.

1.2 Thesis Outline

Following this section, Chapter 2 explores the literature related to gully erosion processes, traditional and more recent techniques for mapping gullies and reviews the use of remote sensing methods for mapping gullies in South Africa. In Chapter 3, details concerning the physical setting and site description of the gully erosion study site are given. In Chapter 4, a description of the data collection and processing methods are examined. In Chapter 5 the result of the analysis of the vegetation indices and classification methods for mapping gullies is provided. Chapter 6 is a discussion of some of the limitations of the study and finally in Chapter 7, the conclusions, and recommendations for future research are discussed.

Chapter 2
Research Context

2.1 Geomorphology Background of Gully Erosion

This thesis attempts to bridge traditional gully mapping methods with current remote sensing techniques. To do so, four fundamental questions were adapted from Klimaszewski (1982) and can be applied to the spatial variability of gullies and the status of gullies in their evolution: (i) How are gullies characterized morphologically (appearance, shape and past characterization)? (ii) How can gullies be characterized by their morphometry (dimensions and geometry)? (iii) What is a gully morphogenesis (origin and development)? and (iv) How are gully morphodynamics characterized (interaction of a gully and the erosion controlling factor)? These questions are addressed in the following sub-sections with specific relevance for gully erosion in South Africa.

2.1.1 Morphology: Gully Characteristics

Successful mapping depends on knowing the characteristics of a gully, and using that information to define the appropriate mapping technique (King, 2002). Gullies have been characterized by a number of different criteria. The Food and Agriculture Organization (FAO) (1965) and Hudson (1985) described gullies simply as geomorphic features that do not allow for normal ploughing. The shape of gully cross-sections and soil material in which a gully develop have also been used to characterize gullies, with V- and U-shaped gully cross-sections subdivided according to the type of sedimentary material present (Imeson and Kwaad, 1980). Morgan (1979) gave a more landscape-based approach defining gullies as "relatively permanent steep-sided eroding water courses that are subject to flash floods during rainstorms." Gullies have been characterized based on the shape/pattern produced by the physical and land use factors influencing drainage as seen in Figure 2-1 (Ireland *et al.*, 1939; Twidale, 2004).

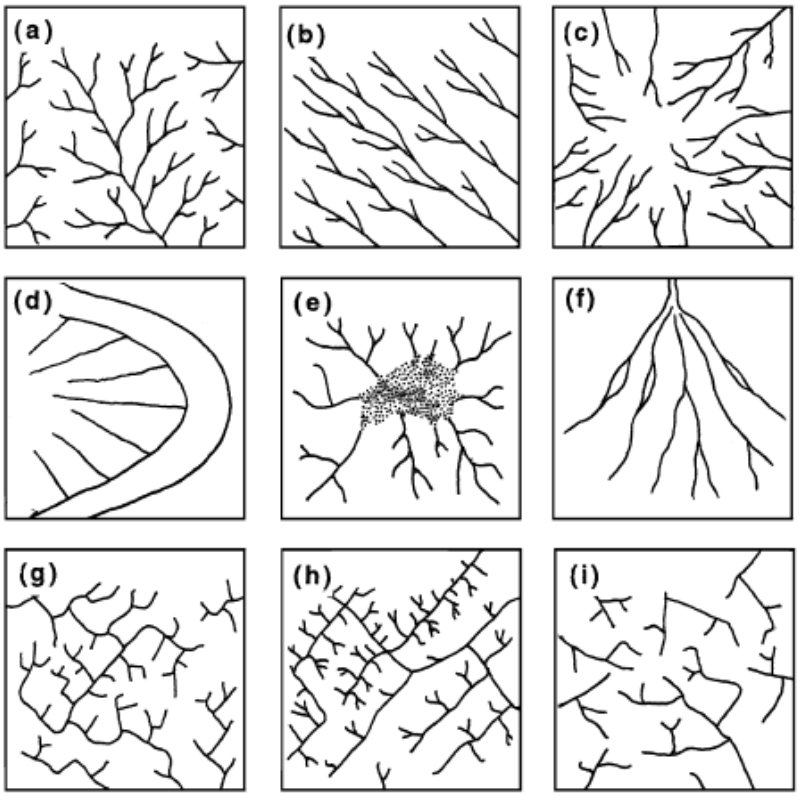

Figure 2-1 An example of different drainage patterns. a) dendritic, (b) parallel, (c) radial, (d) centrifugal, (e) Centripetal, (f) distributary, (g) angular, (h) trellis, (i) annular (adapted from Twidale, 2004)

In South Africa, Dardis (1988) identified nine different gully landforms based on flow type, flow regime, geometry of erosion feature, nature of the host material and dominant processes acting on the particular erosion form. The two dominant types of gullies found in KwaZulu-Natal are: *ravine gullies*, linear, flat-walled channels in soil with unconsolidated thick deposits called colluvium and weathered bedrock; and *organ pipe gullies*, typically dendritic in plan, with distinctive, fluted walls, normally in colluvium (Dardis *et al.*, 1988). Overall, past characterization of gullies is very broad, thus for the purpose of mapping gullies this study characterizes gullies "*as relatively permanent steep-sided eroding water courses* (Morgan, 1986) *that have banks which are usually un-vegetated with some slumping and in some cases vegetation can occur in the base of the gully"*(Thwaites, 1986).

2.1.2 Morphometry: Gully Dimensions

Gully geometry, or cross-sectional form, has been considered an important characteristic for identifying gully types (Heede, 1970; Ireland *et al.*, 1939; Leopold and Miller, 1956). The cross-sectional profile (i.e. planar, u-shaped and v-shaped) of a gully reflects the important relationships between soil erosion and parent material (Harvey *et al*., 1985). However, there is no clearly defined upper limit on the dimensions of gullies (Poesen *et al.*, 2002). Gullies typically range in incision depth of 0.5-30 m, and as wide as 80 m (Garland *et al.*, 2000). Gully length is less frequently reported when gully systems are integrated with drainage networks and the channels can reach lengths of up to several kilometers (Garland *et al.*, 2000). In South Africa, gully dimension vary considerably, ranging from small features such as 22 m wide and 13 m deep gullies in the Eastern Cape to much larger landforms, such as the gully near Stranger on the north coast of KwaZulu-Natal which is 2 km long, 50 m deep and 80 m wide (Garland *et al.*, 2000).

2.1.3 Morphogenesis: Gully Origin and Development

Before gullies can be mapped it is necessary to understand the strong relationship between hydrologic and erosion processes (Bocco *et al.*, 1991) because this influences thr stage dimension of the gully erosion process. Some studies have found a strong positive relationship between the dominance of surficial flows and the development of gully erosion (Bergsma, 1974). Patton and Schumm (1975) described the gully process as occurring when geomorphic threshold is exceeded due to either a decrease in the resistance of the materials or an increase in the erosivity of the runoff, or both.

In South Africa, gully development is best explained by erosion processes that occur at the surface and subsurface level (Bocco *et al.*, 1991; Summer and Meiklejohn, 2000) (Figure 2-2). At the surface precipitation detaches soil particles causing rainsplash erosion (soil particles are displaced by the impact of the raindrop) and sheet erosion (soil particles are detached and transported). The concentrated flow of water from sheet erosion travels in micro-channels and forms rills and extension of rills resulting in gully development. At the subsurface level, infiltrated water saturates the soil leading to percoline flow. This flow moves fine particles within the soil and eventually forms hollow pipes (pipe formation) beneath the surface (Summer and Meiklejohn, 2000). Pipe flow forms mainly in heterogeneous material of variable resistance (Dardis *et al.*, 1988). When these pipes collapse a gully develops at the surface, which is usually termed a discontinuous gully (Leopold and Miller, 1956).

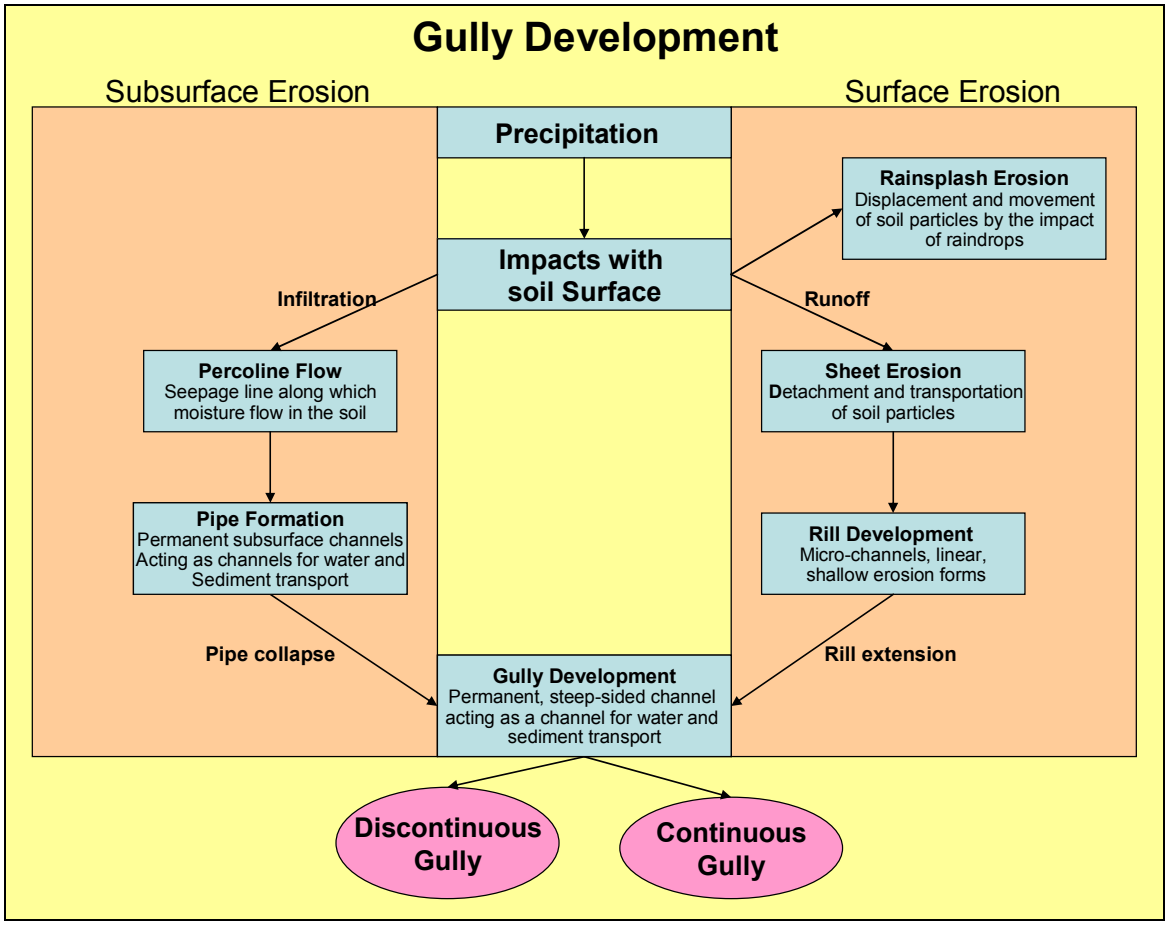

Figure 2-2 Gully development by surface and subsurface soil erosion modified from (Summer and Meiklejohn, 2000)

The two types of gully formation can be described as continuous or discontinuous (Figure 2-3) (Blong, 1966; Heede, 1970; Leopold and Miller, 1956; Mosley, 1972). The discontinuous gully represents the initial stages of development, typically when the more rapid rate of gully development occurs (Sidorchuk, 1999). This occurs during the first 5% of the gully's lifetime, when morphometry characteristics of a gully (length, depth, width, area and volume) are not stable (Figure 2-3: stage 1 and 2). Morphologically they are characterized by a vertical headcut, in a valley floor, with a channel immediately below the headcut. The floor of a discontinuous gully has a gradient that is less steep than that of the surrounding area and is composed of a layer of newly deposited material over an undisturbed alluvium (Leopold *et al.*, 1964). The gully develops through side-wall erosion and collapse, headward erosion and gully deepening, collapsed cavities or soil pipes (Figure 2-3: stage 3)

and eventually becomes a continuous gully by connecting to another discontinuous gully (Bocco, 1991; Dardis *et al.*, 1988) (Figure 2-3: stage 4).

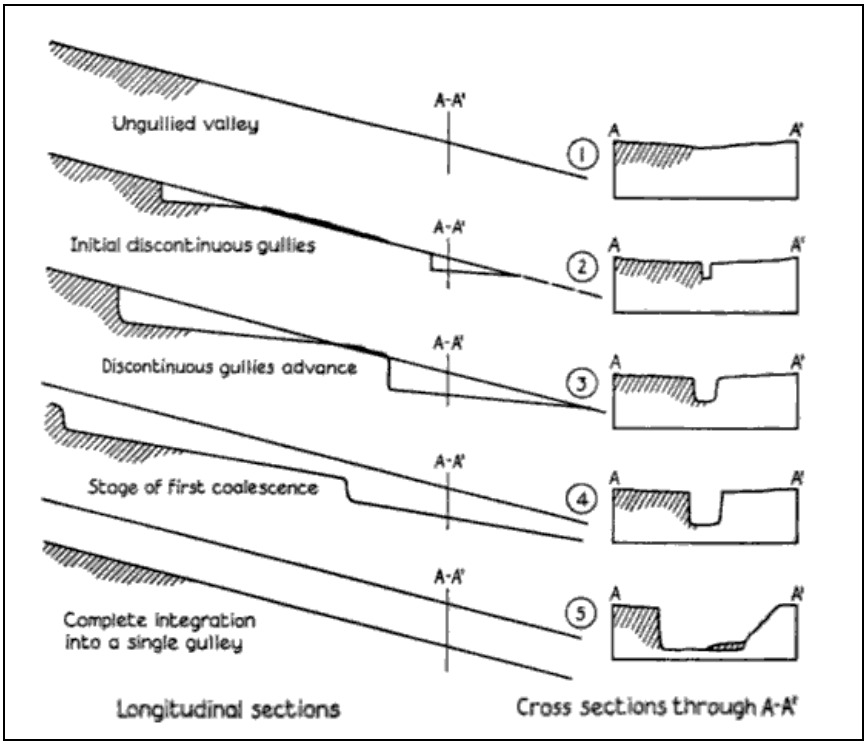

Figure 2-3 Stages of gully development, from discontinuous gullies to a continuous gully, extracted from Leopold *et al.* (1964).

Continuous gullies occur most commonly in stratified colluvium (Dardis *et al.*, 1988). The continuous gully represents the 'early mature' or 'mature' stage which occurs when the gully attains a dynamic equilibrium (Heede, 1975). It is also a much more prominent feature to identify in the landscape than a discontinuous gully because it tends to be larger. It appears relatively easy to classify gully erosion based on processes (discontinuous or continuous), however gullies are the result of multiple processes interacting on the landscape. Thus gully erosion can occur over a large variety of timescales ranging from a single storm to many decades (Le Roux *et al.*, 2007).

2.1.4 Morphodynamics: Interactions of Gully Controlling Factors

For gully mapping it is important to recognize the dominant environmental factors that control erosion because this will determine the rate of the gully erosion process and thus the timescale needed for map updating. Environmental factors that control gully erosion include bedrock type, soil, climate,

topography, vegetation and human activity (Botha, 1996; Weaver, 1991). The rate of gully development and its location is highly dependent on the complex interactions among these factors.

In South Africa, gullies occur more frequently on soils underlain by shale (Berjak *et al.*, 1986) or dolerite (Bader, 1962; Mountain, 1952; Weaver, 1991) as these rocks develop fine grained soils once weathered. Additionally the presence of unconsolidated sediments that are high in silt (colluvial and alluvial sediments) coincides with most of the areas of gully erosion in KwaZulu-Natal (Botha *et al.*, 1994; Garland *et al.*, 2000; Watson, 1997), as these sediments generally have higher run-off rates (due to lower permeability) and can easily detach (Terrence *et al.*, 2002). Such sediments exist as multi-layers in gully sidewalls and are often marked by the embedment of stone lines (Felix-Henningsen, *et al.*, 1997).

Climate can influence the rate of gully erosion directly, through precipitation, temperature, and indirectly, through the conditions that influence the vegetation cover. Rainfall is a major driving force of many erosional processes in South Africa (Moore, 1979) because the amount of detached soil is directly proportional to rainfall intensity (Van Dijk *et al.*, 2002). Rainfall also influences the vegetation cover and type, therefore moderates the erosion intensity of an area (van der Eyck *et al.*, 1969). In KZN gullies have been mostly located in areas that are mild semiarid with very cold to warm temperatures (Scotney, 1978) because climatic areas of this nature are sparsely vegetated. Liggitt (1988) found that in some areas of KZN gullying decreases significantly where mean annual rainfall exceeds 800 mm. This was further confirmed by Liggitt and Fincham (1989) study of the Mfolozi catchment where rainfall less than 900 mm per annum experienced greater erosion. These conclusions demonstrate the complex interactions of climate on gully erosion. An area with high mean annual rainfall promotes lush vegetation that secures the soil by reducing surface runoff, increasing the infiltration rate, root deepening and increasing organic matter, thus making it more resistant to gully erosion (Laker, 2000). Conversely relatively warmer, drier areas limit the growth of vegetation which exposes the soil thus making the area more prone to gully erosion.

Some important topographical properties that control the erosion processes are slope steepness, length and shape (Morgan, 1986). Topography is an important determinant of erosion potential since it controls the energy gradients. Gullies can develop on very gentle to steep slopes, but are most numerous on strongly sloping land (Bergsma, 1974). However, in contrast, Liggitt and Fincham

(1989) found gully erosion in KZN to be inversely related to slope steepness. Where slope gradients are less than 10° gullies occur most frequently (Liggitt and Fincham, 1989) because of the increase in runoff resulting from land clearing, overgrazing, cultivation, and stream channelization, which are more common on gentle slopes. Furthermore, commercial cultivation is done on flatter areas making them more susceptible to gully erosion. In certain parts of South Africa, a strong spatial correlation exists between abandoned cultivated land and gully erosion (Kakembo and Rowntree, 2003). This has been attributed to the little basal cover offered by the type of vegetation that grows when cultivation of fields is no longer active, making the land more vulnerable to erosion by overland flow (Sonneveld *et al.*, 2005). Improvements in spatial mapping of gullies can help identify the factors controlling gully erosion through multi-temporal analysis. See appendix A for a literature review summary on erosion controlling factors in southern Africa.

2.2 Traditional Gully Mapping Methods

Traditional methods of mapping gullies involve digitization of the outer boundary of the gully banks from an aerial photo or satellite image or both (Burkard and Kostaschuk, 1997). Gullies are mapped by extracting information from an image such as size, shape, shadow, tone and colour (reflectance), texture, pattern, and feature association[1] (Teng *et al.*, 1997; Zhang and Goodchild, 2002). In cases where the outline of the gully is not clear (i.e. vegetation cover) ground-truthing and stereographic viewing using air photographs or certain satellite imagery (e.g. SPOT) can minimize the problem (Burkard and Kostaschuk, 1997) because gullies are visualized from different perspectives. Gullies are delineated on a transparent plastic overlay over an air photo or digitized within a GIS (using air photos and satellite imagery), annotated and printed off as a map.

Aerial photos are the most commonly applied instrument for mapping gully erosion (Ritchie, 2000) because most gullies are visible using stereoscopic aerial photography (Morgan *et al.*, 1997; Thwaites, 1986; Watson, 1997). Using 1:10 000 and 1:20 000 air photographs, Thwaites (1986) digitized gullies in the BRAR catchment (372 km²) in South Africa, based on grey tones and feature association and Morgan *et al.* (1997), identified gullies as linear features with a clearly defined depth. Most of the gully erosion research in southern Africa has used air photos to map gullies (Jones and

[1] Association is defined as 'the spatial relationship of objects and phenomena' (Teng *et al.*, 1997)

Keech, 1966; Morgan *et al.*, 1997; Thwaites, 1986). In Zimbabwe, Jones and Keech (1966) used air photo interpretation to measure gully size and therefore assess the severity of gully erosion at a scale of 1:25 000. In South Africa Flugel (2003), Hodchschild *et al*. (2003) and Sindorchuk (2003) used air photos to map gully erosion based on the homogeneity of the erosion response and the heterogeneity of the structure, a concept called erosion response units (ERU[2]). These studies were slight modifications of the van Zuidam (1985) proposed method of terrain analysis which also extracts information from an image such as tone, texture, geometry and so on. This procedure enabled mapping of six different ERU, ranging from slightly eroded (1) to severely eroded (6), at a scale of 1:50 000. More recently and with relevance to the current study area, the study by Sonnevelds (2005) focused on digitizing gullies at the sub-catchment level, delineated as linear erosion features with confined flow.

Many erosion studies applied in developing countries have used satellite imagery to digitize gullies (Dwivedi and Ramana, 2003; Fadul *et al.*, 1999; Kiusi and Meadows, 2006). Satellite imagery offers much broader spatial coverage than individual aerial photos and can be used to map gullies in remote areas due to additional spectral bands that help the interpreter distinguish gullies. Gullies are digitized based on tone, shape, pattern and their high reflectance in all bands (Bocco and Valenzuela, 1988; Bocco and Valenzuela, 1993). In Sudan, Fadul (1999) used Landsat TM to identify gullies based on topography, drainage pattern, tone and land use. In Tanzania, Kiusi and Meadows (2006) delineated gullies based on colour, texture and pattern, using Landsat TM images at a scale of 1:100 000. In India, Dwivedi and Ramana (2003) delineated three categories for gully erosion (shallow, medium and deep) using a false colour image from the Indian Remote Sensing Satellite. In hopes to combat environmental problems such as gully erosion, the ISCW acquired SPOT-5 imagery for the whole of South Africa. This imagery can improve on traditional methods of gully mapping at a local scale because major (>2.5 m) and minor (2.5 m) gullies are visible in the panchromatic band of SPOT-5 (2.5 m). In addition, SPOT imagery can improve on traditional mapping methods in South Africa on a regional scale by offering a seamless coverage.

[2] ERUs are defined as "Distributed three-dimensional terrain units, which are heterogeneously structured and have homogeneous erosion process dynamics characterized by a slight variance within the unit, if compared with neighboring ones." (Flugel *et al.*, 2003).

Although digitization of gullies from an air photo or satellite image has been used extensively, the method is limited to expert knowledge, is inconsistent, lacks quantitative information and can be a very time consuming and costly process. The following points highlight these issues:

- **Expert Knowledge:** The major problem with this method is it relies heavily on the expert's knowledge of the gully erosion processes, governing factors, and characteristics in the image for accurate delineation of gullies. Moreover, the expert may be familiar with gully erosion but lacks knowledge in a particular study area. Thus, application of traditional gully mapping methods, by stakeholders with little expert and background knowledge of the area may be challenging and erroneous.
- **Consistency problems:** Digitization is also limited, but not confined to, the field of view of the instrument used to capture the image which determines the spatial extent of an image. Although images can be mosaicked (if the area to be mapped is larger than the field of view), consistency problems with different image dates and scales, and coordinating with several air photo interpreters, are apparent. This problem is more prevalent when digitizing from aerial photographs and limits the study of erosion systems which are represented in much detail at a regional scale.
- **Lacks quantitative information:** Most of the information extracted when digitizing air photos lack quantitative information on the spatial extent of the gullies. For example gullies digitized using ERU are labeled from 'slight' and 'moderate' to 'severe' erosion. Plus maps produced by gully digitization tend to lack quantitative information on the level of accuracy of the map produced. This lack of information makes it very challenging for stakeholders in gully erosion management to make important decisions and limits their assessment of the gully erosion problem.
- **Issues of scale:** Maps produced using traditional methods of mapping gullies are limited to the scale at which the features are visible (<1:50 000) which limits regionalization of gully studies. Using small scale air photographs (> 1:50 000) to map gullies would mean that small gullies may not be visible. Additionally, traditional methods are not very flexible for mapping gullies at different scales, covering regions of various extents (Hayden, 2008).
- **Time and cost:** Since erosion in South Africa occurs over a large variety of timescales (single storm to many decades) and spatial scales (Le Roux *et al.*, 2007), gully erosion maps may need to be updated 'on the fly.' This can be very time consuming especially when mapping large areas for which each gully needs to be hand digitized and validated in the field

are concerned. The process is also costly due to the number of air photos needed to map a large area and the expense of equipment that would be required to validate the maps.

2.3 Gully Mapping Using Remote Sensing

Through maximization of the spectral, spatial and temporal resolution of a satellite sensor, remote sensing techniques can map gullies with less expert knowledge, time and cost, and provide the appropriate quantitative information necessary for combating erosion in South Africa. In general, these three resolution types allow for characterization of the gullies and the surrounding landscape from the local to global spatial scales (Wilkie and Finn, 1996). Spatial resolution is "a measure of the linear separation between two objects that can be resolved by a remote sensing system" (Jensen, 2005) which dictates the size of the smallest possible feature that can be detected in the satellite image (Wilkie and Finn, 1996). The spatial coverage offered by certain satellite imagery is much larger than a conventional photograph, for example, "it can take 5000 conventional vertical aerial photographs obtained at a scale of 1:15 000 to fit the geographic extent of a single Landsat image" (Jensen, 2005). Such a large spatial coverage allows for a direct perspective of the regional mix of the gully erosion process (regionalization) (Hayden, 2008), provided that the gullies are large enough to be detected by the spatial resolution of the images (Giordano and Marchisio, 1991). The spectral resolution (dimension and number of wavelength regions of a sensor system) allows for feature extraction methods for gully mapping, for example ideal band combinations, vegetation indices and classification algorithms. Such techniques combined with the repetitive coverage of a particular area by satellite systems (temporal resolution[3]) can lessen the time and cost required to produce a gully erosion map. This offers the possibility of monitoring the extent and evolution of gully erosion.

2.3.1 Overview of Candidate Satellite Remote Sensing Instruments

Imagery provided by Landsat optical satellite systems are widely applied in erosion studies (Bocco and Valenzuela, 1988; Dwivedi *et al.*, 1997; Kiusi and Meadows, 2006) and are suitable for gully erosion mapping in South Africa. The family of Landsat includes Multispectral Scanner (MSS), having four bands at 80-m spatial resolution; Thematic Mapper (TM) and the Enhanced TM (ETM+) both carrying seven bands at a spatial resolution of 30m with the thermal band having a additional spatial resolution of 120m (TM) and 60m (ETM+) (Jensen, 2005) (Table 2-1). A great advantage of

[3] Temporal resolution is the measure periodicity of a satellite to obtain imagery of a particular area (Wilkie and Finn, 1996).

using Landsat imagery for gully erosion mapping in South Africa, is that it began imaging the Earth in the 1970s enabling geomorphologists to study gully erosion processes over 30+ years. Even more advantageous is that the USGS now offers all users the Landsat 7 archive data and is soon to offer (December 2008) the Landsat TM and Landsat MSS archive all at no charge using a standard data product format. This accessibility is important not only for South Africa but other developing countries.

Table 2-1 Imagery characteristics

	Landsat MSS	Landsat TM	Landsat ETM+	SPOT 5 HRG
Spatial Resolution	1-4: 80*80m	1-5,7: 30m*30m 6: 120m*120m	1-5,7: 30m*30m 6: 60m*60m Pan: 13*15	1-3: 10m*10m, midIR: 20m*20m, Pan: 2.5m*2.5m
Bands	1 -0. 5-0.6 (green) 2 -0.6-0.7 (red) 3 -0.7-0.8 (NIR) 4 -0.8-1.1 (NIR)	1-0.45-0.52 (blue) 2-0.52-0.60 (green) 3 -0.63-0.69 (red) 4 -0.76-0.90 (NIR) 5 -1.55-1.75 (MIR) 6 -10.40-12.5 (thermal) 7 - 2.08-2.35 (MIR)	1 -0.45-0.515 (blue) 2 -0.52-0.605 (green) 3 -0.63-0.690 (red) 4 -0.775-0.900 (NIR) 5 -1.55-1.75 (MIR) 6 -10.40-12.5 (thermal) 7 -2.09-2.350 (MIR) Pan 0.520-0.900	1-0.50-0.59 (Green) 2– 0.61-0.68 (Red) 3- 0.79-0.89 (NIR) 4–1.58-1.75 (mid IR) Pan– 0.48-0.71
Swath width	185km	185km	185km	60km
Revisit	16 days	16 days	16 days	26 days

Landsat TM has improved spectral and spatial characteristics compared with MSS thereby providing more detailed regional and local gully erosion mapping capabilities. Both Landsat TM and MSS are optical-mechanical whiskbroom sensors; they use oscillating mirrors to provide cross-track scanning during the forward motion of the space platform. TM scans in both directions but MSS scans in one direction. The spatial resolution of TM allows for mapping individual large and medium sized gullies, larger than 30m (Langran, 1983; Millington and Townshend, 1984); whereas the MSS spatial resolution of 80m is too coarse. Furthermore Landsat TM is able to identify small-scale farms (2 to

10ha on average) which are typically found in South Africa. Although MSS spectral resolution of five bands can enable the mapping of eroded areas (Dhakal *et al.*, 2002; Dwivedi *et al.*, 1997; Pickup and Nelson, 1984) Landsat TMs higher spectral resolution of seven bands (two additional mid IR) is better for gully eroded landscapes such as those in South Africa. These seven different bands of Landsat TM record energy in the visible, reflective-infrared, middle-infrared, and thermal infrared regions of the electromagnetic spectrum are appropriate for erosion and peripheral vegetation mapping (Dhakal *et al.*, 2002; Jensen, 2005). Dhakal (2002) found that the visible bands (1, 2, and 3) were effective in detecting erosion areas and flooded areas resulting from an extreme rainfall event. This study proved to be better than field survey studies for distinguishing eroded and non-eroded areas. However one study has found that combining Landsat TM and MSS has provided more detail about the terrain features and allowed for the maximum accuracy for mapping eroded lands (Dwivedi *et al.*, 1997). In this case eroded areas were classified into four classes ranging from non-eroded to severely eroded areas.

Landsat observations of gully erosion are suitable for change detection studies: the imagery dates back to the early 1970s and with NASAs Landsat Data Continuity Mission (Brill and Ochs, 2008), future data are available for any given spot on the Earth every 16 days. This repeat period is ideal for mapping gullies at a regional scale because it allows for monitoring of measurable changes in gully development over a long period of time, a point which is still ignored in gully erosion reviews (Boardman, 2006). The repeat period also reduces the issue of cloud cover which often reduces image availability (Vrielin *et al.*, 2008). With the added higher-resolution panchromatic band in ETM+, which aids in interpretation, Landsat offers the feasibility and affordability for future mapping of gullies in South Africa.

For mapping eroded areas Landsat TM has proven comparable, and in some cases better than other higher resolution satellites. The SPOT (Systeme Pour l'Observation de la Terre) series satellites (SPOT-1,2,3,4) provide a higher spatial resolution sensors called High Resolution Visible (HRV) and High Resolution Visible and Infrared (HRVIR) and are capable of measuring reflected radiance in three bands at a spatial resolution of 20m, or 10m panchromatic and have proven better at distinguishing eroded areas compared to Landsat TM observations (Bocco and Valenzuela, 1988; Dwivedi *et al.*, 1997). While SPOT HRV is better at detecting eroded areas than TM or ETM+, Bocco and Valenxuela (1988) found that the latter performed better at classifying the surrounding areas.

Dwivedi *et al.* (1997) also found that SPOT HRV improved the classification of eroded lands than Landsat TM; however not all the TM bands were utilized in this study. Although SPOT HRV has proven better at mapping eroded areas, its low spectral sampling (4 bands) has proven to be a limitation in mapping gullies (Servenay and Prat, 2003). Serveney and Pratt (2003) found that SPOT was unable to identify outcropping eroded areas even though they had unique spectral signatures (Servenay and Prat, 2003). While there is an insufficient amount of literature on SPOT and Landsat TM comparison for mapping of gullies, it can be assumed that medium spatial resolution and higher spectral resolution Landsat TM may prove to be better at mapping gullies overall because of the spectral sampling capabilities of the sensor. Clearly the combination of both may be the optimal approach.

Alternative available optical satellite instruments have additional qualities for mapping gullies; however they are limited by certain aspects of their resolutions. Imagery from the NOAA AVHRR[4] sensor is able to detect various soil properties (e.g. moisture) which has been used to map and monitor land degradation (Singh *et al.*, 2004) but the low spatial resolution of 1.1km (at nadir) limits its ability to delineate gullies of any size. The 1C sensor LISS-3 on the Indian Remote Sensing Satellites has stereo viewing capability and a spatial resolution (23.5m in visible and NIR) which has enabled for differentiation of gully depth in India (Dwivedi and Ramana, 2003) but the lower spectral (0.52-0.5, 0.62-0.68,0.77-0.86,1.55-1.7) and temporal (24 days) resolution limits its capability for automatic detection and monitoring of gullies.

Although used to a lesser extent in erosion studies, the inclusion of active microwave[5] sensor imagery from JERS-1 SAR[6], has increased the identification accuracy of certain erosion classes but this was in combination with Landsat TM (Metternicht and Zinck, 1998). The final imagery had a spatial resolution of 15m and a cloud-penetrating capability because of its long microwave wavelength (23cm or 1275MHz, HH polarization). This enabled for identification of three classes: badlands, slightly eroded areas and miscellaneous lands. Gully mapping capabilities provided by SAR include their insensitivity to weather conditions and sunlight; however, the drawback of using such data for

[4]Advanced Very High Resolution Radiometer
[5] An active microwave sensor has the capability of transmitting and receiving polarized radar waves across a range of frequencies. The amount of energy returned to the radar antenna is known as radar backscatter.
[6] A Synthetic Aperture Radar (SAR)system active microwave sensor

gully mapping in South Africa is the cost of acquiring such high-resolution data. Furthermore there is geometrical uncertainty in steep terrain such as that found in complex gulley terrain.

Recent satellites such as, SPOT-5 (10m multispectral resolution and 2.5m Panchromatic) (Table 2-1), IKONOS (4m multispectral resolution and 1m panchromatic), and QuickBird (2.44m and 2.88m depending on the angle of tilt of the sensor multi-spectral resolution and 61cm and 0.73 panchromatic) offer high quality data for potential use in gully mapping (Vrieling, 2006); but even these have their limitations for gully mapping in South Africa. Such high resolution data (IKONOS and QuickBird) are very expensive to acquire for mapping gullies in a large area (Vrieling *et al.*, 2008) and may not be affordable for developing countries. Furthermore, they have low spectral sampling capabilities. Other geomorphological studies have found IKONOS cost-benefit offer little advantage over lower resolution air photographs in terms of financial resources necessary (Nichol *et al.*, 2006). SPOT 5 is more affordable than IKONOS and QuickBird, and has already been acquired for the whole of South Africa. SPOT 5 carries an instrument known as HRG (High Resolution Geometry) which can provide imagery that is useful for providing information at a local level (fine-scale) (Lu and Weng, 2007) but its low spectral resolution of three bands, visible, near-infrared, and shortwave infrared (SWIR) bands mean that gullies may be challenging to automatically detect from SPOT's limited spectral observations. Although SPOT 5 lacks the spectral bands useful for multi-spectral analysis, the major advantage it has over Landsat TM is the 2.5-5m panchromatic data which provides high resolution air photo-like quality for gully mapping.

While high spatial resolution air photo or satellite imagery is superior to lower resolution imagery for the purposes of mapping gullies, such high levels of resolution may not be required for the development of gully maps in South Africa. Furthermore they lack the spectral information necessary to resolve automatically mapping gully erosion. Given both multi-spectral capabilities, relatively high spatial resolution capabilities and affordability, Landsat TM has the greatest potential for mapping gullies in South Africa despite the limiting factors for Landsat TM in its ability to identify narrow gullies and areas where vegetation obscures the eroded areas (Vrieling, 2006). Gullies are less detectable with Landsat TM because the dimensions of smaller gullies tend to be less than the pixel resolution of Landsat TM 30m. Advancements in remote sensing techniques can maximize the spectral resolution of Landsat TM imagery by increasing feature separability.

2.3.2 Fundamental Concepts of Remote Sensing of Gullies

2.3.2.1 Remote Sensing: Electromagnetic Energy

Jensen (2005) defines remote sensing as the use of *"aerial platforms (e.g., suborbital aircraft, satellites, unmanned aerial vehicles) and sensors (e.g., cameras, detectors) that can collect information some remote distance from the subject."* The basic principle used is that a sensor detects electromagnetic (EM) energy, at specified wavelength bands[7] (nanometers), that are reflected from a feature on the earth. The full range of reflected EM wavelengths which are subdivided into regions that help interpret the way the EMR interacts with a feature for example visible (0.38-0.72µm), near-infrared (0.72-1.30µm), mid-infrared (1.3-3.00µm), far-infrared (0.7-15.0µm), and microwave (0.3mm to 3000m) (Nizeyimana and Petersen, 1997). These divisions are not strictly defined boundaries. Knowledge of reflected or emitted EM radiation characteristics at different wavelengths is important for selecting information extraction techniques that convert remote sensing observations to thematic maps of Earth surface features, and in the context of this research, especially gullies.

2.3.2.2 Spectral Response of Gullies

The complexity of mapping individual gullies with satellite data lies in the spectral heterogeneity of gullies themselves (King *et al.*, 2005). If a gully is to be mapped as a discrete feature in a landscape, using remote sensing, it is important to understand the spectral response of the features that characterize it. As defined in section 2.1.1 *" gullies can be characterized as relatively permanent steep-sided eroding water courses* (Morgan, 1986) *that have banks which are usually un-vegetated with some slumping and in some cases vegetation can occur in the base of the gully"* (Thwaites, 1986). Hence there are three major features that contribute to the spectral signature of a gully: bare soil, water and vegetation.

The bare soil spectral signature of a gully is influenced by mineral composition, soil texture, moisture and organic matter (Barnes and Baker, 2000; Irons *et al.*, 1989; Sujatha *et al.*, 2000). In general, soils exhibit a bright response in the visible red (0.6-0.7um) and IR (0.7-1.1um) region of the spectrum. Figure 2-4 is a graph showing the differences in the spectral signatures of two bare soils; clay and sand (solid line and large dashed line). The differences in the spectral curves of the clay (2-6% moisture content) and the sand (0-4% moisture content) relates to the differences in soil texture;

sandy soils are coarser grained and tend to be dry and hence give off a stronger reflectance across the visible and infra-red part of the EM spectrum than clay, which is fine textured and smooth and absorbs more of the incoming natural radiation. If soil moisture increases, the spectral response becomes similar to a water spectral signature. As shown in Figure 2-4 the curves of the moist soils exhibit water absorption bands around 1.4 μm and 1.9μm that are related to soil moisture. The low moisture content sand 0-4% does not have these absorption bands. These absorption bands characterize the spectral signature of water which is also influenced by the presence or absence of suspended sediment.

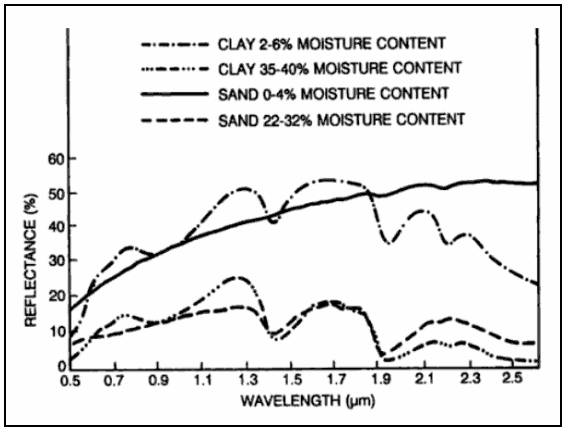

Figure 2-4 Spectral responses of clay and sandy soils from Hoffer and Johannsen (1969)

Organic matter influences the soils cohesiveness and is an important indicator used to assess land degradation (Shonk *et al.*, 1991). When gully erosion occurs it removes organic matter which increases the overall soil albedo (Hill and Schutt, 2000; Ritchie, 2000; Robinovoe *et al.*, 1981).

The presence or absence of vegetation also contributes to the spectral response of the gully. Vegetation has more complex spectral properties than soil (de Asis and Omasa, 2007). It is low (5%) in the visible part of the electromagnetic spectrum (red, blue, green) because it absorbs much of the incident blue, green, and red radiant flux for photosynthetic purposes; then the response increases (30%) in the near-infrared wave lengths because of the high reflectance associated with mesophyll structure of leaves. The spectral response characteristics in the near-IR make it easy to distinguish vegetation from a nonliving feature.

The time and stage dimension of a gully erosion process affects the physical and spectral properties of the soil surface (Ritchie, 2000). For example Figure 2-5 shows a cross-section of a gully system that has developed through incision into a thin colluvium layer overlying mudstones and sandstones in Lugxogxo, South Africa (Dardis, 1991). The spectral response of this gully system would vary. Water may or may not be present in the base of the gully and each of the layers (colluvium, palaeosol, mudstone, dolerite, gravel lag) and each of the stages (1,2,3 and 4) shown in the cross-section, would have different spectral signatures and may also have different types of vegetation growing on them depending on the mix of these surface types. Usually a stabilized gully has more vegetation present than an actively eroding gully in which bare soil dominates. During the rainy season the more stabilized gully would then have more healthy vegetation within the gully meaning that there would be an increase in the reflectance of the NIR in the spectral signature.

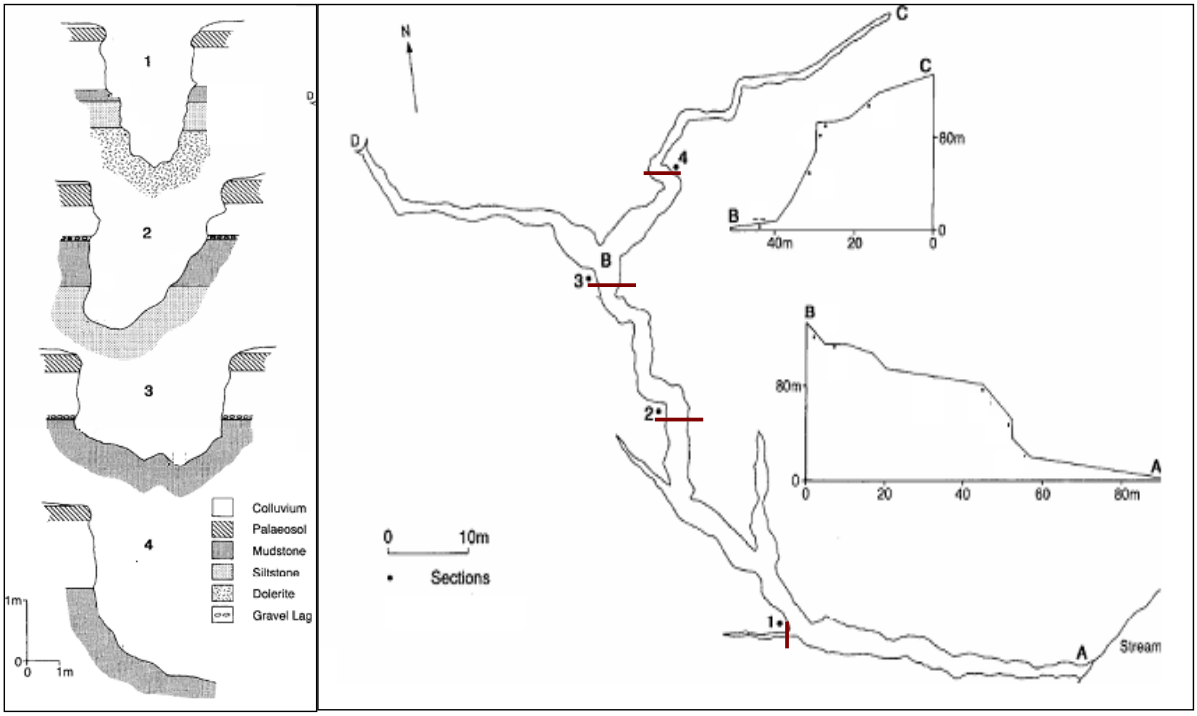

Figure 2-5 An example of soil variability within a gully that has incised into a thin colluvium layer overlying mudstones and subordinate sandstones. Left are four cross-sections of the gully system at different points. Right is an aerial view of the gully system with graphs displaying elevation change in the landscape (A,B,C,and D). Modified from (Dardis, 1991).

Since gullies are complex features to map, the design of a remote sensing gully mapping technique needs to maximize the spectral response of the eroded area (Dwivedi and Ramana, 2003; Metternicht and Fermont, 1998; Pickup and Nelson, 1984; Pickup and Chewings, 1988) and/or the erosion controlling factors (Cyr *et al.*, 1995; Hochschild *et al.*, 2003; Price, 1993). The complex nature of the gullies and of the surrounding terrain, within which they are formed, has brought remote sensing to the forefront of gully erosion mapping with a stated need for improved gully mapping methods using satellite remote sensing (Boardman, 2006; Lal, 2001).

2.3.2.2.1 Spectral Behavior of Gullies in a Landsat TM Imagery

The amount of energy reflected from an object, for example gully or an erosion factor, can be graphed at specific wavelengths to produce a spectral reflectance curve (Jensen, 2005). The spectral reflectance curves are unique to the sample and the environment from which they are derived (Schowengerdt, 2007).

Figure 2-6 displays the spectral response (mean reflectance) of six regions of interests (ROI) in bands 1-5 and band 7 of Landsat TM data of KwaZulu-Natal, South Africa. The lower reflectance of the gully ROI in the visible and near-infrared ranges compared to the other bands is attributed to a shadow component related to depth of the gullies and the irregularities of the surface, trapping more of the incoming sunlight and reducing the amount of reflected energy (Metternicht and Zinck, 1998). The gully and urban ROI, indicated as a brown and purple solid line respectively, exhibits the highest reflectance values in all waveband ranges, except the TM-4 where maximum reflectance values correspond to ROIs consisting of more green vegetation, forest and agriculture. The TM bands 4 and 5 allow for the most separability amongst the ROIs yet in TM bands 1, 2 and 3 the ROIs are less separable because of the similarity in their interactions with the sun's rays. This similarity can cause difficulties when trying to identify gullies spectrally from other features in the landscape; thus most remote sensing studies have focused on extracting erosion controlling factors such as soils (Pickup and Nelson, 1984; Pickup and Chewings, 1988) and vegetation (Singh *et al.*, 2004; Wessels *et al.*, 2004). However, remote sensing techniques do exist that can help enhance separability amongst classes for example vegetation indices and classification algorithms.

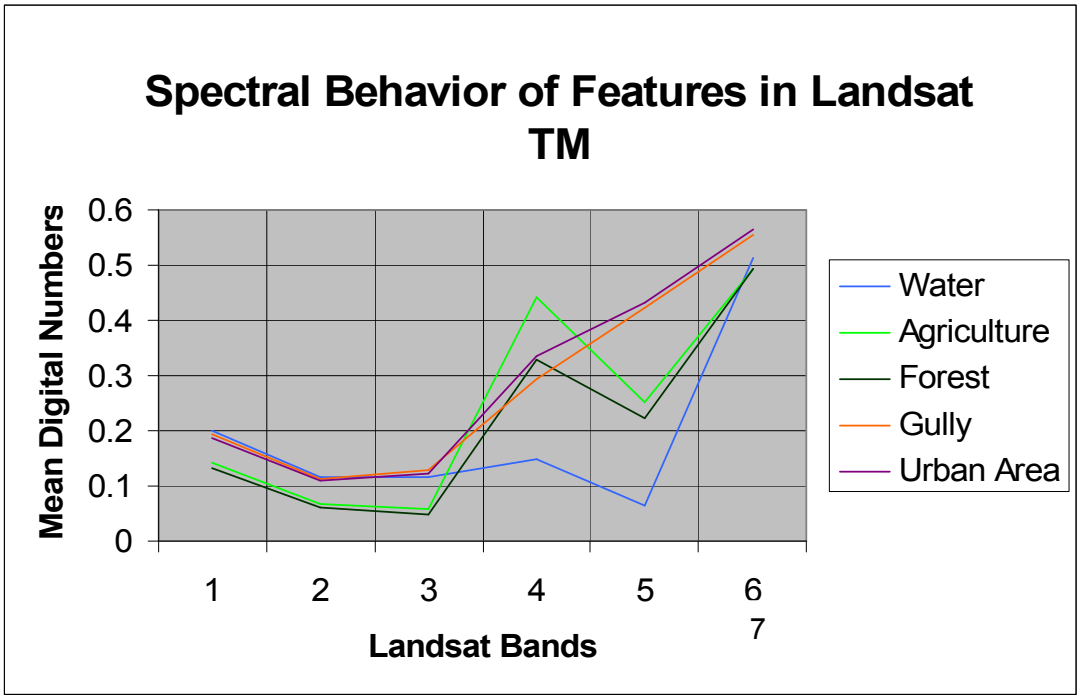

Figure 2-6 Spectral curves of selected regions of interest (Landsat TM),

2.3.3 Semi-automatic Techniques for Mapping Gullies in South Africa

2.3.3.1 Vegetation Indices

Vegetation indices (VI) derived from imagery are one of the primary remote sensing approaches for obtaining information about the Earth's surfaces, and have been used as a simple and quick feature extraction technique for erosion mapping (King, 1993; Manyatsi, 2008; Singh, 2006). A VI provides a greater contrast between vegetation and bare soil, by maximizing on a linear relationship between the red and near-infrared bands (TM-3 and TM-4).

If the assumption is made that if a lack of vegetation is an indication of gullied areas, a VI range could be used to identify those gullies. This can be achieved by selecting a particular VI value or range between values, which represent the vegetation on the ground, to mask out the vegetation in an image, thus leaving the gullied areas. This is called a threshold technique and is usually applied to crop based studies where a particular VI value or a range between two VI values represents a specific

vegetation/crop type (Vaidyanathan *et al.*, 2002). To apply this technique for mapping gullies in South Africa, the selected VI must accurately represent the vegetation on the ground.

2.3.3.1.1 Normalized Difference Vegetation Index

Normalized difference vegetation index (NDVI) can easily be derived from data acquired by a variety of satellites and low value thresholds can be selected to extract eroded areas (Mathieu *et al.*, 1997; Symeonakis and Drake, 2004; Thiam, 2003; Vaidyanathan *et al.*, 2002). Using SPOT imagery, Mathieu *et al.* (1997) mapped gully erosion in northern France by calculating NDVI and doing a maximum similarity with a brightness index (BI) and masking out vegetation, limestone outcrops and built-up areas. Thiam (2003) also used NDVI to produce a three-class (low, moderate, and high) land degradation risk map using multitemporal 1km NOAA/AVHRR. Here NDVI values were averaged for specific soil types which allowed for the evaluation the spatial extent of land degradation risk in southern Mauritius. Symeonakis and Drake (2004) used NDVI as an indicator of vegetation cover to determine areas of desertification over sub-Saharan Africa, using AVHRR. Using imagery from the Indian satellite sensor IRS-1B LISS-II, Vaidyanathan *et al.* (2002) used NDVI thresholds to identify classes for an erosion intensity map in Garhwal. This technique allowed for separation of 4 different classes, snow (NDVI <-0.01), vegetation (0.03 ≥ NDVI > -0.01), Barren (0.03≥NDVI>0.14), Water (0.14 ≥ NDVI > 0.34) (Vaidyanathan *et al.*, 2002).

NDVI measures the slope of the line between the point of convergence and the location of the pixel plotted in red-NIR space (Baugh and Groeneveld, 2006). This index is computed by dividing the difference of the near-IR and visible red bands (bands 3 and 4) by their sum, as seen in the following equation:

$$\mathbf{NDVI = (NIR-R) / (NIR+R)} \qquad \mathbf{(2\text{-}1)}$$

This equation is based on the idea that chlorophyll absorbs incoming radiation in the red/visible band and that the interior structure of the plant leaves reflects strongly in the near-infrared (indication of plants health). Although this equation is simple NDVI has proven to be unsuitable for areas with sparse vegetation. This is because soil is a major surface component that controls the spectral behavior of sparsely vegetated areas (Huete, 1988).

2.3.3.1.2 Soil Line Indices

In attempts to improve the detection of erosion features, in sparsely vegetated areas, other studies have applied vegetation indices developed to minimize the effect of soil, such as the soil adjusted vegetation index (SAVI) (Botha and Fouche, 2000) and the transformed soil adjusted vegetation index (TSAVI) (Hochschild *et al.*, 2003). These indices are designed to be relatively insensitive to variables such as soil background, sun-sensor angular geometry and the atmosphere (Dash *et al.*, 2007), which NDVI is sensitive to.

SAVI was originally developed using ground-based data, but it was later found useful in minimizing soil background effects using satellite imagery (Jackson and Huete, 1991). SAVI has been used in land degradation studies in southern Africa (Botha and Fouche, 2000). Using Landsat TM and MSS, Botha (2000) used SAVI to detect land degradation change. Whereas Dang *et al*. (2003) used Landsat ETM to calculated SAVI for a soil erosion model for Miyun County in China.

SAVI and TSAVI are based on the assumption that bare soil reflectance lies on a single line in the feature space of the red and NIR bands (soil line) (Baret *et al.*, 1993). The red and NIR bands have proven to be very useful for identifying soil erosion through the use of the 'soil line' concept (Mathieu *et al.*, 1997) which is a linear relationship between bare soil reflectance observed in the red and near-IR bands (Richardson and Wiegand, 1977). This soil line is characterized by the following linear equation:

$$\mathbf{NIR = aR+b} \qquad \mathbf{(2\text{-}2)}$$

Where **a** is the soil line slope and **b** is the y intercept. In theory the soil line can be calculated by finding two patches of different soils and calculating the best fitted line in NIR-red spectral space (Baugh and Groeneveld, 2006). In practice, the typical approach is to collect a large number of pixels and plot them on a NIR-red spectral space (y-axis NIR, x-axis red), then use the flat edge as the soil line (Baugh and Groeneveld, 2006). Soil Adjusted Vegetation Index (SAVI) was proposed by Huete (1988). It is derived from NDVI and can be expressed in terms of the NIR and R reflectance and also a constant (L), according to the following:

$$\mathbf{SAVI = [(NIR-R) / (NIR+R+L)] (1+L)} \qquad \mathbf{(2\text{-}3)}$$

The value of L ranges from 0, for very high vegetation cover, to 1 for very low vegetation cover. Huete, (1988) proved that SAVI (L=0.5) successfully minimizes soil variations in both the grass and the cotton canopies (Huete, 1988). Huete *et al.* (1992) showed that SAVI normalized the soil background (dry, wet, and damp soils) across all viewing angles. Some of the drawbacks of SAVI is it only offers an exact solution for study sites where the soil line slope is exactly in unity and the intercept is exactly zero (Fox *et al.*, 2004).

Another VI expression used is the TSAVI which can significantly reduce the effects of soil for areas of sparse vegetation cover or bare soil (Baret and Guyot, 1991; Hochschild *et al.*, 2003). It incorporates soil line parameters which allow for a VI that is designed for a specific area and can be applied in imagery that covers different soil types. Low TSAVI values have been related to potentially degraded areas (Flugel *et al.*, 2003; Hochschild *et al.*, 2003). Calculation of TSAVI requires parameters that are developed from a soil line. It is important to note that these parameters vary with soil type.

$$\mathbf{TSAVI = a(NIR - aRed - b) / (aNIR + Red - ab + X(1 + a^2))} \qquad \mathbf{(2\text{-}4)}$$

Where **a** and **b** are calculated from the soil line as slope and y intercept respectively, and X is a soil adjustment factor (Baret and Guyot, 1991). The benefit of using TSAVI is that it adjusts to a given study area using a well designed soil line; hence it would be expected to perform better than SAVI and NDVI as they are universal (Lawrence and Ripple, 1998). Though there is little literature on the application of soil line vegetation indices (SAVI and TSAVI) in erosion research, they could prove to be beneficial for gully erosion mapping in South Africa.

2.3.3.2 Classification Algorithms

A second approach of applicability to mapping soil erosion using remote sensing is through the use of the powerful capabilities of supervised classification algorithms. The objective of a supervised classification approach is to automatically categorize all pixels in an image based on their spectral clustering behavior, into classes or themes; in the case of this research those classes would be gullies and non gullies. The classification process involves three main steps (i) *Transformation* – the transformation of an image by spatially or spectrally enhancing feature identification, for example Principal Component Analysis (PCA). This helps remove noise in the image and simplifies the calculations performed by an algorithm, (ii) *Training* – selection of pixels which are used to train the classifier to recognize classes, and determination of decision boundaries which partition the feature

space according to the training pixel properties, (iii) *Labeling* – the application of the feature space decision boundaries to the entire image to label all pixels (Schowengerdt, 2007). The final output is a thematic map that categorizes different surface materials or conditions (see Figure 2-7).

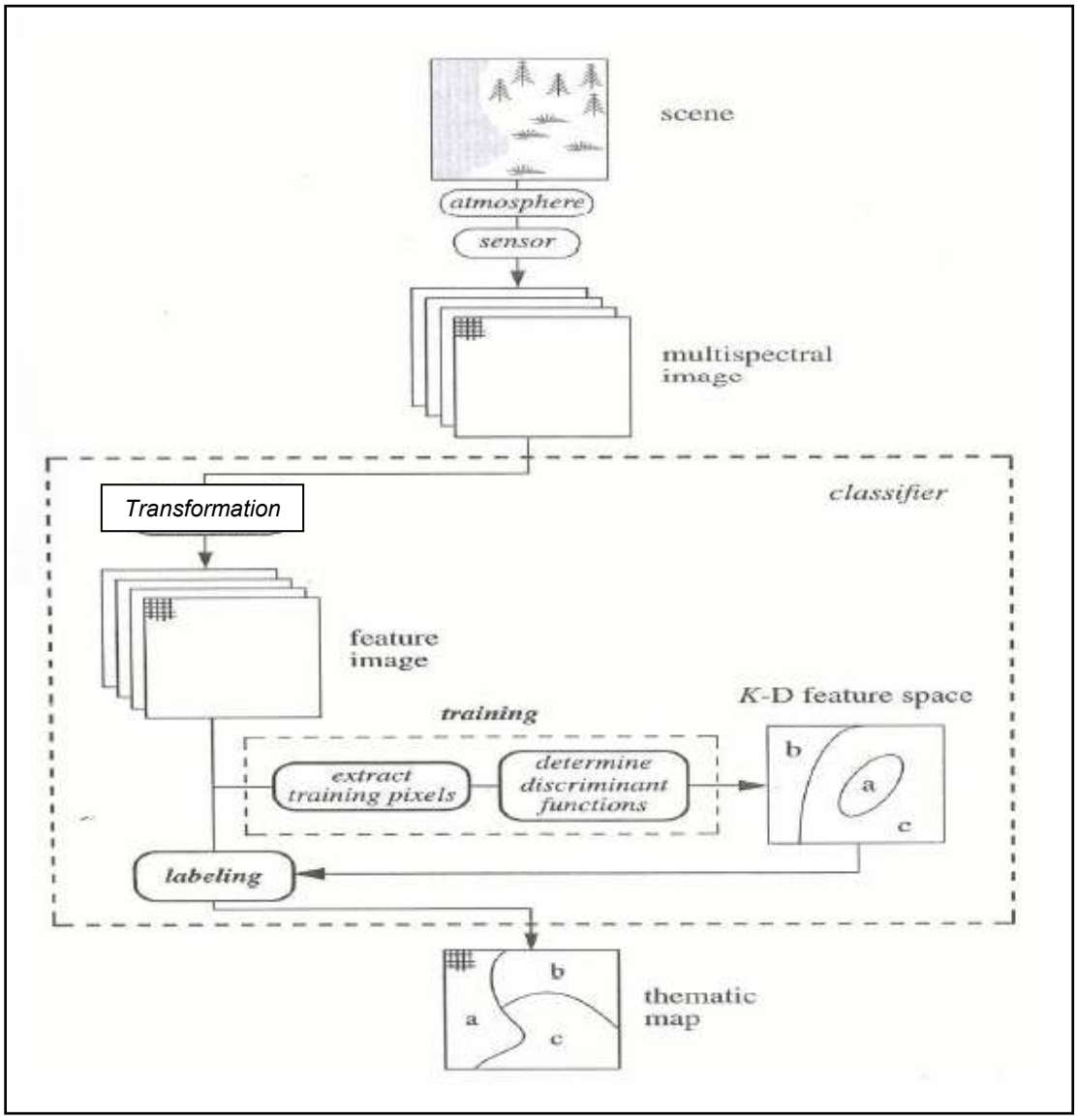

Figure 2-7 The classification process (modified from Schowengerdt, 2002)

Classification algorithms can be parametric or non-parametric. Both require user input, in the form of training data, to guide the image processing software through the classification. A parametric algorithm uses parameters such as mean and variance-covariance matrices for each of the classes to determine its decision boundary between classes; whereas non-parametric algorithms do not make

any assumptions about the distribution of the data used. The most commonly used classification method is based on maximum likelihood; a per-pixel based probabilistic classification. This traditional approach to classification has limitations in resolving complex classes that are not normally distributed. Since gullies and their surrounding areas are spectrally complex, application of this traditional parametric algorithm may be challenging for gully mapping in South Africa. Recently remote sensing literature has given particular attention to the support vector machines (SVM) approach which can produce higher classification accuracies than maximum likelihood classification (MLC) (Gualtieri *et al.*, 1999). SVM classifiers have been applied to multi-spectral (Hermes *et al.*, 1999; Huang *et al.*, 2002; Roli and Fumera, 2001) and hyperspectral data (Gualtieri *et al.*, 1999). SVM classifiers represent a promising non-parametric classification method for identifying gullies from other land cover types. SVMs potential lies in its ability to separate classes by locating a hyperplane that maximizes the distance from the members of each class to the optimal hyperplane. To demonstrate the mapping capabilities of SVM, a comparison is made between its characterization of the decision boundaries with MLC and mahalanobis distance classification (MDC) decision boundaries.

2.3.3.2.1 Conventional Classification Algorithms

The decision surfaces implemented by MLC are quadratic and take the form of parabolas, circles and ellipses. MLC will be explained using two training data classes A, and B, existing in a simple two dimensional feature space (x, y). The MLC algorithm first calculates the probability ellipses separately for class A and class B using a covariance matrix and mean vectors for class A and class B. The mean controls the location of the ellipse in feature space and the covariance controls the spread. These parameters allow for the calculation of the statistical probability of a given pixel being a member of a particular class A or B using the following equation, which is calculated for each class:

$$p_i = -\frac{1}{2}\log_e|V_i| - \left[\frac{1}{2}(X - M_i)^T V_i^{-1}(X - M_i)\right] \quad \textbf{(2-5)}$$

Where: M_i = mean measurement vector for class *i*,

V_i = variance-covariance matrix of class *i* for bands *k* through *l*.

The expression $(X - M_i)^T V_i^{-1}(X - M_i)$ refers to the Mahalanobis distance (MD) squared. The effect is to downgrade pixel values that are relatively far from the mean of the training class (high

MD) taking into account the shape of the probability distribution of the training-class members (Mather, 2004). The unknown pixel is assigned to the class that produces the largest probability.

The above discussion on how an unknown pixel *(w)* is classified, is illustrated in Figure 2-8, which is two classes A and B in a two dimensional feature space (x,y). Here class A has a high positive covariance between the bands x and y whereas class B has a lower covariance, this is demonstrated in the width of the ellipses. The means of each class are located in the centre of the ellipse, point 1 and 2. The contours indicate the degree of probability of point *w* belonging to each class, so as one moves away from the mean or centroid, the probability of the pixel *w* being in that class decreases. The shape of the probability distribution contours also controls the probability of whether or not a pixel should belong in that class as can be seen point *w* is closer the center of class A yet because of the shape of the ellipse point *w* is more likely to be classified as class B rather than class A. Probability thresholds can also be applied if not enough training data are available to estimate the parameters of the class distributions. Applying a threshold also helps remove outliers. Thus the MLC can be regarded as a distance-like classifier because it measures the distance from the unknown pixel to each class however this is modified according to class (Mather, 2004). There exists abundant literature on ML and its application to remote sensing data; for more information a comprehensive overview can be found in (Jensen, 2005; Richards and Jia, 2006).

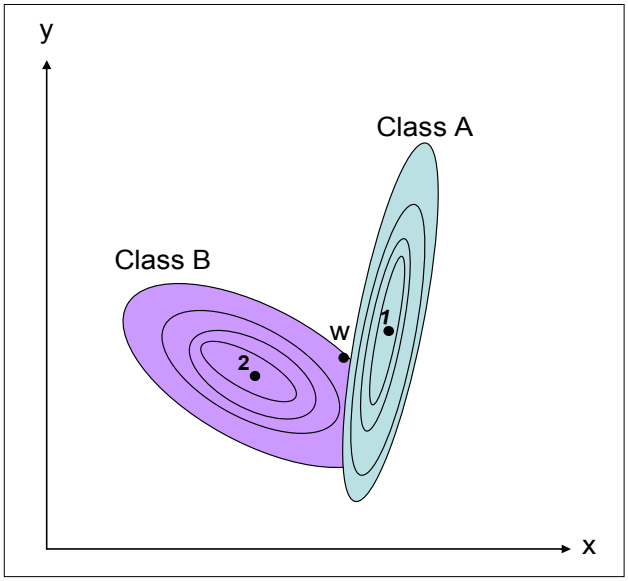

Figure 2-8 Displays class A and class B plotted in an x-y feature space, with hypothetical probability contours and means. Modified from Mather (2004)

The Mahalanobis distance classifier (MDC) is similar to MLC however its decision boundaries assume all class covariance's are equal (Richards and Jia, 2006) and simply measures the MD of an unknown pixel as appose to MLC which calculates the probability density function of each class. Here the MD is defined as the distance of an unknown pixel from the center of a class ellipse (i.e. mean) divided by the width of the ellipsoid in the direction of the unknown pixel (Mather, 2004). An

unknown pixel is classified to the class for which the MD is the shortest (Richards and Jia, 2006). Mathematically this distance can be expressed for a group of pixels in a class with mean $M_i = (\mu_1\mu_2\mu_3,\ldots,\mu_i)^T$ and covariance matrix V_i for a unknown pixel described as a multivariate vector $X = (X_1,X_2,X_3,\ldots X_i)^T$ the MD can be defined as:

$$D = \sqrt{(X - M_i)^T V_i^{-1} (X - M_i)} \quad \textbf{(2-6)}$$

Where: D = Mahalanobis distance of a unknown pixel

M_i = mean measurement vector for class *i*,

V_i = variance-covariance matrix of class *i* for bands *k* through *l*.

Although MLC also uses MD to determine its probability density function, the distances themselves have no upper limit whereas MDC has a fixed covariance for each class. The potential of using MDC for gully mapping lies in its ability to be less affected by outliers in a training class because of this fixed covariance. Hence the effects of outliers in a training class are reduced. This makes the computational processing time faster and simpler than MLC yet still maintaining a degree of direction (Richards and Jia, 2006).

2.3.3.2.2 Support Vector Machines

The Support vector machine (SVM) represents a group of theoretically superior machine learning algorithms (Huang *et al.*, 2002) that aim to determine the location of decision boundaries that produce the ideal separation of classes. Most of the literature and success stories of SVMs are from other pattern recognition applications. Gualtieri *et al.* (1999) were the first to introduce the support vector concept to remote sensing image classification, followed by Burges (1998) and Huang *et al.* (2002).

The application of SVM as a "one class classification" (i.e. when one class is of interest) (Sanchez-Hernandez *et al.*, 2007a; Sanchez-Hernandez *et al.*, 2007b) offers a potential method for mapping gullies in South Africa. Sanchez *et al.* (2007a and 2007b) and Boyd (2006) all found SVM performed successfully (all above 91% overall accuracy) in classifying habitats in Landsat TM imagery.

SVM classification is a nonparametric classifier that attempts to separate the different classes by directly searching for adequate boundaries between them. The process uses the concept of support

vectors[8] to identify the optimal separating hyperplane OHS (multidimensional linear surface) which divides two classes and functions as a decision surface for classification. The orientation of the hyperplane is where there is a maximum separation between the two classes which is essentially called maximizing the margin. If two-classes are linearly separable the SVM selects from among the infinite number of linear decision boundary the one that has low generalization error (Gualtieri *et al.*, 1999).

However most classes are not linearly separable and in such cases the SVM approach uses a kernel which plays an important role in locating complex decision boundaries between classes (Huang *et al.*, 2002). The kernel maps the data to a higher dimensional space and within that space it attempts to find a linear separating surface between the two classes (Gualtieri *et al.*, 1999). The basic idea is the nonlinearly separable data appear in the training algorithm are in the form of dot products (xi*xj) and the kernel maps them to some other Euclidean space where they can be linearly separated. (See Figure 2-9).

[8] Training samples that lie near the boundary between the classes in feature space (Boyd, Sanchez-Hernandez, and Foody, 2006)

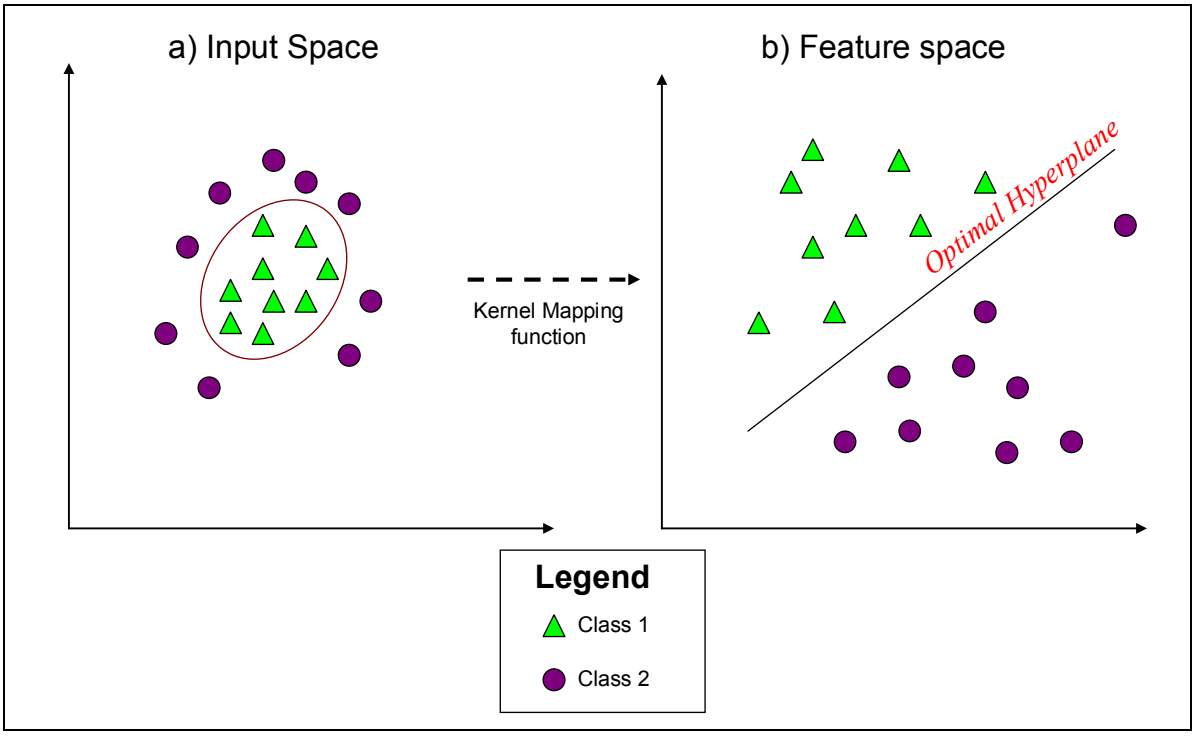

Figure 2-9 The kernel maps the training samples into a higher dimensional feature space via a nonlinear function and constructs a separating hyperplane with maximum margins. Modified from Camps-Valls *et al.* (2004)

How the kernel operates is by introducing positive slack variables (allowed errors) and a penalization parameter C which is applied to the errors (Camps-Valls *et al.*, 2004). The positive slack variables are applied to each sample and indicate the distance the sample is from the OSH. They are used so that the amounts of violation of the constraints are introduced. The constant C is selected by the user and is used to control the magnitude of the penalty that is associated with the samples that lie on the wrong side of the decision boundary (Foody *et al.*, 2006). Parameter C affects the generalization capabilities of the classifier (Camps-Valls *et al.*, 2004). Large values of C may cause the SVM to over-fit the training data and low values may cause an inappropriately large fraction of support vectors to be derived (Foody *et al.*, 2006). Figure 2-10 is a more detailed description of how the SVM operates with linear and nonlinear training data. This binary classification can also be extended to N classes, where N > 2 (Hsu and Lin, 2002), however this is not the focus of the study. For more information the kernel functions and parameters please refer to Vapkin (1995).

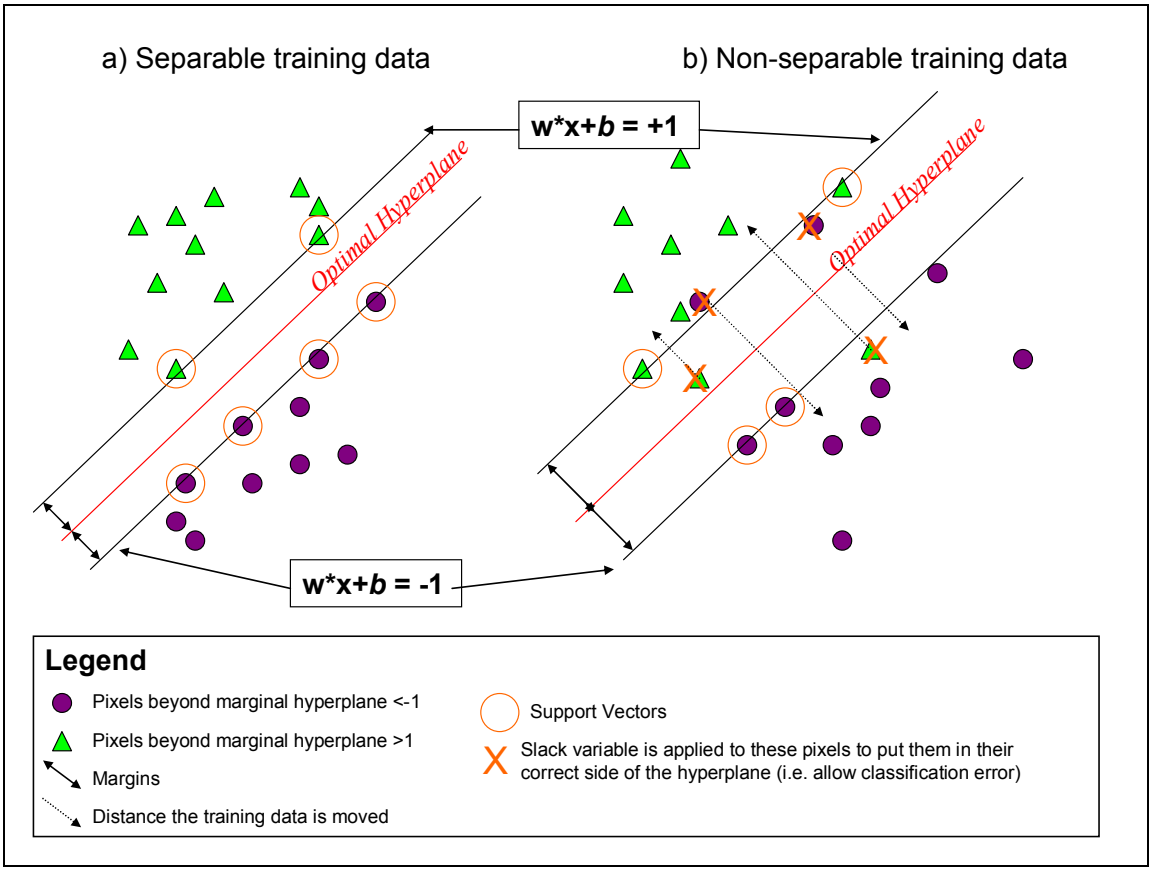

Figure 2-10 a) SMV separating linearly separable classes. In separating classes that are not linearly separable b) the SVMs task is to find the cost separated marginal hyperplanes that minimize the slack variables and maximize the margins.

There is a lack of information on the parameters used and the level of accuracy obtained from using SVM for one class classifications. SVM has been used for forest fire redetection and urban area extraction in SPOT 5 satellite imagery (Lafarge *et al*., 2005). The main focus of their study was on the kernel parameters based on textural information and radiometric information, and their ability to separate in one case forest smoke and in other urban areas. The results were visually impressive; however no accuracy assessment was documented. Authors that have quoted the SVM accuracy, have used overall accuracy, which is the total number of pixels correctly classified divided by the total number of pixels in the map. Foody and Mathur (2004a) used SVM (C=6;γ=0.0039) on SPOT HRV and aimed at assessing the training data size for crop classification. The study proved that a small training site could be used to achieve an overall accuracy of 95.2%. Foody (2006) had a similar aim but assessed the use of mixed pixels and achieved a lower overall accuracy of 91.11%; however

still concluded that SVM was comparable to conventional methods (91.48% overall accuracy). More recently Mathur and Foody (2008) used SVM (C=1; γ=0.000625) to classify crops in South west India. They demonstrated that using only the support vectors, for the SVM classification, still produced a high overall accuracy of 90% which is comparable to the conventional training data which had a 92% overall accuracy.

Rational for using Support Vector Machines for gully mapping in South Africa

- **It has proven successful in binary classifications** (Boyd et al., 2006; Sanchez-Hernandez et al., 2007b; Tax and Duin, 2004) which separate the class of interest from all other classes. In this case gullies from non gully areas.
- **Is well adapted to deal with data of high dimensions:** Since SVM does not rely explicitly on the dimensionality of the training data but uses pattern recognition, regression, and density estimation in high-dimensional spaces to separate the classes (Vapnik, 1998), this means that less time is required in creating training data.
- **Less expert knowledge is required in training data collection:** The nature of SVM's operation allows the use of smaller training data size (Foody and Mathur, 2004b). SVM has also proven useful for mapping unknown classes in a Landsat ETM (Mantero and Moser, 2005). Therefore, SVM implementation is probably more tolerable of less expert knowledge when identifying training data for mapping gullies using this algorithm.
- **Competitive with other classifiers:** It has been proven to be competitive with the best available classification methods such as neural networks and decision tree classifiers (Huang *et al.*, 2002); and typically yields accuracies that are comparable to other classifiers that are widely used in remote sensing (Foody and Mathur, 2004a; Huang *et al.*, 2002). Other classifiers have problems separating unbalanced classes.

If SVM is successful in gully mapping then researchers will be able to extract gully information with little background knowledge of the gully feature/process, rapidly and inexpensively, over large geographic area (50-10,000km²). Fortunately most of the remote sensing literature on SVM classification has provided information on the level of accuracy; however, in most of these studies these values are very misleading and could, once again, contribute to some serious issues when drawing conclusions on maps created using classification algorithms.

2.3.4 Testing and Validation

Map accuracy assessments show users how data accuracy and model choices affect results and, thus, decisions for erosion control. It is necessary to quantitatively assess remotely sensed data classification to determine the accuracy of the remote sensing technique. This can be done using an accuracy assessment which assesses the degree of error in the end-product typically with reference to a thematic map or image. Accuracy assessment results are beneficial to both the user and the producer of the maps. The producer can evaluate and compare the effectiveness of various classification techniques, and can communicate the product limitations to the user.

A variety of measures are available for describing the accuracy of an output map through use of an error matrix. An error matrix is a standard accuracy reporting mechanism that shows a cross-tabulation of the class labels in the classified map against those in the ground truth reference data. It is known to be a very effective way to represent map accuracy because individual accuracies are shown for each category as well as errors of inclusion (commission errors) and errors of exclusion (omission errors) that are evident in the output (Congalton, 1991). It is used to calculate statistics such as the overall accuracy, producer accuracy, user accuracy[9] and the kappa statistic[10]. These can be calculated as follows:

$$\text{Overall Accuracy} = \frac{\text{Total number of pixels correctly classified}}{\text{Total number of pixels in the map}} \quad \textbf{(2-7)}$$

$$\text{Users Accuracy} = \frac{\text{Number of pixels correctly classified as gully}}{\text{Total number of gully pixels in classified map}} \quad \textbf{(2-8)}$$

$$\text{Producers Accuracy} = \frac{\text{Number of pixels correctly classified as gully}}{\text{Number of gully pixels in the reference data}} \quad \textbf{(2-9)}$$

[9] The ratio of the total number of correctly classified pixels to the total number of pixels in each class (Janssen and Wel 1994, Stehman 1997),

[10] Measures the difference between the actual agreement in the confusion matrix and the chance agreement

$$\text{Kappa Statistic} = \frac{n\sum_{i=1}^{k} n_{ii} - \sum_{i=1}^{k} n_{i+}n_{+i}}{n^2 - \sum_{i=1}^{k} n_{i+}n_{+i}} \quad \textbf{(2-10)}$$

Where: n the total number of samples

n_{ii} the number of samples correctly classified into category i

n_{i+} the number of samples classified into category i in the classified image

n_{+I} is the number of samples classified into category j in the reference data set

There are many claims on which measurement is the best for quoting the accuracy of a given classification. Interestingly enough, most of the remote sensing erosion studies have failed to report the accuracy of the output maps (Vrieling, 2006) and those that have provided validation statistics, are often misleading. For example, Ellis (2000) study on classification of soil erosion in Australia used overall accuracy to compare two classifiers performances. However the high overall accuracies reported was mostly a result of two classes which occupied 99% of the study region: `no appreciable erosion' (class 1) and `minor sheet erosion (Ellis, 2000). Other classifications where one class is of interest, have quoted the maps based on either the producer or the user accuracy. For example, both Boyd *et al*. (2006) and Sanchez-Hernandez (2007a) chose the producer accuracy as being more important for identifying habitats for fen identification; whereas, Verling (2007) placed more emphasis on the user accuracy for identifying gullies. Verling (2007) also suggested that using an average of the producer and user accuracy for identifying gullies is less biased than reporting a single value. It is not clear, however, whether such a technique could be used for a comparative study of different classifications. Stehman (1997) favored the kappa statistics for comparison of classified maps using different algorithms.

To illustrate how some of the above accuracy measurements could be very misleading for a comparison of classified maps representing gullies and non gullies in this study, we consider the calculations presented in Figure 2-11. This is a hypothetical example displaying two maps; classified map and reference map each showing different proportions of area for the gully and no gullied class. The accuracy assessment is illustrated in the bottom left and shows correctly classified pixels as solid colour and errors of commission and omission as patterned areas. The error matrix in the top right now displays the values which are used in the calculation of the accuracy measurements.

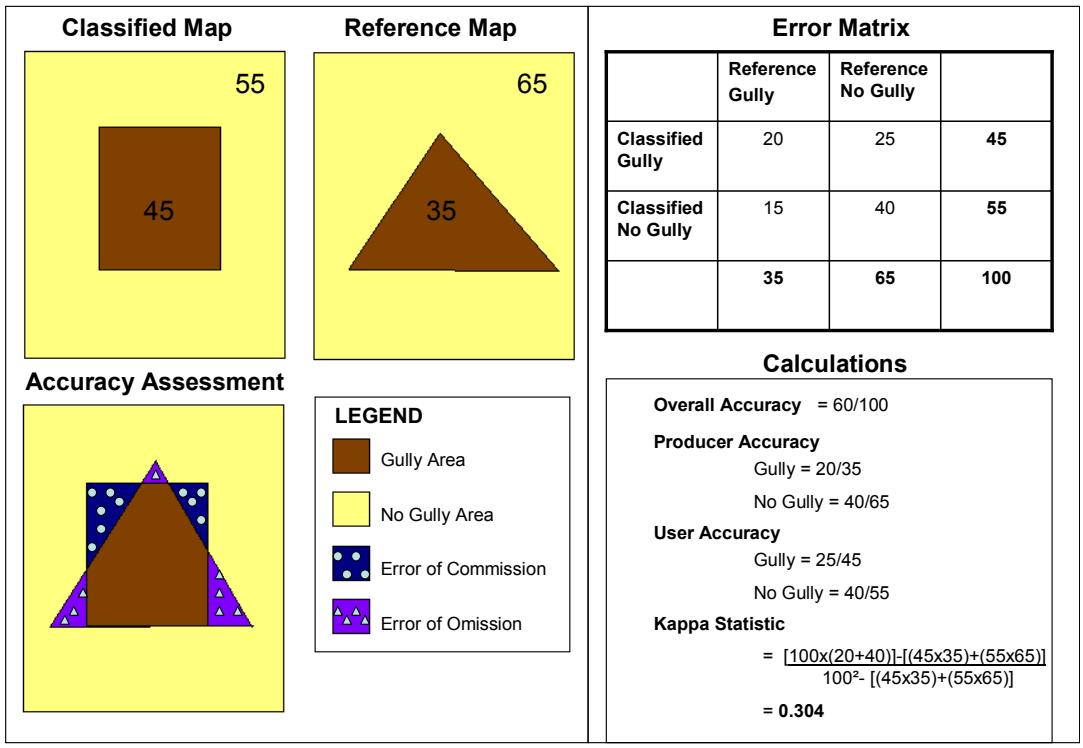

Figure 2-11 A simple accuracy assessment illustrations

The overall accuracy, which is the total number of pixels correctly classified divided by the total number of pixels in the map, i.e. (20+40)/100, only takes into account those pixels that were correctly classified. Using such a measurement to assess the accuracy in our case study could be very biased because of the larger spatial coverage of the non gullied class. The no gullied area would have a greater number of correctly classified pixels which could overpower the actual pixels classified as gully. Selection of a classification technique simple based on single accuracy values such as a producer (20/35) or user accuracy (25/45), could also be extremely misleading because they both are important values for the following:

- A high producer's accuracy indicates that most of the actual gully pixels in the reference data are also classified as gully, which is said to be a measure of error of omission (Story and Congalton, 1986); it is an expression of how well the map producer identified a gully on the map from the imagery.

- A high user's accuracy indicates that few actual non gully pixels are classified as gully, which is considered a measure of commission (Story and Congalton, 1986). It expresses how well a user will find that gully feature on the ground.

Since both the user and the producer accuracy are important, the Kappa statistic is more applicable for assessing the accuracy of a classification output because it takes into account the overall statistical agreement of an error matrix (Lu and Weng, 2007). The kappa statistic measures the difference between the actual agreement and the chance agreement and takes into account the whole error matrix (Congalton, 1991). The value of the kappa statistic ranges from 0 to 1 with values greater than 0.80 indicating a positive correlation between the classified image and the reference data and values between 0.4 and 0.8 representing a moderate level of agreement (Jensen, 2005). A major advantage of using the kappa statistic is it allows for a statistical test of the significance of difference between two techniques (Congalton, 1991) which allows for better comparison.

2.4 Specific Objectives

From this literature review, the main aim of this study is to assess the relative merits of using vegetation indices and classification algorithms for mapping gullies in a Landsat TM imagery of KZN South Africa. Gullies mapped in a SPOT 5 Pan image using traditional digitization provide a comparative basis for this assessment. The specific objectives are to compare and evaluate the classification map accuracy, achieved form each technique with changes in scale of the study area from the gully system level- continuous and discontinuous to the sub-catchment. The kappa statistic is the main accuracy assessment metric used. These main objectives can be summarized as follows:

A. Vegetation Indices for mapping gullies:

- To determine the input parameters for TSAVI.
- To determine the best threshold range for gully mapping using NDVI, SAVI and TSAVI.
- To determine the accuracy assessment of the sub-catchment subset using thresholds obtained from the continuous gully subset.
- To determine the classification accuracy, using the kappa statistic, of the gully maps produced from NDVI, SAVI and TSAVI in the continuous and discontinuous and sub-catchment subsets.

B. Classification algorithms for mapping gullies:

- To test the need for image transformation for MLC, MDC and SVM for mapping gullies.
- To test the effect in classification accuracy with different training data sizes
- To determine the SVM parameters for gully mapping using Landsat TM.
- To determine the classification accuracy, using the kappa statistic, of the gully maps produced from MLC, MDC, and SVM in the continuous and discontinuous and sub-catchment subsets.

The experiments reported in this thesis were undertaken in order to achieve the objectives listed above, while at the same time addressing a variety of other issues that are extremely important for successful applications of remote sensing for gully mapping in South Africa such as cost, time and expert knowledge required.

The final question is whether "medium resolution multi-spectral satellite observations, such as Landsat TM, combined with information extraction techniques, such as Vegetation Indices and multispectral classification algorithms, can provide a semi-automatic method of mapping gullies and to what level of accuracy?". By addressing this question, it may be possible to determine whether or not such techniques could improve the ability of developing countries, such as South Africa, to create gully maps for a large area on 'the fly', economically and with little expert knowledge.

Chapter 3
Site Description

3.1 Location

The study region is located in the province KZN, South Africa approximately 30º18´39.399´´ E, 27º49´24.6´´S (Figure 3-1). The availability of satellite imagery and the occurrence and high levels of gully erosion were important criteria for the selection of the study site. The study region covers an area of approximately 2000 km² and is located the Buffalo River (Buffels) sub-catchment which is approximately 4000 km² (Figure 3-2). The Buffalo River catchment is one of the two large drainage systems that make up the Tugela Basin. It stretches from the Drakensberg escarpment to the Indian Ocean flowing in a general southeast direction, roughly at a right angle to the coast. The study area consists of the Belelasberg plateau in the north, which lies at an altitude of approximately 1800m with lowlands in the interior part of the study region, approximately 1200m in altitude (van der Eyck *et al.*, 1969).

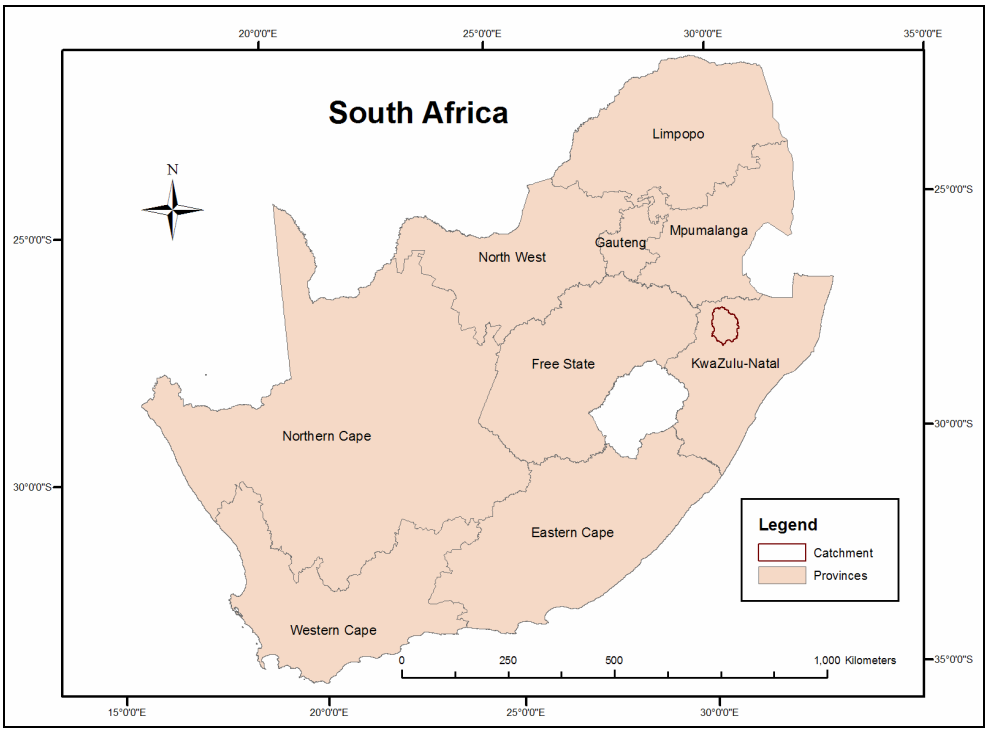

Figure 3-1 Location of study area in South Africa (spatial data source: ARC, (2007))

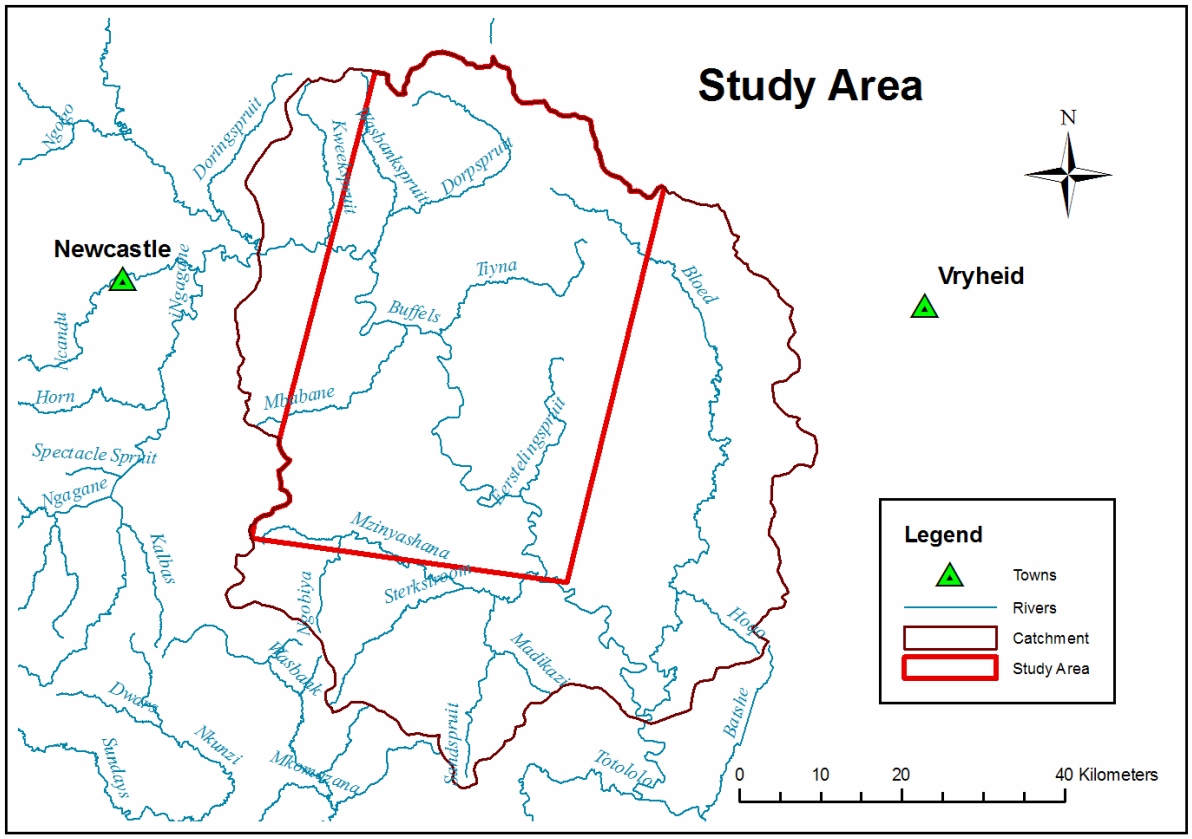

Figure 3-2 Location of study region within Buffalo River sub-catchment (spatial data source: rivers (DWAF, 2007) towns and catchment (ARC, 2007))

3.2 Climate

The climate of the study area is semi-arid with dry winters and rainy summers. The area generally experiences a mean annual rainfall between 800-1000mm with most of the precipitation falling between the summer months of October to March (Schulze *et al.*, 1997). In the upper catchment in the north of the study area, mean annual rainfall ranges from 780—1,300mm; whereas the interior part of the study area has a lower mean annual rainfall ranging from 750-980mm. The monthly minimum and maximum daily temperatures are approximately 11 ºC and 25ºC, respectively; however temperatures can reach as high as 39ºC in the summer months (October-March). The two main ecological regions present in the study area are the Highlands in the north and the Interior Basin which covers most of the study region.

3.3 Vegetation

The study region is located within two Biomes: Grassland biome and Savanna biome (Munica and Rutherford 2006). Within these biomes a total of three bioregions are present: Mesic Highveld Grassland, Sub Escarpment Grassland and the Sub-escarpment Savanna. These three bioregions represent a total of eleven different vegetation units which are characterized based on geology, soils, topography and precipitation (see Appendix B: Bioregion and vegetation unit map) The vegetation unit description is provided in Appendix C and additional information can be found in Munica and Rutherford (2006).

The most dominant vegetation unit is the Income Sandy Grassland (approximately 80% of the study area) which has the greatest erosion intensity compared to the other vegetation units in the study region (Mucina and Rutherford, 2006). The two vegetation units of the Mesic Highveld Grassland bioregion are located on the escarpment in the northern part of the study region. The sub-escarpment Savanna Bioregion covers a very small area found in the south east of the study region. The other vegetation types are dispersed through out the study region with the Eastern Temperate Freshwater wetlands occurring close to the rivers and the Northern Afrotemperate Forest occurring on the high levels of the escarpment.

3.4 Geology and Soils

The study region is underlain by rocks of the Karoo Supergroup which is a sedimentary rock that formed from the filling of the Karoo basin during the Permo-Carboniferous to Early Jurassic times (van der Eyck *et al.*, 1969). The sedimentary formation includes four layers: Dwyka, Ecca, Beaufort and Stormberg series. The majority of the study area (approximately 85%) consists of the Vryheid and Volkrust formations of the Ecca series and the Normandien formation of the Beaufort series. The Vryheid formation consists of thick beds of whitish to yellowish, mostly coarse-grained sandstones and massive grits, often rich in feldspars (Catuneanu *et al.,* 2005). The Volkrust formation consists of blue shales that were deposited under lacustrine conditions (van der Eyck *et al.*, 1969) (see Figure 3.3). The Normandien formation consists of coarse grained sandstone interbedded with mudstone that has been deposited by meandering streams (Catuneanu *et al.,* 2005). Scattered within the study area are intrusive dykes and sills made of a volcanic rock called Karoo Dolerite, as well as alluvial and colluvial deposits made up of silt, clay and larger particles of sand.

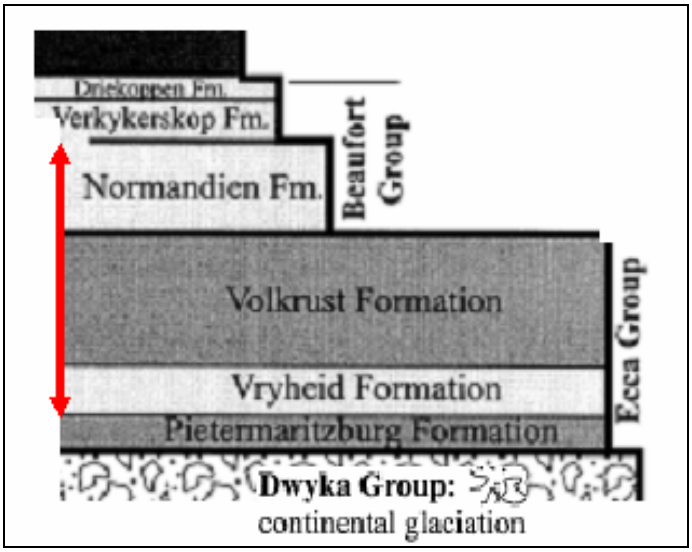

Figure 3-3 Lithostratigraphy of the Karoo Supergroups present in the study area

The soils generated from these sedimentary rocks tend to be shallow, poorly drained, sandy soils (BA, EA, EB). These soils are highly erodible and are of poor quality because of the poor vegetation cover and species composition (Income sandy grassland). The soils generated from the Karoo Dolerite are strongly structured red or black (DA) clayey soils and are reasonably resistant to erosion and grazing pressure (Whitmore *et al.*, 2006). Most of the study area is made up of strongly structured soils with marked clayey accumulation (CA).

3.5 Land Use

Commercial and communal farms are the dominant land use practiced in the study area with some urban areas (high population density) which are located in the eastern side of the study region. Most KZN studies indicate that gullied lands are more common in communal farms than commercial farming areas because informal grazing and intensive crop agriculture (Meadows and Hoffman, 2003; Weaver, 1988). Some of the other land use practices evident in the study region that make it more susceptible to erosion are listed in Table 3.6.

Table 3.6 Land use practices and contribution to erosion

Landuse Practices	Contribution to the erosion problem
Overgrazing and fire	Destroy the protective vegetation cover
Compaction of the soil through pathways and animal tracks	Reduce infiltration rates which increases surface runoff and erosion by surface wash and rills
Poor agricultural practices	Cause loss in organic carbon and dilution of nutrients which make the soil less stable (Felix-Henningsen *et al.*, 1997)
Communal grazing	Usually over stock the lands leading to overgrazing (Mills and Fey, 2003)
Artificial channeling of surface runoff	(Beckedahl and Dardis, 1988)

3.6 Erosion Status

One of the main characteristics of the area is the dissection of the landscape by numerous gullies. The study region lies between two erosion "hot spots"[11]: Swaziland (Morgan *et al.*, 1997) and Lesotho, which has the highest erosion hazard of any single country in central or southern Africa (Chalela and Stocking, 1988). Within the study region the magnitude of soil erosion differs from one physiographic region to another. The plateau is fairly uneroded however the slopes include some broad shaped gullies that have a mix of bare soil and vegetation. Within valley there is a mix of sheet erosion, rill erosion and discontinuous and continuous gullies occurring mostly in the cultivated areas.

3.7 Summary

The gully erosion study site is found in KZN, South Africa where the most serious cases of erosion have been identified. The area has sparse vegetation consisting mostly of grasslands which occur on shallow, poorly drained, sandy soils and more lush vegetation types which occur in wetlands and on the escarpment. The topographic relief consists of a plateau in the north and a valley bottom which is dissected by two rivers flowing in a south east direction into the Buffalo River. The geology generates highly erodable soils originating from shale's and coarse grain sandstones. The major land use type is agriculture both commercial and communal, with the latter being the most severely vulnerable to

[11] Hot spots refer to areas in Africa that experience severe cases of soil erosion

gully erosion. The combination of high rainfalls, sparse vegetation cover, highly erodable soils and poor land management, are all contributing factors to the gully erosion problem in the area.

Chapter 4
Methodology

The imagery used in this thesis was made available by the ARC of South Africa and included Landsat (TM) 2005, SPOT (HRG) 2006 and SPOT (Pan) 2006 images for the defined study area (refer to Table 2-1 for imagery characteristics). Only Landsat TM was used for the VI gully mapping methods and both Landsat (TM) and SPOT (HRG) were used for the classification gully mapping methods. The SPOT (Pan) was used to create the ground truth map for the accuracy assessment of the semi-automatically produced gully maps. Figure 4-1 summarizes the procedures used to assess the explored semi-automatic methods for gully mapping.

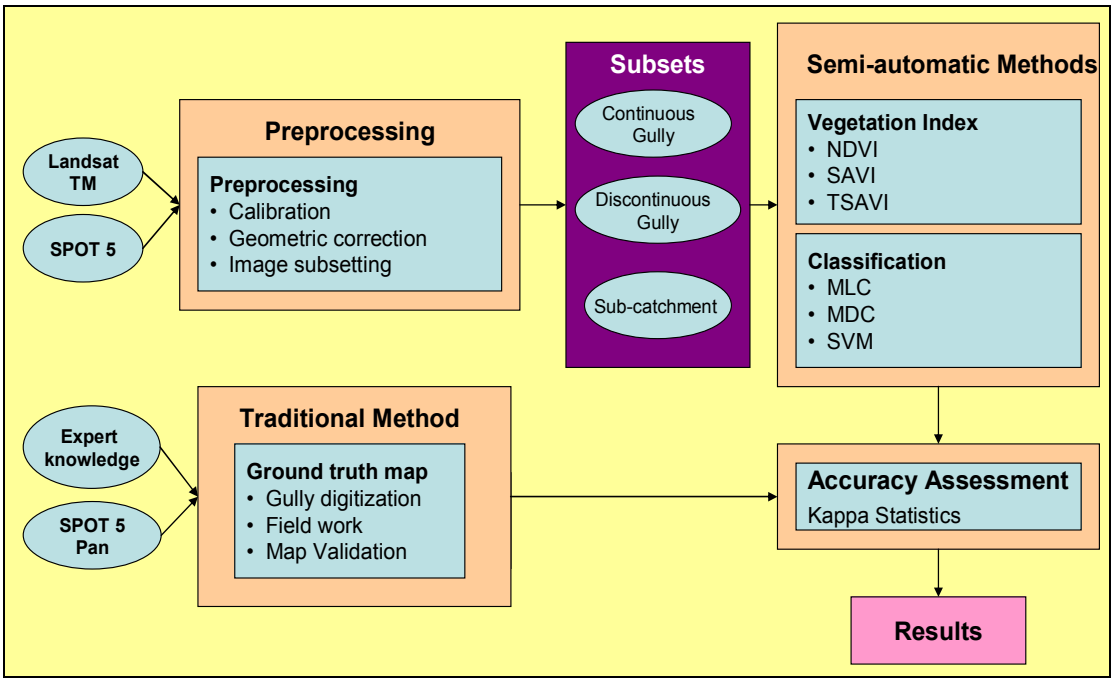

Figure 4-1 Methodology flow diagram

4.1 Preprocessing

Image preprocessing is necessary before information is extracted from the image because it ensures that the image is as close to the true radiant energy and spatial characteristics at the time of data

collection. The preprocesses carried out in this study were radiometric calibration, atmospheric correction, geometric correction and Image subsetting

4.1.1 Calibration

A typical radiometric calibration involves several different steps. First the sensor's digital numbers (DN) need to be converted to at-sensor radiances (sensor calibration). Second, the at-sensor radiance values need to be transformed to radiances at the earth's surface and this stage involves incorporation of the atmospheric condition at the time of image capture (atmospheric correction). The last stage of calibration is done by correction for slope and aspect, atmospheric path length variation due to topographic relief, solar spectral irradiance, solar path atmospheric transmittance, and down-scattered skylight radiance (Schowengerdt, 2007). Not all of the procedures were necessary for this particular study area because the terrain is not complex (Song *et al.*, 2001).

4.1.1.1.1 Sensor Calibration

The sensor calibration procedure involves converting the DN values to radiances using calibration coefficients called "gain" and "offset". The output is units of radiance-per-DN. It is often assumed that the gain and offset are constant throughout the sensor's life; hence the Landsat TM image was processed to reflectance using a Landsat TM model in ERDAS. This procedure reduced between scene variability by accounting for sensor gains, offsets, solar irradiance, and solar zenith angle (Schowengerdt, 2007). It also removed the thermal band 6 in Landsat TM, which was not necessary for this study. SPOT 5 was kept at DN values because only a small subset of the image was used for this study; thus between-scene variability would be minor.

4.1.1.1.2 Atmospheric Correction

Atmospheric correction is the removal of effects of the passage of radiation through the atmosphere. The amount of atmospheric correction depends upon the wavelength of the bands and the atmospheric conditions (Sabins, 1996). For both Landsat TM and SPOT, scattering is the dominant atmospheric effect (Song et al., 2001) with band 1 of each image having the highest component of scattered light and band 7 of Landsat TM having the least.

The Dark Pixel Subtraction technique was used to remove the additive effect of scattered light because it is one of the oldest, simplest and most widely used procedures for adjusting digital remote sensing data for effects of atmospheric scattering (Song *et al.,* 2001). However, it is recognized that

this is not a complete atmospheric correction. Dark pixel subtraction assumes that the dark object, water in the case of this study domain, has uniformly zero radiance for all bands, and that any non-zero measured radiance must be due to the atmospheric scattering into the objects pixels (Song et al., 2001). In ENVI 4.3 the dark pixel reflectance values were subtracted from every pixel in the corresponding band for both TM and SPOT.

4.1.2 Geometric Correction

The scanning of remote sensing images introduces a number of geometric distortions that are classified as systematic and nonsystematic distortions (Sabins, 1996). Nonsystematic distortions are caused by variations in the spacecraft such as attitude, velocity, and altitude. Systematic distortions are distortions whose effects are constant and are corrected before the data are distributed. To remove the nonsystematic distortions a geometric correction was performed by conducting an image to map registration of the Landsat TM and SPOT 5 images to the national georeferenced Topographic Map of South Africa. A minimum of 20 ground control points were collected and the average root mean square (RMS) error of 0.85 pixels was achieved. Ideally one would want an RMS error less than 1 and as close to 0 as possible. These steps were necessary to ensure that any additional spatial data would overlap exactly.

4.1.3 Image Subsetting

Image subsetting reduces the processing time and allows for behavior trends within techniques. Three different subsets were obtained: a sub-cathment area of 2000km², and two sample areas, each approximately 150km² that were characteristic of the study region. One sample included a continuous gully system and the other included discontinuous gullies (Figure 4-2). The large sub-catchment subset was selected based on the area of overlapped by two Landsat scenes, a 1991 and 2005 (Figure, 4.2). This allowed for change detection studies in the area using the techniques presented. The smaller continuous gully subset (150 km² window) consisted of a large representative connected gully system. The smaller discontinuous gully subset (150 km² window) was chosen in an area that had representative discontinuous gullies (small not connected eroded areas). Both Landsat TM and SPOT 5 Pan were spatially clipped to the three subset areas. Figure 4-2 displays the sub-catchment subset location within the Buffalo River sub-catchment area (left) and the locations of the continuous (A) and discontinuous (B) gully subsets, within a preprocessed true colour Landsat TM image that was clipped to the sub-catchment subset.

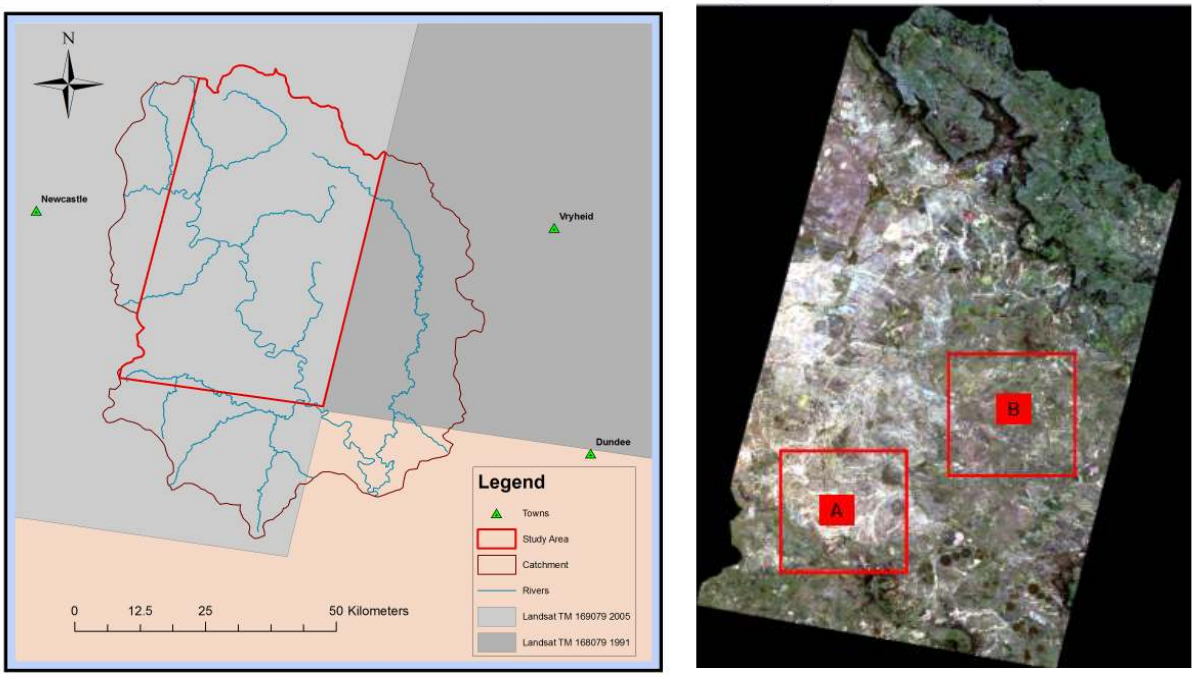

Figure 4-2 Left: Map illustrating the sub-catchment level of the study area and the Landsat TM track/row. Right: The locations of the chosen subsets within the selected preprocessed Landsat TM sub-catchment subset. Label 'A' is the continuous gully system, and label 'B' is the discontinuous gullies

4.2 Mapping Methodology

The objective of this study was to compare semi-automatically created gully maps with maps created using traditional gully mapping methods. Thus a gully map created traditionally is assumed to be a 'ground truth' map i.e. everything in the map is assumed to be true. Ground truth based comparison is a form of accuracy assessment where the whole image is used in the accuracy assessment rather than randomly selected pixels (see, section 2.3.4). Ground truth accuracy assessment was chosen over a ground truth point approach because it: avoided issues in choosing the sampling design used to select reference data; it reflected the 'true' class proportions for gully and no-gullied areas; and the approach enabled identification of misclassified pixels (Congalton, 1991).

4.2.1 Traditional Methods

The specific objectives:

- To determine the location of gullies in the catchment using expert knowledge
- To create a gully erosion map that could be used as a "ground truth" basis for assessing the semi-automatically created gully erosion maps.

A commonly accepted practice for assessing products derived from coarse resolution data is the use of a higher resolution satellite data as a reference (Cihlar *et al.,* 2003). Ground truth maps were created using the traditional gully mapping methods mentioned in section 2.3.4, in the SPOT 5 panchromatic image sub-catchment subset. The procedures used to create the assumed "ground truth" gully map are summarized in Figure 4.3.

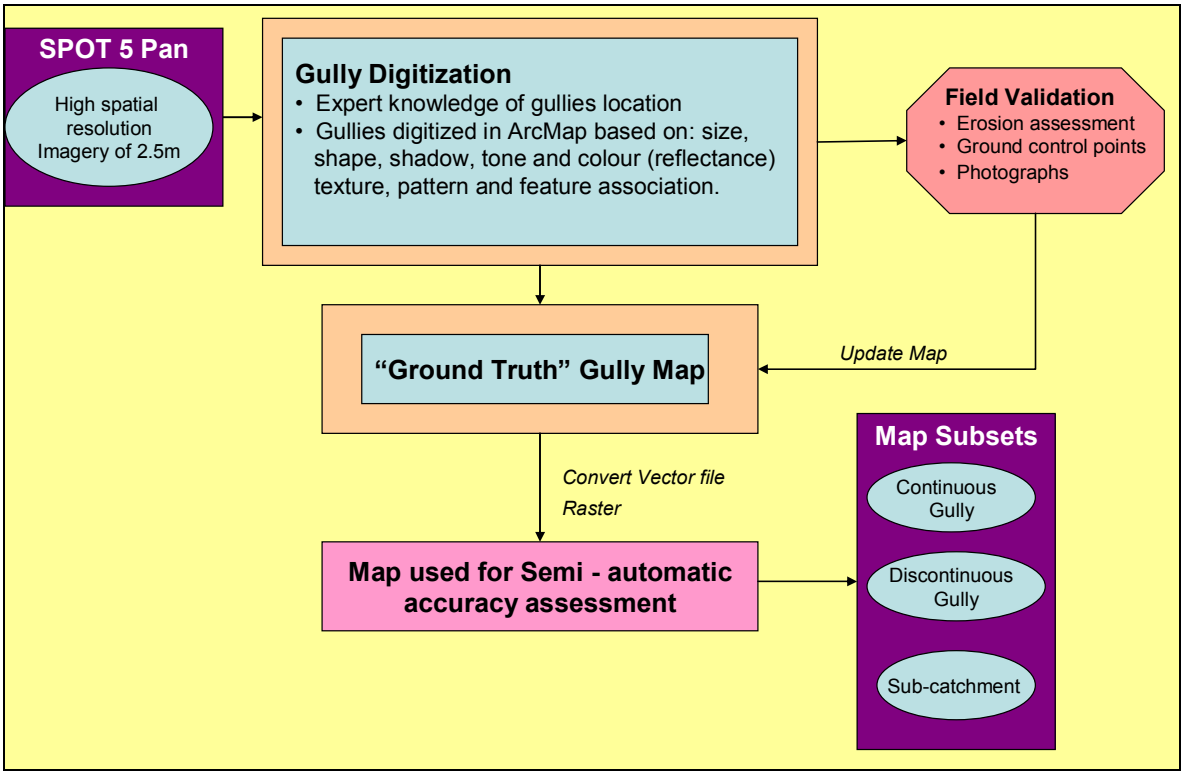

Figure 4-3 Flow diagram of the "Ground Truth" gully maps

Creating the ground truth map involved manually digitizing individual gullies in the SPOT 5 Pan sub-catchment subset using ArcMap. This was carried out by gully mapping experts at the ARC. Ground truthing was necessary to validate the digitized gully map and involved confirming that the locations of the gullies mapped were actually present on the ground. This was conducted during a one week field study that involved: i) documenting the erosion status (sheet, rill, gully), vegetation cover (%), land use type, (ii) visual assessment of the erosion extent which was limited to visibility from the road because most gully areas were on private property, (iii) collection of photographs, and (iv) collection of ground control points (GCP) using a global positioning system (GPS). Previously collected soil sample data, in the form of a shape file (point), offered additional information on the erosion assessment. The GCPs and erosion assessment information were imported into ArcMap and overlaid with the digitized gully map. Erosion experts corrected the errors of omission or commission by re-digitizing or deleting features in the gully map. Appendix D displays the location of the expert mapped gullies, soil samples, and ground truth sites and illustrates the location of a few gully photographs taken during field research.

Once the corrections were made in the ground truth gully map the created vector file was converted to a binary raster representing two classes: gullies and non gully classes. This is essentially a gully map which was then subsetted to the selected discontinuous and continuous subsets. Figure 4.5 displays the gully distribution within the discontinuous (A) and continuous (B) gully subsets. A1 and B1 are SPOT 5 true colour composites of the area with expert digitized gullies overlaid in red; and A2 and B2 are the ground truth maps created using traditional mapping methods with the white and black representing gullies and non gullied areas respectively.

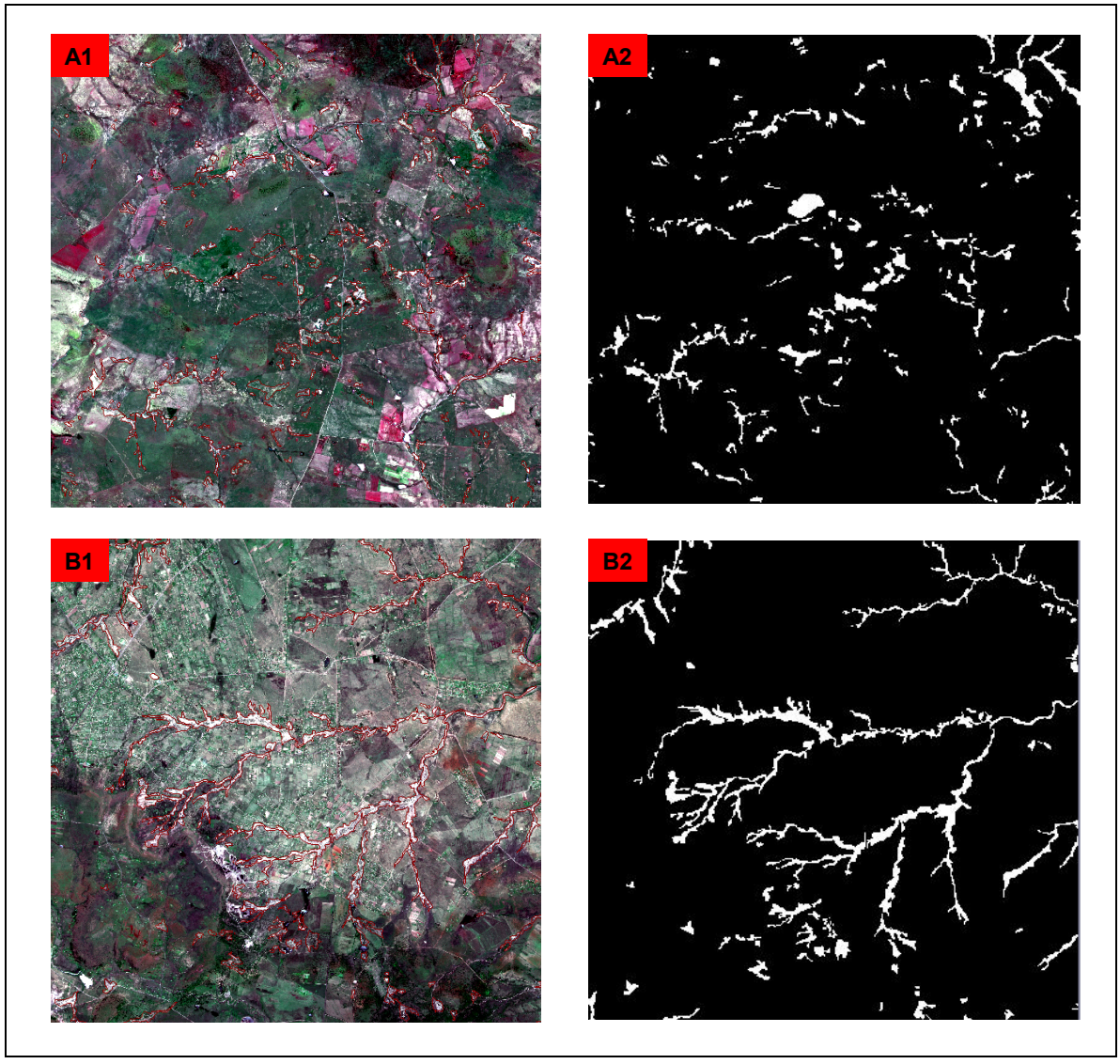

Figure 4-4 A1 and B1 are the digitized gullies, in red solid line, on a true colour composite of SPOT 5. A2 and B2 are the gully maps created for the discontinuous and continuous subsets respectively.

4.2.2 Semi-automatic Methods

The following section discusses the semi-automatic techniques used to create a gully map. Each of the output maps created were enhanced using a majority analysis. This analysis involved using a 3*3 majority filter where the center pixel in the filter was replaced with the class present in the most of the surrounding pixels. This process removes spurious pixels that cause noise ('salt and pepper' effect) and in some cases it can increase the accuracy of the map (Jensen, 2005). All semi-automatically created gully maps assessed based on the ground truth maps created in section 4.2.1 using the accuracy assessment discussed in section 2.3.4.

4.2.2.1 Mapping Gullies from Vegetation Indices

The specific objectives of this section are:

- To determine the input parameters for TSAVI.
- To determine the best threshold range for gully mapping using NDVI, SAVI and TSAVI.
- To determine the classification accuracy, using the kappa statistic, of the gully maps produced from NDVI, SAVI and TSAVI in the continuous and discontinuous and sub-catchment subsets.

4.2.2.1.1 Vegetation Index Implementation

NDVI, SAVI and TSAVI were applied to the continuous and discontinuous subsets defined in section 4.1.2.3. NDVI was calculated by inserting the NIR and Red bands in the NDVI model which was already built in ENVI 4.3. The SAVI formula (equation 2-3) was translated into a band math equation (equation 4-1) in ENVI 4.3. Since over 70% of the study area is made up of Income Sandy Grasslands, SAVI L parameter was chosen to be 0.5 because it is the most ideal value for areas with such sparse vegetation type (Baret and Guyot, 1991; Huete, 1988; Schowengerdt, 2007):

$$(((b4-b3)/(b4+b3+0.5))*(1+0.5)) \quad (4\text{-}1)$$

where b3 is the red reflectance band and b4 the NIR band.

For calculation of TSAVI, a manual approach was used to obtain the soil line parameters for the equation. This involved pseudo-randomly selecting bare soil pixels (200) in the subset; plotting the pixels in a NIR-Red spectral space and manually calculating the best fitted line. Figure 4.6 below is a graph of the NIR-Red reflectance for the selected bare soil pixels. The soil line was drawn in manually as a straight solid line arranged along the lower edge of the points in this feature space.

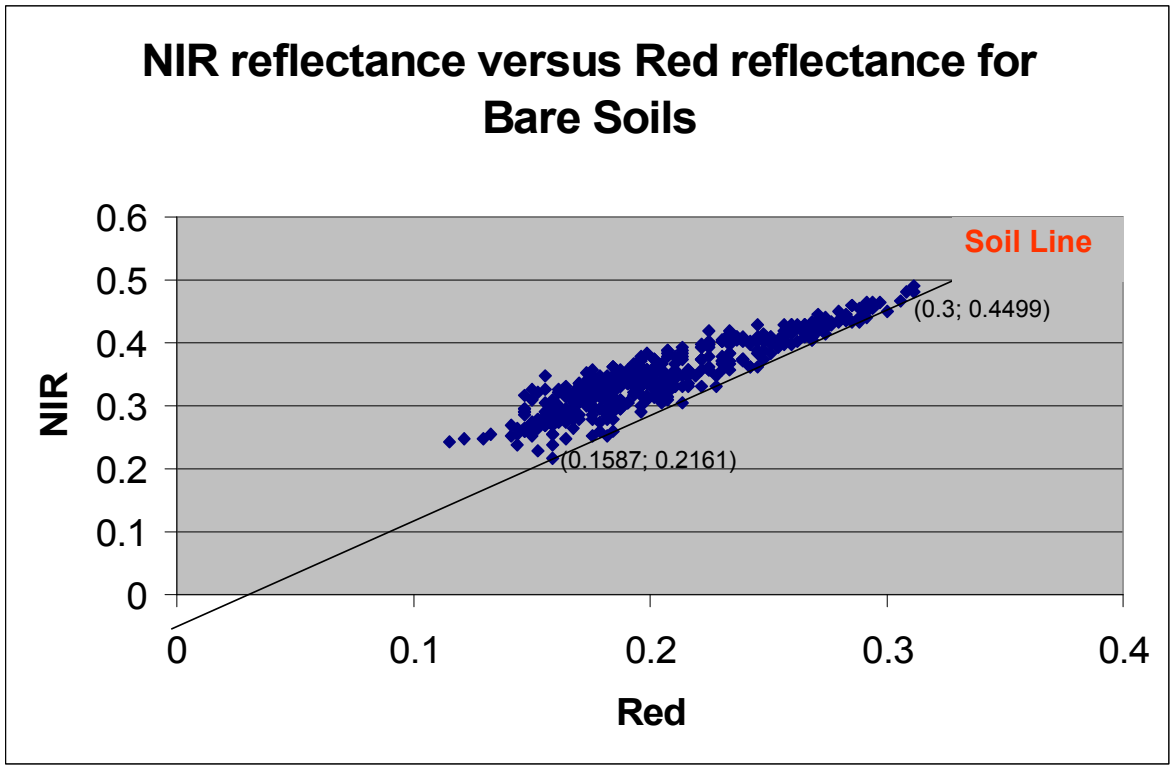

Figure 4-5 A NIR/Red 2-D scatter plot of 200 bare soil pixels. The straight solid line corresponds to the soil line for this particular data set.

The calculated gradient for the soil line equation (equation 2-3) was **1.6545** and the y-intercept was estimated to be **-0.5,** which completed the final soil line equation for TSAVI (equation 4-2). The value of X in the TSAVI equation (equation 2-5) was set to 0.08 which is a typical value set for sparse vegetation (Baret and Guyot, 1991). These values were then inserted into the band math equation as seen in equation 4-3.

$$NIR=1.655R-0.5 \quad (4\text{-}2)$$

$$\text{TSAVI} = \frac{((1.655 * (b4 - (1.655 * \text{float}(b3)) - (-0.5)))}{((1.655 * \text{float}(b4)) + b3 - (1.655 * (-0.5)) + (0.08 * (1 + (1.655 * 1.655)))))} \quad \textbf{(4-3)}$$

Where: B3=Red,

B4=NIR

The calculated VI values were confirmed by selecting a pixel within the subsets of the original Landsat TM image and identifying its corresponding reflectance in the red and NIR bands and manually calculating the expected NDVI, SAVI and TSAVI.

4.2.2.1.2 Threshold Selection

Threshold selection was done in the continuous gully subset because it best represented the gully erosion in the study area. The spatial profiler tool in ENVI 4.3 was used to visually select a vegetation index lower and upper threshold within which pixels values were assigned to soil that is assumed to be gully erosion. This was done by drawing a transect across ten different locations on the continuous gully and visually identifying the corresponding value, for each VI. This interactive process helped identify a range of candidate values that could be used as thresholds to map gullies. Similar transects were visually evaluated to estimate VI thresholds to test for gully mapping. Once thresholds were identified for each vegetation index in each subset, they were used to create a gully mask using a similar technique as applied by Cyr *et. al* (1995). This mask was then transformed into a gully map by applying the ISODATA unsupervised classification with a limit of two classes labeled gullied area and non gullied area. It is important to note that this classification was only used to label the already created mask, no analysis was run. This process is essentially developing classification rules to map gullies, for example an associated rule for classifying gullied areas using NDVI would look similar to the following rule:

If NDVI $\geq$0.4 then the pixel belongs to gullied area

If NDVI $\leq$ 0.4 then the pixel belongs to non gullied area

Threshold selection was an optimization process which was run several times, using random values for each subset, until a maximum accuracy was achieved (maximum kappa statistic) for each vegetation index. It was assumed that approximately 70% of the gullies in the study area were continuous gullies, thus the threshold that produced the maximum kappa statistic for the continuous gully subset was applied to the sub-catchment subset and tested in the discontinuous gully subset.

4.2.2.1.3 Summary

Figure 4-7 displays a summary of the procedures used to achieve the above objectives. First the parameters and bands required for each VI were identified then applied to the continuous and discontinuous subsets and formulas were verified in excel. Different lower and upper thresholds were selected and applied to each VI. These thresholds were tested for their accuracy in mapping the two different gully types (accuracy assessment). The VI threshold which provided the maximum accuracy for the continuous gully subset was applied to the sub-catchment subset. Each vegetation index gully map produced was assessed based on their kappa statistic.

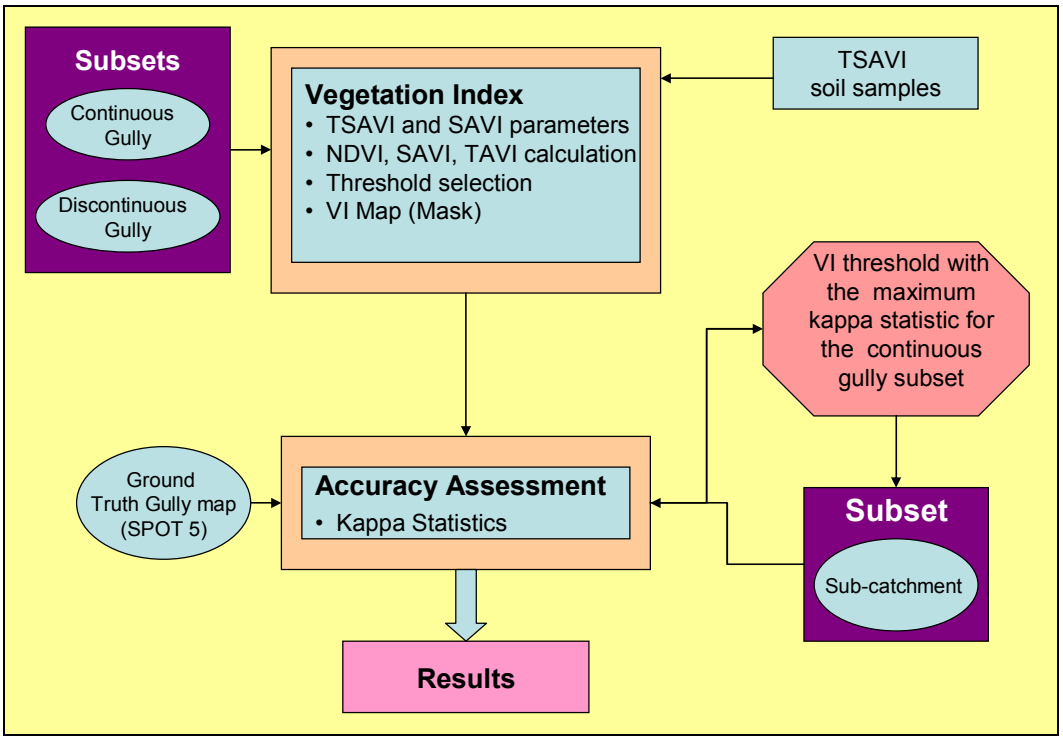

Figure 4-6 Flow diagram of Vegetation Index gully maps

4.2.2.2 Gully Mapping from Multi-spectral Classification Techniques

MLC, MDC and SVM were the three classifiers used in this section. For comparison purposes it is difficult to account for all the variables (band selection, training data size, classifier parameters) required by these classifiers. However it is important that each classifier performs to the best of their ability. Since it is assumed that over 70% of the gully erosion type is continuous gullies, different classification variables were tested on the continuous gully subset. Parameters that produced the

highest kappa statistic were selected as input parameters for the sub-catchment subset. The objective of this section is:

- To test the need for image transformation for MLC, MDC and SVM for mapping gullies.
- To test the effect in classification accuracy with different training data sizes
- To determine the SVM parameters for gully mapping using Landsat TM.
- To determine the classification accuracy, using the kappa statistic, of the gully maps produced from MLC, MDC, and SVM in the continuous and discontinuous and sub-catchment subsets.

4.2.2.2.1 Principal Component Analysis

A principal component analysis (PCA) was run to ensure that the maximum accuracy for mapping gullies was achieved with conventional classification algorithms. PCA is a process that compresses the information content from a number of bands into a few principal components which are uncorrelated and easier to interpret (Jensen, 2005). It has proven to increase classification accuracies of conventional classification algorithms (Wu and Linders, 2000).

PCA was run on the Landsat TM discontinuous and continuous subset and two tests were run using the first 5 PC bands (Test 3) and first 4 PC bands (Test 4). The last principal components were disregarded because they contained most of the noise in the image. This aim was to assess whether the classification accuracies improved when applied to an uncorrelated image with less noise (PCA image) rather than the original preprocessed Landsat TM image which is assumed to carry more noise.

4.2.2.2.2 Training

Although it is important to consider the classifier when choosing the training data, for comparative purposes, the same training data was used for each classifier. Two classes of training data were used in this study: gully and non gully. The number of pixels chosen for each class was based on Jensen (2005) general rule that states "*the number of pixels used for the training data from n bands should be >10n.*" The total number of Landsat TM bands used were six, thus the number of training pixels selected was >60.

Training was conducted in continuous and discontinuous gully subsets and involved an on-screen selection of polygonal training data for the gully and non gully classes. It was assumed that a person with little expert knowledge would be collecting the training data, thus only a small proportion of gully training pixels (1000) were selected within the expert digitized gully vector file created in section 4.3. The non gully training data were selected as areas outside of the expert digitized gullies (section 4.3) and a variety of land cover types were selected (buildings, commercial and subsistence agricultural fields, forest, roads and water bodies). To test if additional training data was necessary two different non gully training data sizes were tested for the discontinuous and continuous gully subsets. The gully training data size was kept constant because it was a small class. Table 4.1 and 4-2 displays the large (Test 1) and small (Test 2) training data sizes for each class in the selected subset.

Table 4-1 Test 1: Training data sizes with a large non gully class size

Classes	Discontinuous gully	Continuous gully
Gully class	1000	1500
Non gully class	26500	18500

Table 4-2 Test 2: Training data sizes with a small non gully class size

Classes	Discontinuous gully	Continuous gully
Gully class	1000	1500
Non gully class	2500	2500

4.2.2.2.3 Classification Implementation

Implementation of each of the classification algorithms was conducted in ENVI 4.3. For the MLC and MDC the only parameter required was the probability threshold. No threshold was used because this would have created a null class in the classification and it was important that all the features were classified. Implementation of the SVM was more complex than MLC and MDC because the performance of the classifier depended on (i) the choice of kernel used for mapping the data and its

parameters, and (ii) the choice of user-defined parameters C (which controls the penalty associated with misclassifications) (Boyd *et al.,* 2006).

Selecting the most accurate parameters for the SVM was critical in this study because inappropriately selected parameters could produce very low accuracies and thus inadequate gully mapping results. Four main kernels are discussed in the literature- linear, polynomial, radial basis function (RBF), sigmoid- however it is difficult to distinguish which one gives the best generalization for mapping gullies. Furthermore there is little guidance in literature on the choice of the kernel and the ideal parameters to use (Mantero and Moser, 2005; Pal and Mather, 2005). Therefore in this study the four different kernels were tested on the continuous gully because it was assumed to represent most of the sub-catchment area and it was small enough to reduce processing time. The kernel that produced the highest kappa statistic, with default values, was then used to test a range of values for parameters C (varying from 1-5000) and γ (0-60). The parameters that produced the highest accuracy for the continuous gully subset were then used to classify the discontinuous and sub-catchment gully subset.

4.2.2.3 Summary of Classification Algorithm Tests

The classification gully mapping procedures involved in this study required five main tests which are listed below and illustrated in Figure 4-8. Test 1-6 were conducted using both the discontinuous gully and the continuous gully subset whereas the SVM parameter tests were only conducted on the latter.

1. Training data test
    - Large training data size (Test 1)
    - Small training data size (Test 2)
2. SVM Parameter tests
    - kernel selection
    - C parameter
    - γ parameters
3. Principal component analysis
    - Principal components 1-4 (Test 3)
    - Principal components 1-5 (Test 4)
4. Sub-catchment subset (test for regionalization)
    - Apply classification variables that produced the maximum kappa statistic for continuous gully subset, to the sub-catchment subset (Test 5)

5. SPOT 5 test

- Test the classification algorithms on higher spatial resolution SPOT 5 imagery (Test 6)

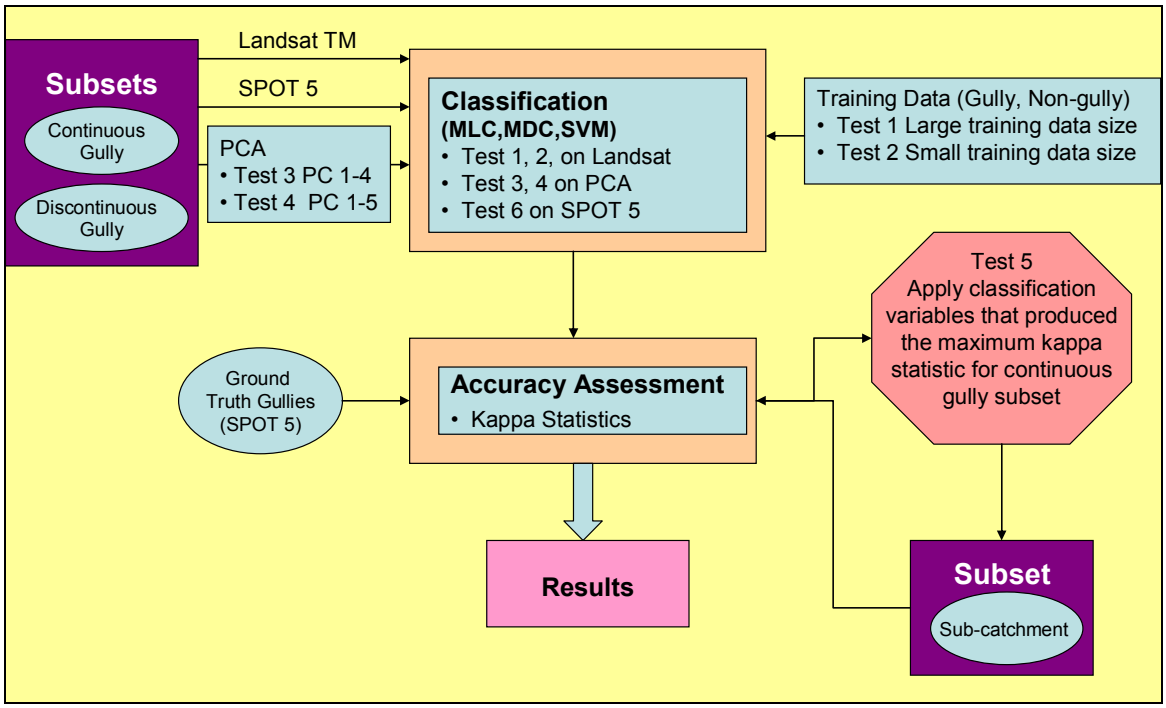

Figure 4-7 Flow diagram of classification gully maps

Chapter 5
Results

5.1 Vegetation Indices

The spatial profile tool in ENVI 4.3 helped compare the range of values for each vegetation index (Figure 5-1). Figure 5-1 displays graphs with extracted NDVI, SAVI and TSAVI pixel values (y-axis) of different transects (x-axis) crossing over selected land cover types. The yellow arrow indicates the location of the particular land cover type on the transect. The general range of the VIs was between +1 to 0 with values close to zero being bare soil and values close to one representing very healthy vegetation. There were some cases of negative values for NDVI and SAVI which were located in areas of deep water; however TSAVI had no negative values. The trend for each VI was slightly similar, TSAVI produced generally higher values, except in healthy vegetated areas (agriculture and wetlands) where NDVI was higher, then NDVI ranked second for other land cover types, followed by SAVI which produced much lower values. Data from vegetated areas, for example agriculture, wetlands and grasslands, yielded high VI values due to high near-infrared and low red or visible reflectance (Jensen, 2005). Water produced low VI values (NDVI=0.1, SAVI=0.08 and TSAVI=0.45) because it has a higher reflectance in the red or visible bands than the NIR (top right of Figure 5-1). SAVI results were similar to NDVI, except the values were slightly lower. For NDVI and SAVI bare soil areas coincided with low positive values close to zero because bare soil generally has similar reflectance in the NIR and red or visible bands (Jensen, 2005). The bare soil values were similar to that of gullies (Figure 5-3 and Figure 5-4). TSAVI values were also low for bare soil compared to other land cover types but values were close to 0.5 rather than zero.

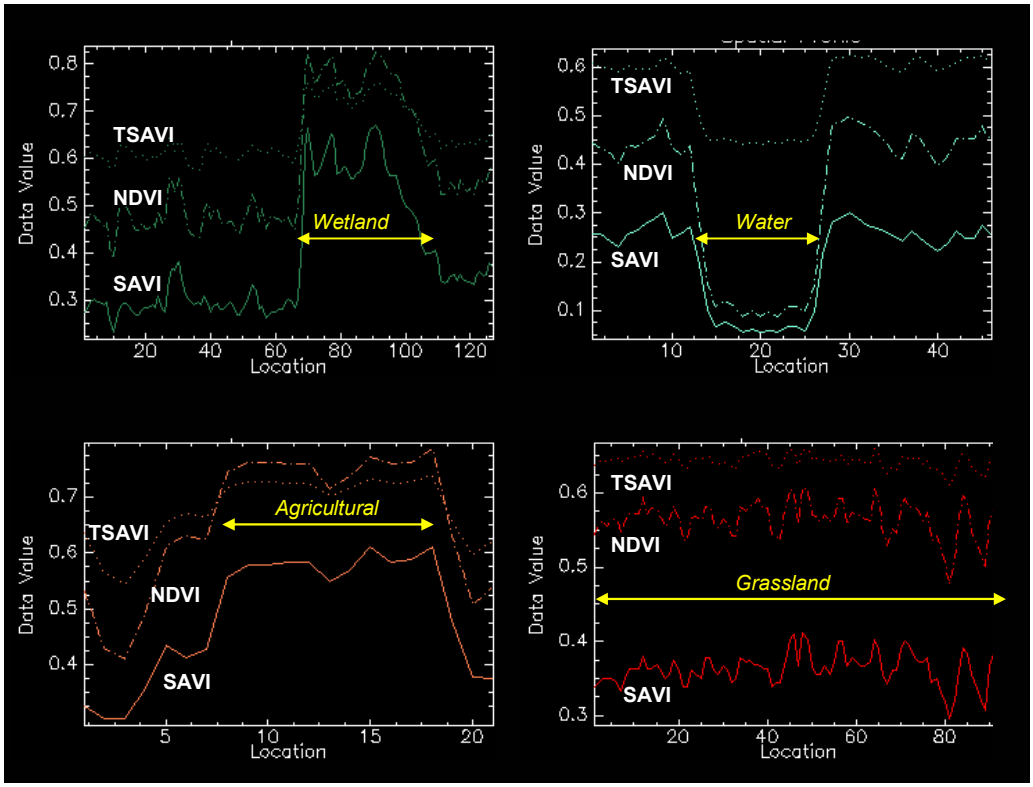

Figure 5-1 Spatial profile of NDVI, SAVI and TSAVI values across different land cover types in the study area

5.1.1 Vegetation Index Threshold

More specific to this study was the range of NDVI, SAVI and TSAVI values within a gully system. Figure 5-2 displays a Landsat TM false colour composite of the continuous gully subset and the three corresponding calculated vegetation index results.

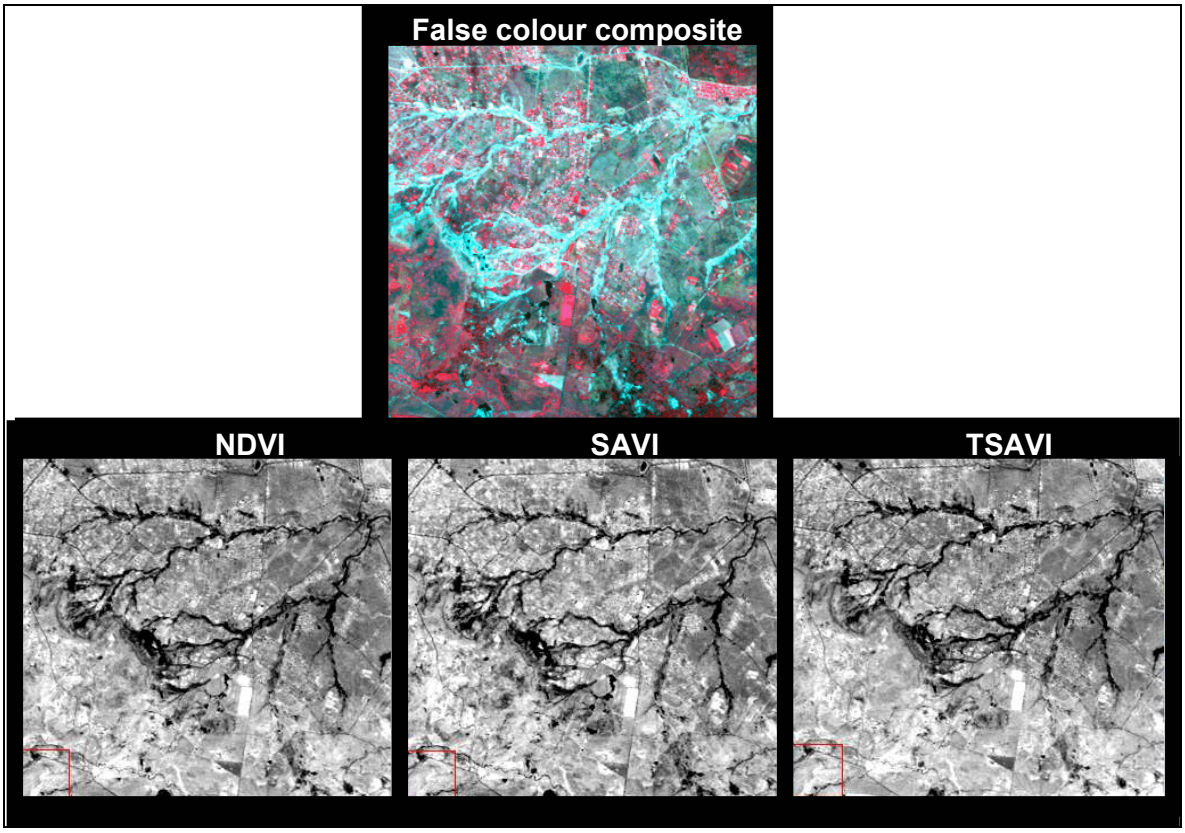

Figure 5-2Top image is a false colour composite of the continuous gully subset. Bottom (left to right) are the NDVI, SAVI and TSAVI results for the continuous gully subset.

Figure 5-3 is a gully with a transect (A-B-C) across its channel (B), displayed is a false colour image made up of TSAVI, NDVI and SAVI entered into the red, green and blue colour guns, respectively. The corresponding graph illustrates the VI values (y-axis) of extracted pixel along the transect (A-B-C), that passes from an area of non gully (A) to gully (B) to non gully (C) (solid line A-C in gully image).

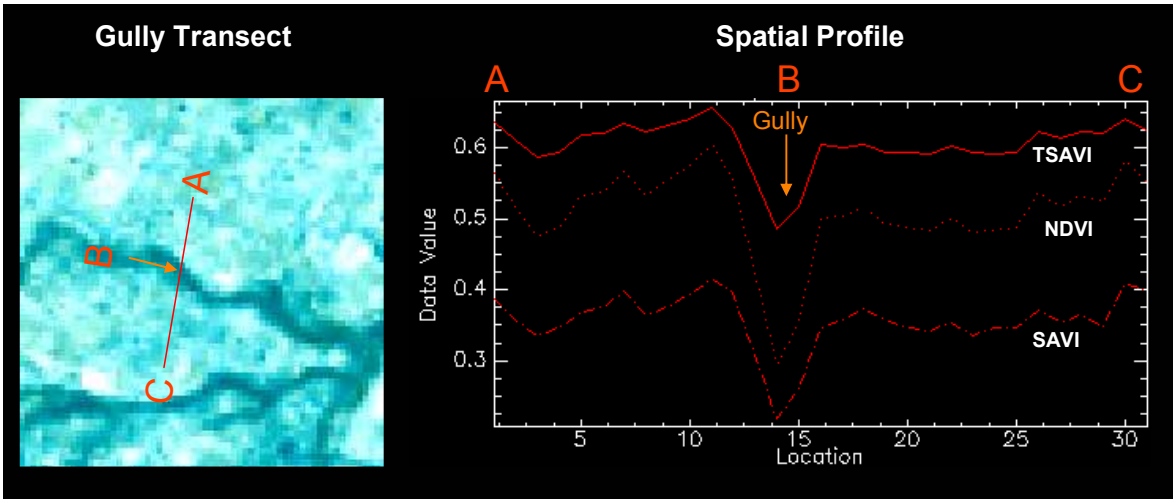

Figure 5-3 Spatial profile of NDVI, SAVI, TSAVI values across a gully

Figure 5-4 displays five transect graphs extracted along a continuous gully channel, using the same method in Figure 5-3. It can be observed that the VI values at the base of the gully are generally low for NDVI, SAVI and TSAVI, compared to no gully areas. The NDVI, SAVI, TSAVI values for the base of the gully (B) are approximately 0.3, 0.27 and 0.5 respectively. These low VI values could be attributed to the moisture conditions of the gully bottom (Vrieling *et al.,* 2008). The observed VI values have a similar trend across the gully channel, with NDVI values generally range between SAVI and TSAVI values. Mapping of gullies using Landsat TM seems to be feasible following the comparison of these VI values with surrounding areas.

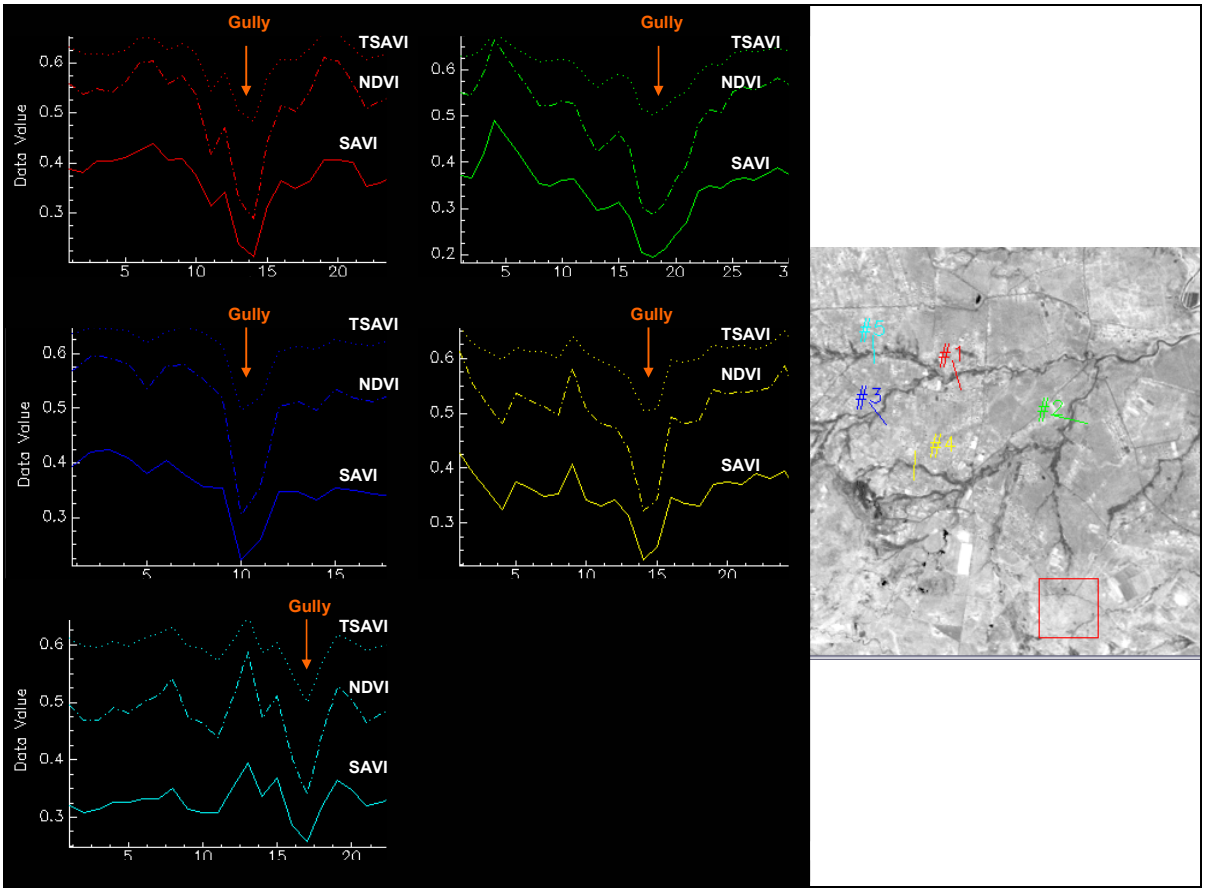

Figure 5-4 Spatial profiles of VI values across transects along a continuous gully

The selected lower threshold for gully mapping using NDVI and SAVI was zero and for TSAVI 0.41. Table 5-1 lists the top five kappa statistics achieved with the tested upper VI thresholds for the continuous gully subset. Figure 5-5 displays the kappa statistics trend for each tested VI threshold. The selected upper thresholds used to represent each VI were the ones that produced the maximum kappa statistic (bold values in Table 5-1). The chosen thresholds used to classify the image can be explained using the following rules:

If $0 \leq NDVI \leq 0.40$ then pixel belongs to gullies, else non gully

If $0 \leq SAVI \leq 0.274$ then pixel belongs to gullies, else non gully

If $0.41 \leq TSAVI \leq 0.55$ then pixel belongs to gullies, else non gully

Table 5-1 Tested upper VI thresholds that produced the highest kappa statistic for gully mapping in the continuous gully subset

Tested Upper Threshold	The top five kappa statistics		
	0 ≤ NDVI	0 ≤ SAVI	0.41 ≤ TSAVI
0.27		0.4903	
0.273		0.4949	
0.274		**0.4961**	
0.275		0.4958	
0.280		0.4928	
0.380	0.5330		
0.390	0.5474		
0.400	**0.5555**		
0.405	0.5541		
0.410	0.5534		
0.530			0.4485
0.540			0.5373
0.550			**0.5580**
0.555			0.5569
0.560			0.5492

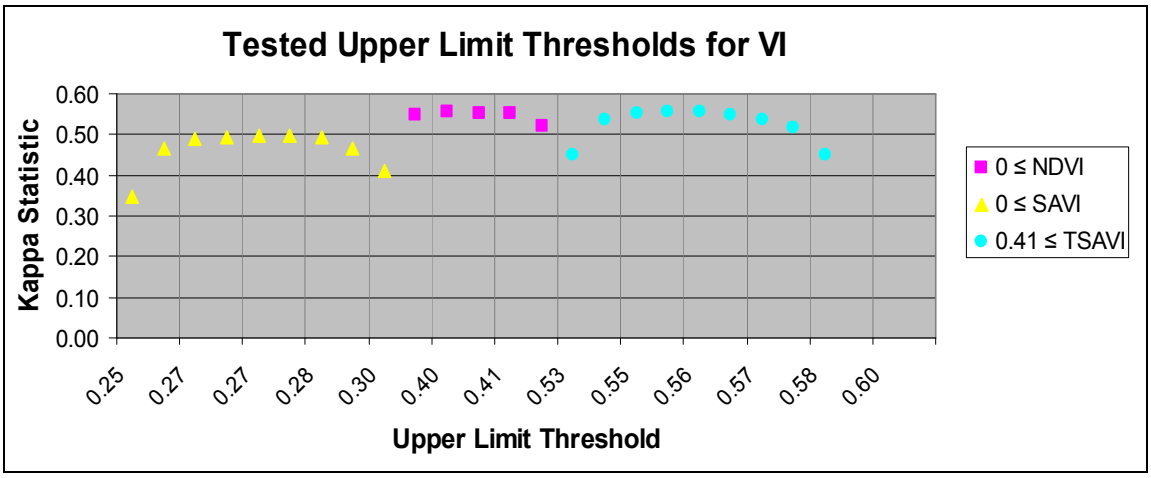

Figure 5-5 A graph of the tested upper thresholds for each vegetation index

5.1.2 Gully Maps from Vegetation Indices

Figure 5-6 displays the VI gully maps produced when the selected threshold values were applied to the continuous gully subset. TSAVI performed the best with an accuracy of 0.5580 followed by NDVI, with an accuracy of 0.555, and last SAVI, with an accuracy of 0.496.

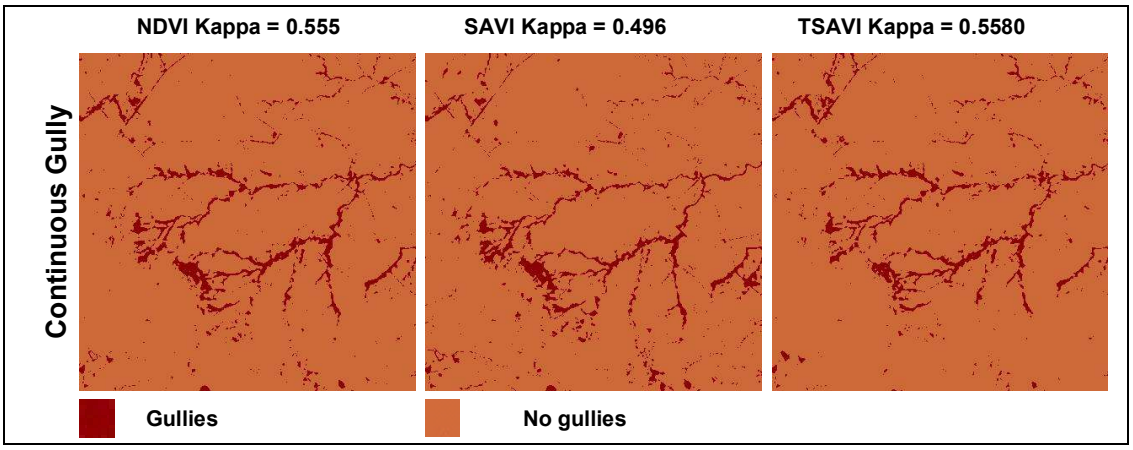

Figure 5-6 VI continuous gully map with kappa statistic results

Figure 5-7 displays the VI gully maps produced when the selected threshold values were applied to the discontinuous gully subset. The results achieved were very low compared to the continuous gully map. SAVI had the highest kappa statistic of 0.2216, followed by NDVI with an accuracy of 0.2088 and TSAVI with accuracy of 0.1793.

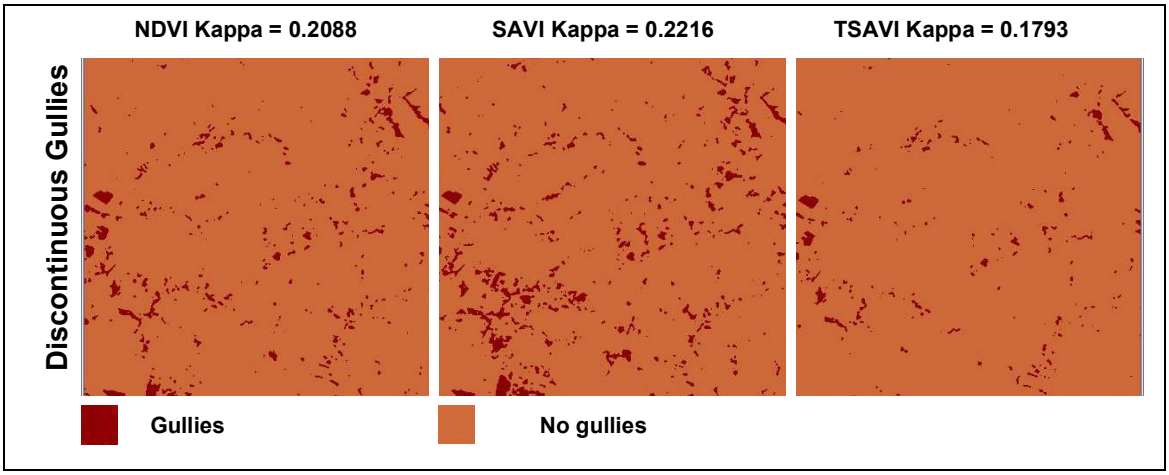

Figure 5-7 VI discontinuous gully map with VI kappa statistic results

Table 5-2 lists the VI accuracies produced when the selected threshold values were applied to the sub-catchment gully subset. NDVI had the highest kappa statistic of, 0.3616, followed by TSAVI with 0.3337 and SAVI with 0.2997. The maps produced were not very clear for representation in this document; however results are discussed in terms of the distribution of error in section 5.1.5.1

Table 5-2 VI kappa statistic results for the Sub-catchment gully map

VI	Sub-catchment
NDVI	**0.3616**
SAVI	0.2997
TSAVI	0.3337

5.1.3 Gully Map Accuracy Assessment from Vegetation Indices

Figure 5-8 and Table 5-3 is a summary of the kappa statistic results for the three VI subset maps. The continuous gully subset was mapped with the highest kappa statistic across all the vegetation indices ranging around 0.5, followed by the sub-catchment scale around 0.3 and the discontinuous gullies around 0.2. All the indices performed better at identifying the continuous gully system, than their performance in the other two subsets. TSAVI produced the most accurate continuous gully map (0.558), SAVI produced the most accurate discontinuous gully map (0.2216) and NDVI ranked first at mapping gullies in the sub-catchment subset (0.3616).

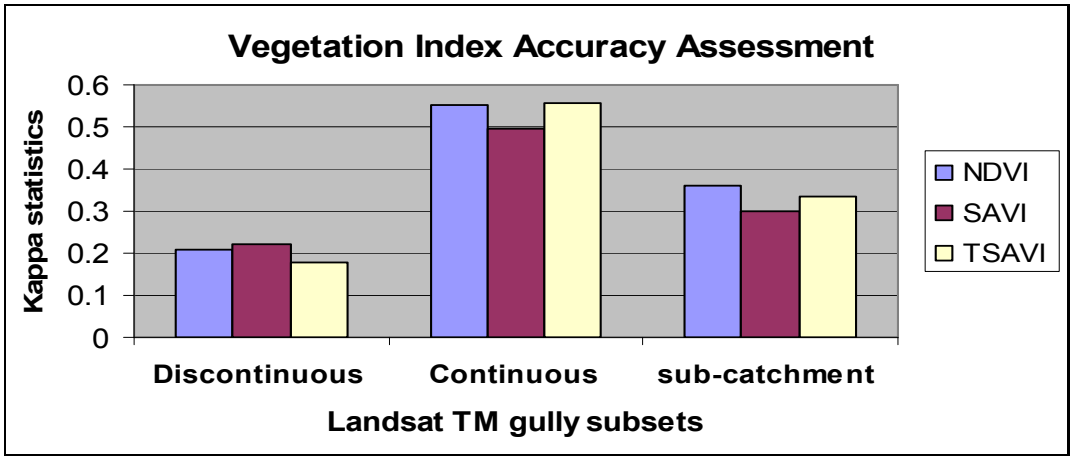

Figure 5-8 Kappa statistics graph comparing the VI results for each gully subset

Table 5-3 VI kappa statistic results for gully mapping in each subset

VI	Discontinuous gully	Continuous gully	sub-catchment
NDVI	0.2088	0.5508	**0.3616**
SAVI	**0.2216**	0.4961	0.2997
TSAVI	0.1793	**0.558**	0.3337

5.1.4 Discussion

Although individual studies have compared the use of VI based on their effectiveness to estimate and detect water erosion (Baugh and Groeneveld, 2006; Cyr, *et al.,* 1995); no comprehensive study has attempted to compare the accuracy of VI for mapping gullies. Cyr *et al.* (1995) performed a comparative study of vegetation indices derived from the ground and from satellite images, to find the best index for estimating soil protection against water erosion. Whereas Baugh and Groeneveld, (2006) compared fourteen VI for mapping erosion.

With the potential of the soil line indices (SAVI and TSAVI) being better at identifying vegetation, it is disappointing that these indices did not out-perform NDVI for gully mapping because most of the vegetation would be identified and masked out; NDVI had the highest accuracy over the sub-catchment subset at 0.3616 It is possible that NDVI was more accurate in the sub-catchment subset because the soil line for the whole area was not that much different than NDVI assumed soil line

(Lawrence and Ripple, 1998). The TSAVI and SAVI soil line parameters were probably not exemplary for the sub-catchment subset soil line because they were obtained in the continuous gully subset. For TSAVI, soil line parameters may have been obtained from the same soil type. Therefore when the index was applied to the sub-catchment and discontinuous gully subsets, a majority of the soils may have been different. Although SAVI parameter L which was assumed at 0.5 is said to be most ideal for minimizing soil variations in sparse vegetation (Huete, 1988), it may not have been the ideal parameter value for the type of vegetation in the study area. It is also possible that most of the gullies in the study region had vegetation within them and if this is the case the soil line indices performed successfully, at identifying vegetation, to the extent that the vegetation within the gullies was removed resulting in a lower kappa statistic because of errors of commission. This highlights the importance of ancillary data, such as soil and rainfall data, when using remote sensing to draw conclusions on areas where one has little knowledge. Although substantial success has been achieved through the use of soil adjusted vegetation indices for the prediction of vegetation variables, this study proves that simple NDVI achieves equivalent or better results without much additional effort for mapping gullies.

Although TSAVI performed the best in the continuous gully subset, with an accuracy of 0.5580 it is recommended that NDVI still be selected, because of the computational cost of the TSAVI soil line parameters. TSAVI performed well in the continuous gully subset because the soil line parameters were modeled to the area. But NDVI was only 0.0072 less accurate than TSAVI, which is not significantly different considering the amount of time and additional information necessary (soil line parameters) to calculate TSAVI.

While NDVI performed the best overall, some of the major limitations are its sensitivity to atmospheric conditions, soil, and view/sun angle conditions (Dash *et al.,* 2007). The atmospheric conditions lower the NDVI of vegetated areas and in areas where the vegetation is on darker soil substrates, the NDVI produces higher vegetation index values (Huete, 1988), as shown in the wetland graph in Figure 5-1. An additional limitation is that the NDVI is insensitive to very high and very low chlorophyll content, which is an important biochemical property that varies with vegetation type (Gilabert, *et al.* 2002). Lastly when compared across different soil types, NDVI has been found to be affected (Huete, 1988) especially during open plant canopy periods. All these limitations restrict the NDVI quantitative capabilities to characterize the vegetated surface (Huete, *et al.* 1992) and therefore

a limitation in gully erosion mapping. But given the presented challenges of trying to assume the vegetation type for SAVI and difficulties in obtaining soil line parameters for calculating TSAVI, NDVI is still the final recommended technique for mapping gullies in South Africa.

5.1.5 Vegetation Index Choice for Gully Mapping – some guidelines

This study has successfully compared three VI for gully mapping in KZN. The results presented confirm that NDVI and TSAVI can be used to map a continuous gully with a moderate level of agreement using little knowledge when compared to traditional methods of gully mapping. Overall, NDVI proved to be more accurate at the sub-catchment level than TSAVI, which was ideal for identifying a continuous gully system and SAVI was best for a discontinuous gully system. Explanation for the distribution of error (omission and commission) can only be validated with additional information such as rainfall patterns prior to image acquisition and the distribution of soil types. For improvements in TSAVI, it is recommended that the selected soil patches be random across soil types, this will ensure that the VI parameters are generalized for the whole study region. When little is known about the study region and little expert knowledge is available, NDVI is recommended to identify erosion.

The experiments carried out in this study can be used to form a number of guidelines that can greatly facilitate the use of VI for gully erosion mapping using Landsat TM. The list of guidelines presented is ranked from highest to lowest and are given as follows:

A. Time required

1. TSAVI – slow process involved in selecting bare soil pixels for soil line equation.
2. SAVI – average amount of time spent on calculating the formula.
3. NDVI – quick, because model was already built in the ENVI 4.3 program

B. Expert knowledge required

1. TSAVI - required extensive expert knowledge, for collecting bare soil pixels, calculation was very complex
2. SAVI – average
3. NDVI - easiest, required little knowledge

C. Accuracy for mapping continuous gullies

1. TSAVI - high

2. NDVI – medium
3. SAVI - low

D. Accuracy for mapping discontinuous gullies

1. SAVI - high
2. NDVI - high
3. TSAVI - low

E. Accuracy in mapping sub-catchment level

1. NDVI – high
2. TSAVI - medium
3. SAVI - low

5.2 Gully Mapping Results from Multi-spectral Classification Techniques

5.2.1 Support Vector Machine Parameters

Appendix E is a list of the tested SVM parameter and the following are the selected values:

- RBF was the chosen kernel function which performed the best (0.5794) compared to the other three kernels. This kernel is known for its capability to separate classes that are not linearly separable with less numerical difficulties (Hsu, *et al.* 2008).
- The chosen value of C was 1000 which provided the highest kappa statistic of 0.601. Values were not tested above 1000 because increasing the penalty parameter would increase the cost of misclassifying points and would create a model that would not generalize well.
- The γ parameter is a kernel specific parameter that controls the width of the RBF kernel. The chosen value for γ was 0.167, which concurred with previously tested γ values which typically ranged between 0 and 1 (Joachims, 1998; Vapnik, 1995). Haung *et al.* (2002) provides details on the effect of γ on the decision boundary.

5.2.2 Training Sample Size

Table 5-4 is the classification accuracy results for a large and small non gully training data size (test 1 and test 2) for the discontinuous and continuous gully system. The values in brackets indicate the change in accuracy when a smaller training data set was used (↓ = decrease and ↑= increase). MDC performed the best within test 1 with a kappa statistic of 0.353 for the discontinuous gully subset and 0.5719 for the continuous gully subset. All classifications improved after test 2 with the most

significant increase in accuracy produced by SVM, in both continuous and discontinuous gully subset, which increased by 0.0227 and 0.0363, respectively. However MDC was the most accurate in mapping gullies within test 2 in the discontinuous gully subset producing an accuracy of 0.374.

Table 5-4 Classification kappa statistics results using different training data sizes

Tests	Discontinuous Gully	Continuous Gully
Test 1: Large Sample Size		
MLC	0.3155	0.4265
MDC	0.353	0.5719
SVM	0.3365	0.5647
Test 2: Small Sample Size		
MLC	0.3516 *(↑0.0361)*	0.5196 *(↑0.0931)*
MDC	0.3740 *(↑0.0210)*	0.5804 *(↑0.0085)*
SVM	**0.3592** ***(↑0.0227)***	**0.6010** ***(↑0.0363)***

5.2.3 Principal Component Analysis

Table 5-5 are the kappa statistic results obtained after applying the classifiers to two PCA images one with the first five PC (Test 3) and the other the first four PC (Test 4). The values in brackets, in Table 5-5, indicate the amount of increase compared to the small sample size classification (Test 2). The PCA increased the accuracy of MLC and MDC in both PC combinations, except the MDC test 4 in the discontinuous gully subset which decreased (↓0.0100). The PCA test 3 had a more significant increase than test 4 for MLC and MDC. MLC had the most significant increase in accuracy in these two tests with an accuracy increase of 0.0609 in the continuous gully subset. The SVM classifier experienced a decrease in accuracy using PCA. The bold values in Table 5-4 and 5-5 are the selected accuracies used to represent each subset gully maps and were the set procedures that were applied to the sub-catchment gully subset.

Table 5-5 Classification kappa statistics results with selected PCA bands

Tests	Discontinuous Gully	Continuous Gully
Test 3: PCA 1_2_3_4_5		
MLC	**0.3573** ***(↑0.0057)***	**0.5805** ***(↑0.0609)***
MDC	**0.3598** ***(↑0.0068)***	**0.5835** ***(↑0.0031)***
SVM	0.3569 *(↓0.0023)*	0.5842 *(↓0.0168)*
Test 4: PCA 1_2_3_4		
MLC	0.3540 *(↑0.0024)*	0.5803 *(↑0.0607)*
MDC	0.3640 *(↓0.0100)*	0.5830 *(↑0.0026)*
SVM	0.3575 *(↓0.0017)*	0.5854 *(↓0.0156)*

5.2.4 Gully Maps from Multi-spectral Classification Techniques

With reference to Figure 5-9, visual comparison of SVM produced a continuous gully map that was less speckled and the gully was more defined than in the other MLC and MDC continuous gully maps. It is challenging to visually assess the classifiers performance in the discontinuous gully subset and is actually insignificant because of the low accuracy achieved.

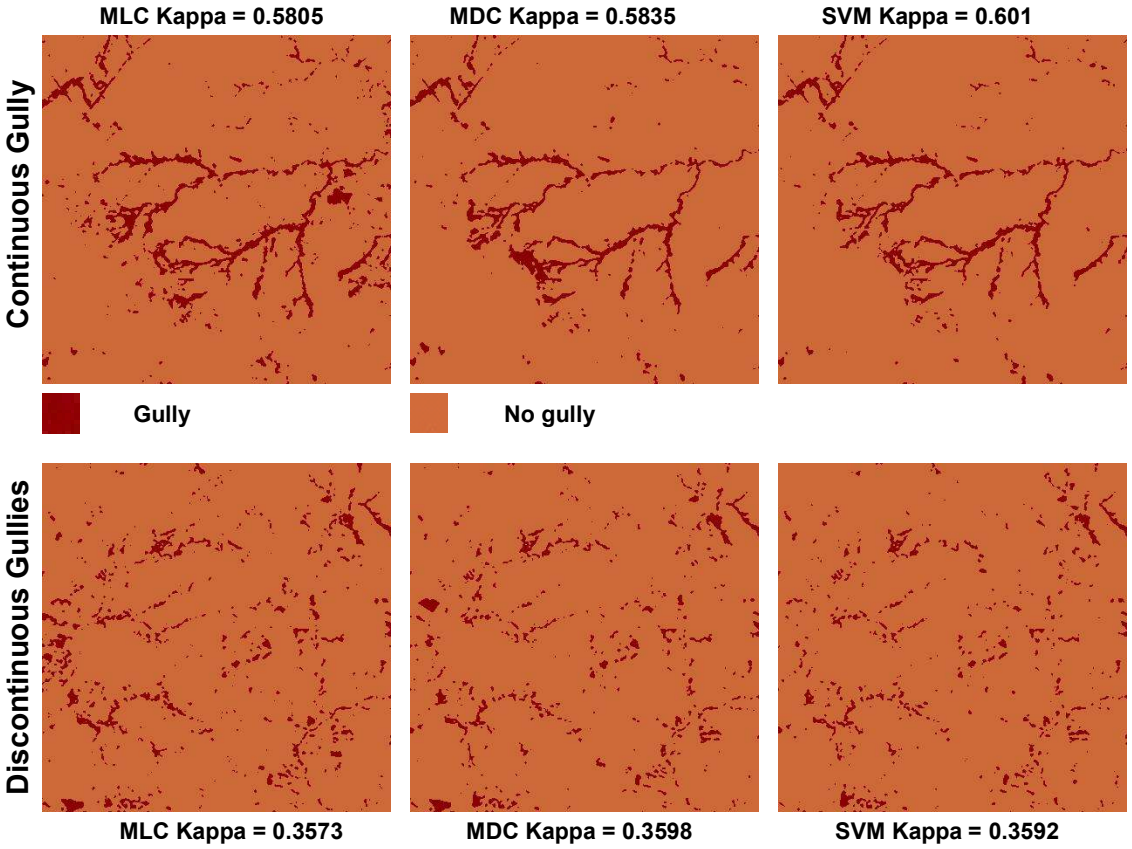

Figure 5-9 Classification gully maps with kappa statistic results

5.2.5 Gully Map Accuracy Assessment from Multi-spectral Classification Techniques

Table 5-6, Figure 5-10 and summarizes the maximum kappa statistics achieved for the continuous and discontinuous subsets as well as the results for the sub-catchment gully subset (Test 5). Figure 5-10 suggests that the continuous gully subset was the only one that produced a high accuracy for all three classifiers. All three classifiers produced similar results for the discontinuous gully subset with a low accuracy of approximately 0.36. Both MLC and MDC poorly classified the sub-catchment gully subset with a low accuracy of 0.2589 and 0.2499 respectively; however, the SVM classified sub-catchment with a higher accuracy (0.4063), compared to its performance in the discontinuous gully subset at (0.3592).

Table 5-6 Classification kappa statistics results for mapping gullies in subsets

Algorithms	Discontinuous Gully	Continuous gully	Sub-catchment gully
MLC (Test 3)	0.3573	0.5805	0.2589
MDC (Test 3)	0.3598	0.5835	0.2499
SVM	0.3592	0.601	0.4063

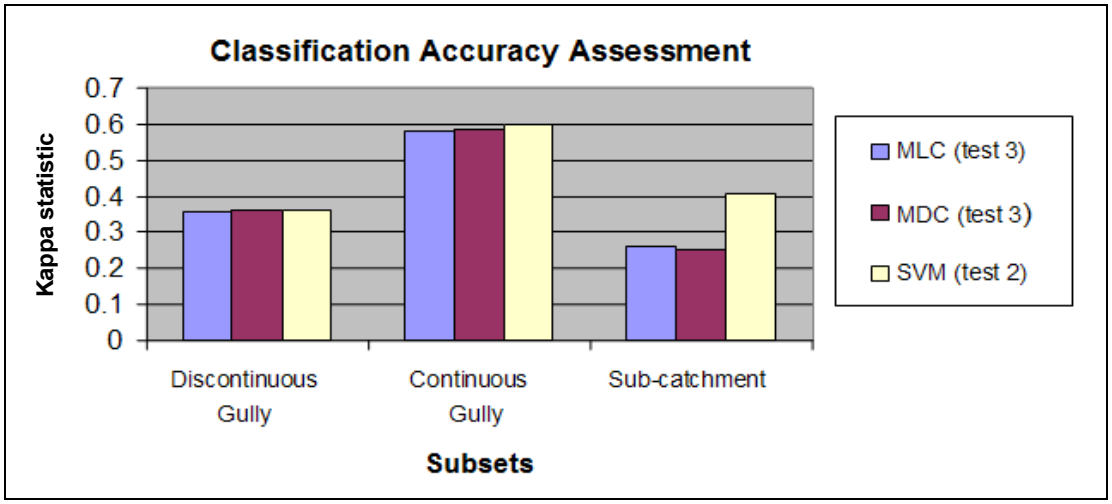

Figure 5-10 Classification kappa statistic results for mapping gullies in each subset

5.2.5.1 Results Using Multi-spectral Classification Techniques on SPOT 5 Imagery

Table 5-7 are the results obtained when the classifiers were applied to SPOT 5 data, the values in brackets are the differences in value from Table 5-6. All the classification algorithms performed poorly in the discontinuous and continuous gully subsets values. MLC and MDC had a more significant decrease in accuracy, for both subsets compared to SVM.

Table 5-7 Classification kappa statistics results with SPOT 5

Test 6	Discontinuous Gully	Continuous Gully
MLC	0.2291 *(↓-0.1282)*	0.4100 *(↓-0.1705)*
MDC	0.2308 *(↓-0.129)*	0.4717 *(↓-0.1118)*
SVM	0.3042 *(↓-0.055)*	0.5331 *(↓-0.0679)*

5.2.6 Discussion

The following discussion addresses the performance of the classificaiton algorithms for mapping gullies, in terms of training data separability and size, and the algorithm decision boundaries. These differences build the case for the selection of the most ideal classifier for gully mapping in South Africa.

5.2.6.1 Issue of Class Spectral Separability

The main obstacle in achieving high accuracies of the gully erosion maps derived from medium resolution (Landsat TM) satellite data is the heterogeneous nature of the gullies because they can consist of water, vegetation, and bare soil (section 2.3.2.2). The inherently high heterogeneity of gullies made it challenging for traditional classifiers to detect gullies because features that existed in the gully class also existed in the non gully class. This is an issue of class spectral separability.

The issue of spectral separability between the gully and the non gully class can be observed in Figure 5-11. This image displays the gully and non gully training data from Test 2, projected in a five band feature space. It illustrates the complexity of identifying a boundary that best separates the classes because the gully training data, indicated as green, and the non gully training data, indicated as yellow, both have overlapping regions in feature space. This area of over lap (fuzzy area) illustrates the region where features that are present in the gully class are also present in the non gully class.

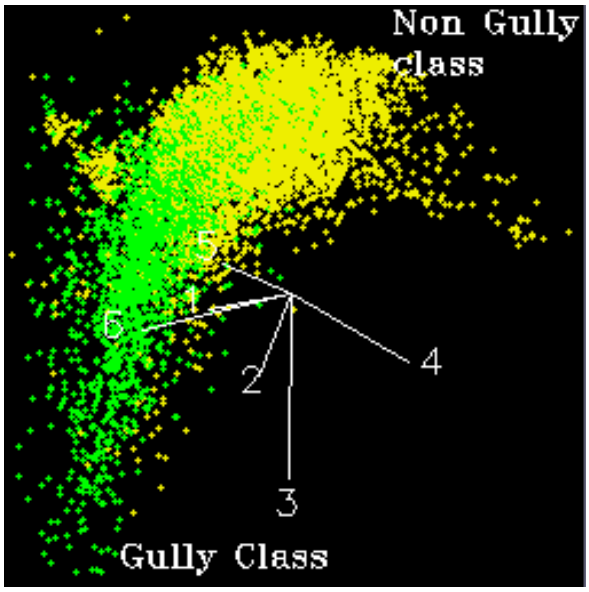

Figure 5-11 The Gully and Non Gully training data in a five band feature space

5.2.6.2 Training Data Size

Training data size is related to the "number of spectral bands, to which statistical properties are to be estimates, the number of those statistical properties, and the degree of variability present in the class" (Mather, 2004). Research has found a positive relationship between the size of the training set and classification accuracy for various classifiers (Foody and Arora, 1997; Foody and Mathur, 2004a). However acquiring large training sets is costly and time consuming and therefore may not be ideal for mapping gullies in South Africa. Interestingly enough this study has proven that a smaller training data size (Test 2) for the non gully class is more suitable for mapping gullies than a larger training data size (Test 1) (Table 5-4). In the following paragraph addresses the possible reasons for these results in hopes to obtain an ideal algorithm for mapping gullies in South Africa.

Some insight is gained into why the classifiers are producing significantly different accuracy results with different training data sizes, by looking at how the classifiers work. MLC and MDC are based on statistical descriptions of the classes generated from the training data (Mathur and Foody, 2008). It would be expected that these two classifiers would improve with a larger training data set because all classes would be exhaustively defined (Sanchez-Hernandez *et al.,* 2007b). Although a large training data for the non gully class does capture all the land cover types in the area; the multimodality of the class defies the MLC assumptions of normality thus feeding to the low accuracy results. MLC had the most significant increase in accuracy using a smaller training data size (Table 5-4), most likely because the training data size allowed for greater separability between the two classes. On the other hand, MDC was not significantly affected by the change in training data size (from Test 1 to Test 2) because it does not take into account possible data multimodality (Lai *et al.,* 2002), such as the non gully class. MDC assumes all class covariance's are equal (Richards and Jia, 2006) and bases its classification decisions on the mahalanobis distance rather than the probability of a pixel being in a class. This assumption of equal covariance's reduced the spectral complexity within the classes and allowed for the decision boundaries to be more concise. In doing so MDC is less affected by outliers in the training data because an unknown pixel is classified based on the distance of an uknown pixel from the center of a class ellips (i.e mean) divided by the width of the ellipsoid in the direction of the unknown pixel. This explains why MDC did not increase significantly when the training data size was reduced.

Figure 5-12 is used to explain this difference in the classification performance of MLC and MDC. The figure is an illustration of a hypothetical example of Test 1 and Test 2 where the training data of the gully and non gully class are plotted in a x-y spectral feature space. The dark tone purple and light tone purple indicate the Test 1 and Test 2 trianing data sizes, respectively. The light blue is the training data size for gully and the outer dashed line is the hypothetical location of the actual gully class in x-y feature space. The broad ellipse of the non gully class expresses the multimodality of the non gully area which increase the variance in the class. The gully training data is probably unimodal because it does not represent as many land cover types and thus has a lower variance. The unknown pixel (yellow diamond) lies within the dotted line illustrating that theoretically it should belong to the gully class in the final classification.

In classifying the gullies Figure 5-12 shows that there is greater separability between the training data (ellipses) when a smaller training data size is applied. If MLC was used to classify the unknown pixel (yellow diamond) using a small training data size (Test 2), it would still classify the pixel as non gully when it should be a gully. This is because the multimodality of the class increases the variance (width of the ellipse) which then increases the chances of a unknown pixel being in the non gully class. However MDC would classify the unkown pixel as gully in both Test 1 and Test 2 because the distance from the unknown pixel to the mean of the gully class (1) divided by the width of the ellipsoid in the direction of the unknown pixel, is shorter, in both Test 1 and Test 2,than the non gully MD disdance.

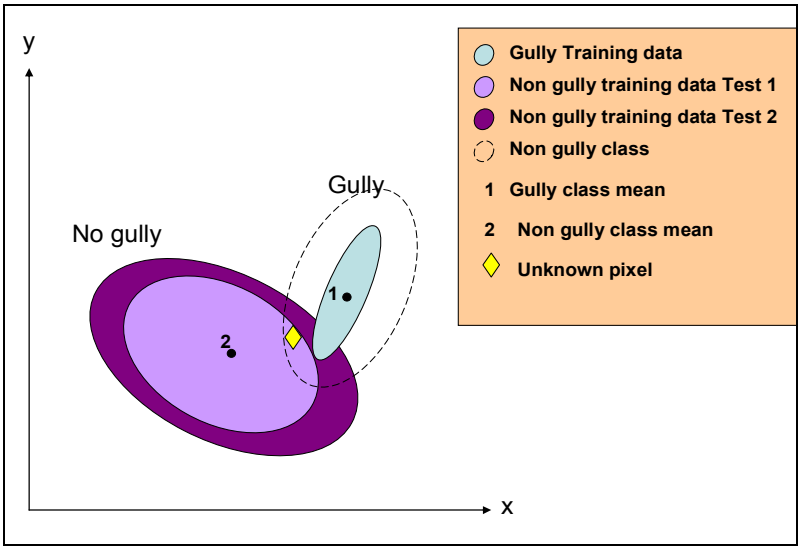

Figure 5-12 MLC and MDC classification illustration of a hypothetical classification

SVM does not rely explicitly on the dimensionality of the training data but uses pattern recognition, regression, and density estimation in high-dimensional spaces to separate the classes (Vapnik, 1998). Visual assessment of Figure 5-9 suggests that the SVM has mapped the continuous gully subset more accurately than the conventional classifiers. More importantly, the results in Table 5-4 prove that SVM can still produce higher accuracies than MLC and MDC even with smaller training data. This is because SVM is non parametric and only uses the support vectors which lie in the region where the classes meet (Foody and Mathur, 2006) and not the whole training data set. Thus SVM maximizes on the complexity of the classes at the boundary and is unaffected by the within class variance. These results mean that application of SVM for gully mapping requires less time, effort and expert knowledge required in training on the classes that are of no interest (Foody *et al*., 2006).

5.2.6.3 Principal Component Analysis

The Principal component analysis was used to test the need for image transformation by the classifiers. The results show that using PCA increased the accuracy for MLC and MDC in Test 3 but decreased the accuracy for SVM, but SVM still produced higher accuracies (Table 5-5). The obtained results confirm the strong superiority of SVMs over the other classifiers even in lower dimensional feature spaces (Table 5-5). Greater efforts could be put in place, in this analysis, to increase the accuracy however this can be very time-consuming. The bottom line is that SVM is not affected by the presence of noise in an image whereas conventional classifiers are. SVM can then be used without any additional expert knowledge and time needed to run an image transformation; thus it is applicable for gully erosion mapping in South Africa.

5.2.6.4 Algorithm Time Requirements

The training speeds of the three classifiers were substantially different. In all cases training the MLC and the MDC did not take more than a few minutes on an IBM thinkPad workstation, while training the SVM took hours and in some cases days, especially when the training data was large. The SVM also had the greatest challenge when classifying discontinuous gullies which took three hours. The long computation time required by SVM expresses the difficulties encountered by the SVM in identifying a separation between the two classes (Huang *et al.* 2002; Melgani and Bruzzone, 2004). The training speeds of these algorithms were affected by the size of the study area, with the sub-catchment subset taking the longest. Although SVM did require a longer computational time during

the process, the removed need for PCA and the higher accuracies across all the subsets still make SVM superior.

5.2.6.5 SPOT 5 Imagery for Gully Mapping

The classification algorithm test on SPOT 5 imagery (Test 6) was conducted to identify the need for higher resolution imagery for gully mapping. It would be expected that as the spatial resolution increases, so the amount of spatial variation, and thereby, the amount of information revealed about the gullies would increase (Atkinson and Tate, 1999), but with SPOT this is not the case. The classification results in Table 5-7 (pg 81) show that medium resolution Landsat TM data imagery out performed the higher resolution SPOT5 imagery for mapping gullies using all classifiers in the continuous and discontinuous subset. One would have expected that the SPOT image would produce a more accurate classification because of the finer spatial resolution; however it appears that the spectral resolution of Landsat TM was more important for identifying the gullies. This is probably due to the spectral variability within the gullies as explained in section 2.3.2.2., gullies can be composed of water, bare soil and vegetation. The heterogeneity of the gully makes it difficult for the classifiers to identify the gullies if less spectral information is provided as in the case of SPOT 5 which only provides 3 spectral bands. However, while the Landsat TM image classification retains more information than the SPOT classification (as evident in the kappa statistics), the resultant predictions still display a large degree of uncertainty.

5.2.7 Multi-Spectral Classification Algorithm Choice – some guidelines

Although the methods presented vary in complexity the study represents some of the inputs, issues and potential of selecting a classifier for gully mapping. Semi-automatic gully detection is very challenging due to the variability in appearance of the gullies and surrounding terrain. This study has shown that using state-of-the-art learning algorithms, which have worked well in other pattern recognition and vision problems, is successful in increasing the detection accuracy of gullies. The best result achieved from the SVM was the classification of the continuous gully system with an accuracy of 0.601. Although the computational time for running SVM was greater than the MLC and MDC, the processing time of SVM was still less than a traditional gully mapping method. The presented results can be summarized by the following guidelines:

A. Time required

1. SVM – slow process involved in running the algorithm.
2. MLC – average amount of time spent training data collection.
3. MDC – quickest

B. Expert knowledge required

1. SVM - required extensive expert
2. MLC – average
3. MDC - easiest, required little knowledge

C. Accuracy for mapping continuous gullies

1. SVM - high
2. MDC – medium
3. MLC - low

D. Accuracy for mapping discontinuous gullies

1. SVM - high
2. MDC - medium
3. MLC - low

E. Accuracy in mapping sub-catchment level

1. SVM – high
2. MDC - medium
3. MLC – low

F. Accuracy with SPOT data for mapping continuous and discontinuous gullies

1. SVM – high
2. MDC – medium
3. MLC – low

5.3 Summary of Results

If we assess these results based on Landis and Koch (1977) characterization of kappa statistics where: a value greater than 0.80 represents strong agreement, a value between 0.40 and 0.80 represents moderate agreement, and a value below 0.40 represents poor agreement, then most of the continuous gully system results performed are reputable as they are within the moderate level of agreement. Only the sub-catchment subset result for SVM (0.4063) lies within this category. Thus Landsat TM combined with SVM can be used to produce a gully erosion map at a sub-catchment scale with a

moderate level of accuracy. Possible incorporation of a digital elevation model and removal of conflicting features such as urban areas would improve the accuracy of all these results.

Table 5-8Kappa Statistic Results Summary

	Discontinuous	Continuous	Sub-catchment
NDVI	0.2088	0.5508	0.3616
SAVI	0.2216	0.4761	0.2997
TSAVI	0.1793	0.5580	0.3337
MLC (PCA)	0.3573	0.5805	0.2589
MDC (PCA)	0.3598	0.5835	0.2499
SVM	**0.3592**	**0.601**	**0.4063**

Chapter 6
Discussion

6.1 Issue of Detectability

Some of the low accuracy results achieved using the proposed semi-automatic techniques can be explained in terms of detectability - described as the degree of ease or difficulty that is encountered in extracting a gully using a vegetation index or classification algorithm. The low results for mapping discontinuous gullies are an issue of detectability both spatially and spectrally. Spatially the issue relates to the size of discontinuous gullies, which in some cases tends to be less than the pixel size 30*30m². This means that the gully is imbedded in a spectrally mixed pixel that contains components of non gully areas. Therefore spectral detectability of gullies in a landscape becomes more difficult, and accuracy in mapping the gully decreases, as the complexity of the background increases (Adams and Gillespie, 2006). The continuous gully subset produced the highest kappa statistic because the continuous gully system is a very prominent feature in the landscape, with most of the pixels being bare soil whereas the discontinuous gully pixels are a mix of vegetation and bare soil. The issue of detectability also explains the low accuracy results at the sub-catchment subset. First it contains a mixture of continuous and discontinuous gullies with the latter probably decreasing the accuracy levels. Second the sub-catchment subset includes a wider range of spectrally similar features to gullies, such as built up areas and quarries. Figure 6-1 is a TSAVI gully map and the ground truth gully map illustrating some of the features that were commonly miss-classified as gullies (errors of commission).

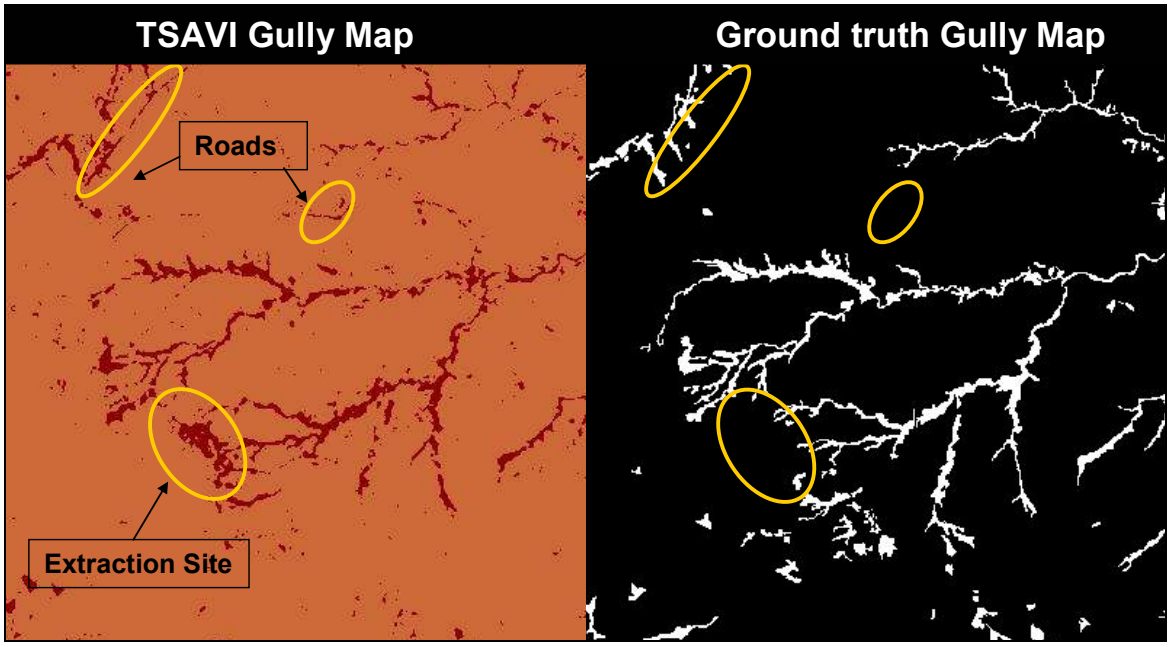

Figure 6-1 Right: Spectrally similar features that were mapped as gullies. Left: TSAVI gully map and right is the ground truth gully map

Despite the superior performance of some of the proposed semi-automatic gully mapping techniques at the continuous gully level, several parts and entire gullies remain unmapped at the sub-catchment level. Most of the proposed mapping techniques were unable to identify gullies along the escarpment (error of omission). A possible explanation could be the inclusion of some vegetation within the gullies which can be seen as a slight pink colour within the expert digitized gully outline in white colour in Figure 6-2 D. This is an issue of up-scaling, i.e. the application of methods to a larger area. It is also possible that this error occurred due to elevation distortions because these gullies are located on a slightly steeper slope than those chosen in the experiments. This steeper slope could have caused elevation distortions in the VIs; additionally this area could have a perched water table causing the exposed soil to be on the darker section of the soil line. Thus affecting the proposed soil line VIs and classification algorithms because these techniques were modeled to the continuous gully subset. A possible way to overcome this situation would be to apply geographical stratification, based on elevation. This can be done by using a digital elevation model to observe whether the spectral response of gullies changes with elevation.

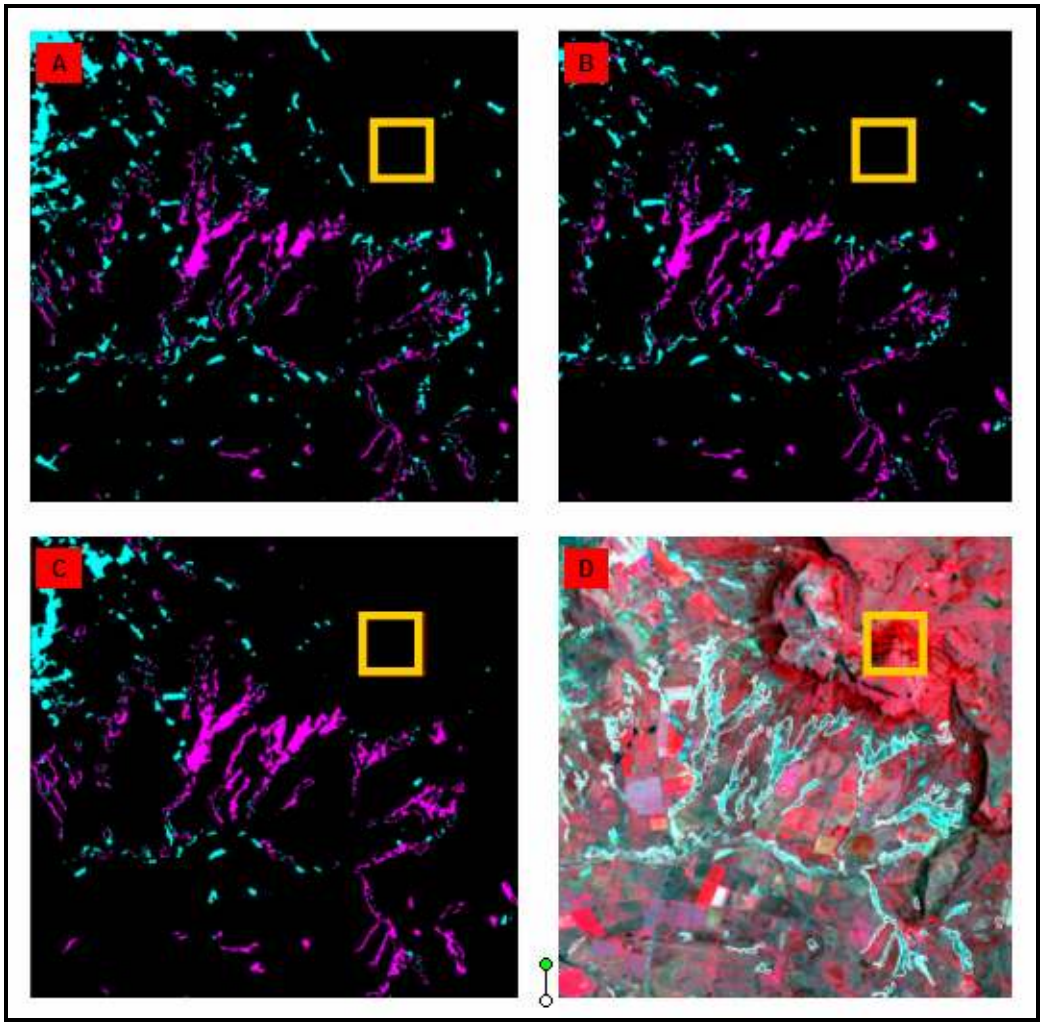

Figure 6-2 The location where gullies were not identified using NDVI (A), SAVI (B) and TSAVI (C); false colour composite (D) with red indicating vegetation and light blue indicating bare soil; the purple and light blue areas in A, B and C are the errors of omission and commission.

6.2 Possible Explanations for Low Accuracy of Maps

The low accuracy levels obtained overall could also be explained because of the methods used in the accuracy assessment. First, this case study is unique to most remote sensing accuracy assessments because it has considered all the pixels in the study region as a sample size since it is a representative of the entire mapping domain. However, in the real world such as situation may not be possible as it is time consuming and costly to obtain information about every pixel (digitization). In areas where there is little known about the erosion status or expert knowledge is unavailable, a sample of pixels

can be used to estimate the classification accuracy. However it is important that the map user is cautions on the decisions made based on these maps because the higher accuracy levels can be very misleading especially when the area being mapped is only a small percentage of the map. For example a random sample of 100 non gully points and 75 gully points was generated to test the accuracy of the SVM sub-catchment map. Using the ground truth image accuracy assessment discussed in the study, the SVM map had an accuracy of 0.4063, but using the ground truth points the accuracy increased to 0.55 with an overall accuracy of 80%, which are both misleadingly high results.

Second, the low accuracy could be explained by the temporal resolutions of the imagery used in the study. The SPOT 5 image used to digitize gullies was taken in 2006 whereas the Landsat TM used to create the semi-automatic maps was taken in 2005. The major issue is the assumption that a gully system had not changeover a one year period. As presented in section 2.1.1.3 gully erosion rates can vary. In one year changes such as flashfloods, human induced factors, vegetation growth and removal could have caused drastic changes in the landscape and thus gully system. This highlights the importance of additional information on past events that may have occurred prior to the image capture. Third the confidence put into the ground truth gully map could cause some discrepancies. As mentioned earlier there are difficulties in the literature with the characterization of a gully and thus it can also be expected that the experts digitizing the gully made errors. These are all possible explanations for the results obtained and can only be justified with further investigation.

Chapter 7
Conclusions and Recommendations

As presented in this thesis traditional techniques for mapping gullies were inappropriate for regional erosion control in South Africa because of the limited resources (expert knowledge, time and money). Furthermore traditional techniques have proven challenging to use because gullies vary in their characterization, dimension, development and also in their governing factors. The literature review discussed how satellite remote sensing can overcome some of the limitations of traditional gully mapping methods. In this section a detailed overview of candidate satellite remote sensing instruments for erosion mapping was presented and Landsat TM had the greatest potential for gully mapping in South Africa. Landsat TM was then combined with selected semi-automatic techniques for mapping gully erosion in Kwazulu-Natal South Africa.

The complex nature of gully erosion and its surrounding areas also proved to be challenging for gully mapping using some of the explored vegetation indices and conventional classifiers. The heterogeneity of the gullies themselves limited the mapping capabilities of the vegetation indices because the thresholds masked the area based on vegetated and non vegetated, not necessarily gully and no gully. The application of the conventional classification algorithms, MLC and MDC, were not appropriate for mapping gullies in this case study because they assume implicitly that the set of classes were exhaustively defined which was not the case because only two classes were being used to map the area, gully and non-gully area. However, SVM proved to be superior over all the explored methods and is recommended for future gully erosion mapping studies in South Africa because it:

- Required less expert knowledge in the training stages:
    - SVM produced a moderate accuracy level by successfully separating the gully class from the non gully class using a small training data set.
- Required less time:
    - In processing because no image transformation was necessary
    - In training data collection, small training data size.
- The achieved accuracies were comparable to traditional gully mapping methods.

- Once the parameters were defined the algorithm was simple to run.

SVM can be beneficial for erosion control, not only in South Africa, but other regions around the world. The potential of using SVM to map areas of severe erosion provides a means of obtaining valuable information on the extent, nature and magnitude of gully erosion in remote areas. This study has demonstrated that SVM can be used for the spatial assessment of the driving forces present at different scales- defined as subcatchment, continuous and discontinuous, which is considered to be relevant in future steps towards controlling erosion in South Africa (Sonneveld *et al.,* 2005). Stakeholders in erosion management can have added benefit of knowing the accuracy of the maps produced and thus make better decisions quickly because the technique is repeatable. The technique is also affordable and requires less expert knowledge. However users must be aware about the scale (discontinuous, continuous or sub-catchment) at which they require the gully maps because as demonstrated in this thesis higher accuracies are more achievable when the gully erosion feature is more prominent, as in the continuous gully scale. The overall accuracies achieved were low because of the methods used in the accuracy assessment and also possible because of the temporal resolution of the imagery. For improved accuracy in gully mapping for future studies the following is recommended:

- Higher spatial and spectral resolution imagery. This would be necessary to for a more accurate local gully erosion map 1:10,000 (Thwaites, 1986).
- Incorporation of ancillary information: e.g. elevation, slope, and aspect could improve the understanding of how the terrain affects the radiation of features. For example with the SVM, information on soil moisture levels and other properties could help in the training data acquisition process in order to identify the most informative training samples (Mathur and Foody, 2008).
- Combining SPOT and Landsat TM imagery: could provide a higher accuracy for mapping gullies because the classifiers would have the advantage of having both a high spatial resolution from SPOT and a high spectral resolution from the Landsat TM.
- Mask out spectrally similar features such as, urban built up areas, prior to mapping the gullies with the proposed techniques.
- Use ground truth imagery with the same temporal resolution.

- Design and explore other indices for mapping gullies because there are currently none that are specific to geomorphic features that contain vegetation and bare soil.

References

Adams, J. B., and Gillespie, A. R. (2006). *Remote sensing of landscapes with spectral images: A physical modeling approach*. Cambridge: Cambridge University Press.

ARC. (2007). *Agricultural research council: Spatial data.* Unpublished manuscript.

Atkinson, P. M., and Tate, J. N. (Eds.). (1999). *Advances in remote sensing and GIS analysis*. West Sussex, England: John Wiley and Sons Ltd.

Bader, C. J. (Ed.). (1962). *Typical soils of the east London district. the border region, natural environment and land use in the eastern cape.* Cape Town: Oxford University Press.

Baret, F., and Guyot, G. (1991). Potentials and limits of vegetation indices for LAI and APAR assessment. *Remote Sensing of Environment, 35*(2-3), 161-173.

Baret, F., Jacquemoud, S., and Hanocq, J. F. (1993). The soil line concept in remote sensing. *Remote Sensing Reviews, 7*(1), 65-82.

Bergsma, E. (1974). Soil erosion sequences on aerial photographs. *The ITC Journal,* (3), 342-376.

Barnes, E. M., and Baker, M. G. (2000). Multispectral data for mapping soil texture: Possibilities and limitations. *Application of Engineering and Agriculture, 16*, 731-741.

Baugh, W. M., and Groeneveld, D. P. (2006). Broadband vegetation index performance evaluated for a low-cover environment. *International Journal of Remote Sensing, 27*(21), 4715.

Beckedahl, H., and Dardis, G. F. (1988). The role of artificial drainage in the development of soil pipes and gullies: Some examples from Transkei, southern Africa. In G. F. Dardis, and B. P. Moon (Eds.), *Geomorphological studies in southern Africa,* (pp. 229-245). Rotterdam, Netherlands: Balkema.

Bergsma, E. (1974). Soil erosion sequences on aerial photographs. *The ITC Journal,* (3), 342-376.

Berjak, M., Fincham, R., Liggitt, B. and Watson, H. (1986). Temporal and spatial dimensions of gully erosion in northern natal, south Africa. *Commission IV of the International Society for Photogrammetry and Remote Sensing and the Remote Sensing Society,* Pollock Halls, Edinburgh, Scotland.

Blong, R. J. (1966). Discontinuous gullies on the volcanic plateau. *New Zealand Journal of Hydrology, 5*, 87-99.

Boardman, J. (2006). Soil erosion science: Reflections on the limitations of current approaches. *Catena, 68*(2-3), 73-86.

Bocco, G. (1991). Gully erosion: Processes and models. *Progress in Physical Geography, 15*(4), 392-406.

Bocco, G., Palacio, J. L. and Valenzuela, C. R. (1991). Gully erosion modeling using GIS and geomorphological knowledge. *ITC Journal, 3*, 253-261.

Bocco, G. and Valenzuela, C. R. (1988). Integration of GIS and image processing in soil erosion studies using ILWIS. *ITC Journal, 4*, 309-319.

Bocco, G. and Valenzuela, C. R. (1993). Integrating satellite-remote sensing and geographic information systems technologies in gully erosion research. *Remote Sensing Reviews, 7*(3-4), 233-240.

Botha, G. A. (1996). The geology and palaeopedology of late quaternary colluvial sediments in northern KwaZulu-natal. *Council for Geoscience, South Africa, Memoir 83*, 165.

Botha, J. H., and Fouche, P. S. (2000). An assessment of land degradation in the northern province from satellite remote sensing and community perception. *South African Geographical Society, 82*, 70-79.

Botha, G. A., Wintle, A. G. and Vogel, J. C. (1994). Episodic late quaternary palaeogully erosion in northern KwaZulu-natal, South Africa. *Catena, 23*, 327-340.

Boyd, D., Sanchez-Hernandez, C., and Foody, G. M. (2006). Mapping a specific class of interest for priority habitats monitoring from satellite sensor data. *International Journal of Remote Sensing, 27*(13), 2631-2644.

Brill, J., and Ochs, B. (2008). *NASA: Landsat data continuity mission.* Retrieved November, 01, 2008, from http://ldcm.nasa.gov/

Bull, L. J. and Kirkby, M. J. (1997). Gully processes and modeling. *Progress in Physical Geography,* (21), 354-374.

Burges, C. J. C. (1998). A tutorial on support vector machines for pattern recognition. *Data Mining and Knowledge Discovery, 2*, 121-167.

Burkard, M. B. and Kostaschuk, R. A. (1997). Patterns and controls of gully growth along the shoreline of lake Huron. *Earth Surface Processes and Landforms, 22*, 901-911.

Camps-Valls, G., Gomez-Chova, L., Calpe-Maravilla, J., Martin-Guerrero, J. D., Soria-Olivas, E., Alonso-Chorda, L., et al. (2004). *Robust support vector method for hyperspectral data classification and knowledge discovery*

Chalela, Q., Stocking, M. (1988). An improved methodology for erosion hazard mapping: PartII. application to Lesotho. *Geographiska Annaler, 10A*(3), 181-189.

Charlton, R. (2008). *Fundamentals of fluvial geomorphology*. New York: Routedge, Taylor and Fancis Group.

Cihlar, J., Latifovic, R., Beaubien, J., Guindon, B., and Palmer, M. (2003). TM-based accuracy assessment of a land cover produce for Canada derived from SPOT VEGETATION data. *Canadian Journal of Remote Sensing, 29*(2), 154-170.

Congalton, R. G. (1991). A review of assessing the accuracy of classifications of remotely sensed data. *Remote Sensing of Environment, 37*(1), 35-46.

Cogalton, R. G., and Green, K. (1999). *Assessing the accuracy of remote sensed data: Principles and practices*. London New York: Lewis Publishers.

Cyr, L., Bonn, F., and Pesant, A. (1995). Vegetation indices derived from remote sensing for an estimation of soil protection against water erosion. *Ecological Modeling, 79*(1-3), 277-285.

Dang, A., Zhang, S., He, X., Tang, L., & Xu, H. (2003). *Case study on soil erosion supported by GIS and RS*

Dardis, G. F. (1991). The role of rock properties in the development of bedrock-incision rills and gullies: Examples from South Africa. *GeoJournal, 23*(1), 35-40.

Dardis, G. F., Beckedahl, H., Bowyer-Bower, T. A. S. and Hanvey, P. M. (1988). Soil erosion forms in southern Africa. In G. F. Dardis and B. P. Moon (Eds.), *Geomorphological studies in southern Africa* (pp. 187-213). Rotterdam, Netherlands: Balkema.

Dash, J., Mathur, A., Foody, G. M., Curran, P. J., Chipman, J. W., and Lillesand, T. M. (2007). Land cover classification using multi-temporal MERIS vegetation indices. *International Journal of Remote Sensing, 28*(6), 1137.

de Asis, A. M., and Omasa, K. (2007). Estimation of vegetation parameter for modeling soil erosion using linear spectral mixture analysis of Landsat ETM data. *ISPRS Journal of Photogrammetry and Remote Sensing, 62*(4), 309-324.

de Jong, S. M. (1994). *Applications of reflective remote sensing for land degradation studies in a Mediterranean environment*. University Utrecht: Netherlands: Faculteit Ruimtelijke Wetenschappen.

Dhakal, A. S., Amada, T., Aniya, M., and Sharma, R. R. (2002). Detection of areas associated with flood and erosion caused by a heavy rainfall using multitemporal landsat TM data. *Photogrammetric Engineering and Remote Sensing, 68*(3), 233-239.

DWAF. (2007). *Geospatial data*. Pretoria: Department of Water Affairs and Forestry.

Dwivedi, R. S., Kumar, A. B., and Tewari, K. N. (1997). The utility of multi-sensor data for mapping eroded lands. *International Journal of Remote Sensing, 18*(11), 2303-2318.

Dwivedi, R. S., and Ramana, K. V. (2003). The delineation of reclamative groups of ravines in the indo-gangetic alluvial plains using IRS-ID LISS-III data. *International Journal of Remote Sensing, 24*(22), 4347-4355.

Dwivedi, R. S., RaviSankar, T., Venkataratnam, L., Karale, R. L., Gawande, S. P., SeshagiriRao, K. V., et al. (1997). The inventory and monitoring of eroded lands using remote sensing data. *International Journal of Remote Sensing, 18*(1), 107-119.

Ellis, F. (2000). *The application of machine learning techniques to erosion modeling.* Unpublished manuscript.

Eswaran, H., Lal, R. and Reich, P. F. (2001). Land degradation: An overview. *Response to Land Degradation* , 20-35.

Fadul, H. M., Salih, A. A., Imad-eldin, A. A. and Inanaga, S. (1999). Use of remote sensing to map gully erosion along the Atbara River, Sudan. *International Journal of Applied Earth Observation and Geoinformation, 1*(3-4), 175-180.

Felix-Henningsen, P., Morgan, R. P. C., Mushala, H. M., Rickson, R. J. and Scholten, T. (1997). Soil erosion in Swaziland: A synthesis. *Soil Technology, 11*(3), 319-329.

Flu̇gel, W., Marker, M., Moretti, S., Rodolfi, G. and Sidorchuk, A. (2003). Integrating geographical information systems, remote sensing, ground truthing and modeling approaches for regional erosion classification of semi-arid catchments in South Africa. *Hydrological Processes, 17*(5), 929-942.

Food and Agriculture Organization (FAO). (1965). *Soil erosion by water. some measures for its control on cultivated lands.* No. 81). Rome: FAO Agricultural Paper.

Foody, G. M., and Arora, M. K. (1997). An evaluation of some factors affecting the accuracy of classification by an artificial neural network. *International Journal of Remote Sensing, 18*, 799-810.

Foody, G. M., and Mathur, A. (2004a). A relative evaluation of multiclass image classification by support vector machines. *IEEE Transactions on Geoscience and Remote Sensing, 93*, 1335-1343.

Foody, G. M., and Mathur, A. (2004b). Toward intelligent training of supervised image classifications: Directing training data acquisition from SVM classification. *Remote Sensing of Environment, 93*, 107-117.

Foody, G. M., and Mathur, A. (2006). The use of small training sets containing mixed pixels for accurate hard image classification: Training on mixed spectral responses for classification by a SVM. *Remote Sensing of Environment, 103*(2), 179-189.

Foody, G. M., Mathur, A., Sanchez-Hernandez, C., and Boyd, D. S. (2006). Training set size requirements for the classification of a specific class. *Remote Sensing of Environment, 104*(1), 1-14.

Fox, G. A., Sabbagh, G. J., Searcy, S. W., and Yang, C. (2004). An automated soil line identification routine for remotely sensed images. *Soil Science Society of America, 68*, 1326-1331.

Fox, R. C. and Rowntree, K. M. (Eds.). (2001). *Redistribution and reform: Prospects for the land in the eastern cape province, South Africa.* Kluwer Academic Publishers: Dordrecht.

Garland, G. G., Hoffman, T. and Todd, S. (2000). *Soil degradation in a national review of land degradation in South Africa.* Retrieved 06/01, 2008, from

Gilabert, M. A., González-Piqueras, J., García-Haro, F. J., and Meliá, J. (2002). A generalized soil-adjusted vegetation index. *Remote Sensing of Environment, 82*(2-3), 303-310.

Giordano, A., and Marchisio, C. (1991). Analysis and correlation of the existing soil erosion maps in the Mediterranean basin. *Quaderni Di Scieza Del Suolo, 3*, 97-132.

Gualtieri, J. A., Chettri, S. R., Cromp, R. F., and Johnson, L. F. (1999). *Support vector machine classifiers as applied to AVIRIS data.* Unpublished manuscript.

Hadley, R. F., Lal, R., Onstad, C. A., Walling, D. E. and Yair, A. (1985). Recent developments in erosion and sediment yield studies. *Technical Documents in Hydrology,*

Harvey, M. D., Watson, C. C. and Schumm, S. A. (1985). Gully erosion. *Technical Note,* (366)

Hayden, R. S. (2008). *NASA geomorphology: Mapping.* Retrieved October/10, 2008, from http://disc8.sci.gsfc.nasa.gov/geomorphology/GEO_11

Heede, B. H. (1970). Morphology of gullies in the Colorado rocky mountains. *Bulletin International Association of Science and Hydrology, XV*(2), 78-89.

Heede, B. H. (1975). *Stages of development of gullies in the west* No. ARS-S-40). Washington: US Department of Agriculture.

Hermes, L., Frieauff, D., Puzicha, J., and Buhmann, J. M. (1999). Support vector machines for land usage classification in Landsat TM imagery. Hamburg, Germany. 348-350.

Hill, J., and Schutt, B. (2000). Mapping complex patterns of erosion and stability in dry Mediterranean ecosystems. *Remote Sensing of Environment, 74*(3), 557-569.

Hoffer, R. M., & Johannsen, C. J. (1969). Ecological potentials in spectral signature analysis. In P. L. Johnson (Ed.), (pp. 1-29). Athens: University of Georgia Press.

Hoffman, T. and Ashwell, A. (2001). *Nature divided land degradation in South Africa*. Cape Town: University of Cape Town Press.

Hsu, C., Chang, C., and Lin, C. -. (2008,). A practical guide to support vector classification.

Huang, C., Davis, L. S., and Townshend, J. R. G. (2002). An assessment of support vector machines for land cover classification. *International Journal of Remote Sensing, 23*(4), 725-749.

Huete, A. R. (1988). A soil-adjusted vegetation index (SAVI). *Remote Sensing of Environment, 25*(3), 295-309.

Huete, A. R., Hua, G., Qi, J., Chehbouni, A., and van Leeuwen, W. J. D. (1992). Normalization of multidirectional red and NIR reflectance's with the SAVI. *Remote Sensing of Environment, 41*(2-3), 143-154.

Hudson, N. W. (1980). Erosion prediction with insufficient data. In M. D. E. Boodt and D. Gabriels (Eds.), *Assessment of erosion* (pp. 279). Great Britain: John Wiley and sons.

Imeson, A. C. and Kwaad, F. J. (1980). Gully types and gully prediction. *Geografisch Tijdschrift, XIV*(5), 430-41.

Ireland, H. A., Sharpe, C. F. and Eargle, D. H. (1939). Principles of gully erosion in the piedmont of South Carolina. *Technical Bulletin,* (633)

Irons, J. R., Weismiller, R. A., and Petersen, G. W. (1989). Soil reflectance. In G. E. Asrar (Ed.), *Theory and applications of optical remote sensing* (pp. 66). New York: Wiley.

Jackson, R. D. (1983). Spectral indices in *N-space*. *Remote Sensing of Environment, 13*(5), 409-421.

Jackson, R. D., and Huete, A. R. (1991). Interpreting vegetation indices. *Preventive Veterinary Medicine,* (11), 185-200.

Jensen, J. R. (2005). *Introductory digital image processing* (3rd ed.). United States of America: Pearson Prentice Hall.

Joachims, T. (1998). Text categorization with support vector machines learning with many relevant features. Berlin. 137-142.

Jones, R. G. B. and Keech, M. A. (1966). Identifying and assessing problem areas in soil erosion surveys using aerial photographs. *Photogrammetric Society, 5*(27), 189-197.

Jurgens, C., and Fander, M. (1993). Soil erosion assessment and simulation by means of SGEOS and ancillary digital data. *International Journal of Remote Sensing, 14*(15), 2847-2855.

Kakembo, V. and Rowntree, K. M. (2003). The relationship between land use and soil erosion in the communal lands near peddie town, eastern cape, South Africa. *Land Degradation and Development, 14*, 39-49.

King, R. B. (2002). Land cover mapping principles: A return to interpretation fundamentals. *International Journal of Remote Sensing, 23*(18), 3525-3545.

King, C., Baghdadi, N., Lecomte, V., and Cerdan, O. (2005). The application of remote-sensing data to monitoring and modeling of soil erosion. *Catena, 62*(2-3), 79-93.

Kiusi, R. B. and Meadows, M. E. (2006). Assessing land degradation in the monduli district, northern Tanzania. *Land Degradation and Development, 17*, 509-525.

Klimaszewski, M. (1982). Detailed geomorphological maps. *ITC Journal, 3*, 265-271.

Lai, C., Tax, D. M. J., Duin, R. P. W., Pekalska, E., and Paclik, P. (Eds.). (2002). *On combining one-class classifiers for image database retrieval*. Berlin Heidelberg: Springer-Verlag.

Lafarge, F., Descombes, X., and Zerubia, J. (2005). Textural kernel for SVM classification in remote sensing: Application to forest fire detection and urban area extraction. *IEE,*

Laker, M. C. (2000). Soil resources: Distribution, utilization and degradation. In R. Fox and K. Rowntree (Eds.), *The geography of South Africa in a changing world* (pp. 326). Cape Town: Oxford University Press Southern Africa.

Lal, R. (2001). Soil degradation by erosion. *Land Degradation and Development, 12*(6), 519-539.

Langran, K. J. (1983). Potential for monitoring soil erosion features and soil erosion modeling components from remotely sensed data. *Proc. IGARSS 83,*

Lawrence, R. L., and Ripple, W. J. (1998). Comparisons among vegetation indices and band wise regression in a highly disturbed, heterogeneous landscape: Mount St. Helens, Washington. *Remote Sensing of Environment, 64*(1), 91-102.

Le Roux, J. J., Newby, T. S. and Summer, P. D. (2007). Monitoring soil erosion in South Africa at a regional scale: Review and recommendations. *South African Journal of Science, 103*, 329-335.

Leopold, L. B. and Miller, J. P. (1956). Ephemeral streams, hydraulic factors and their relation to the drainage net. *US Geological Survey, 282-A*

Leopold, L. B., Wolman, G. M. and Miller, J. P. (1964). *Fluvial processes in geomorphology*. United States of America: W.H. Freeman and Company.

Liggitt, B. (1988). *An investigation into soil erosion in the Mfolozi catchment.* Unpublished manuscript.

Liggitt, B. and Fincham, R. J. (1989). Gully erosion: The neglected dimension in soil erosion research. *South African Journal of Science, 85*, 18-20.

Lu, D., and Weng, Q. (2007). A survey of image classification methods and techniques for improving classification performance. *International Journal of Remote Sensing, 28*(5), 823-870.

Lawrence, R. L., and Ripple, W. J. (1998). Comparisons among vegetation indices and band wise regression in a highly disturbed, heterogeneous landscape: Mount St. Helens, Washington. *Remote Sensing of Environment, 64*(1), 91-102.

Mantero, P., and Moser, G. (2005). Partially supervised classification of remote sensing images through SVM-based probability density estimation. *IEEE Transactions on Geoscience and Remote Sensing, 43*(3), 559-570.

Mather, P. M. (2004). *Computer processing of remotely-sensed images* (Third ed.). England: John Wiley and Sons Ltd.

Mathieu, R., King, C., and Le Bissonnais, Y. (1997). Contribution of multi-temporal SPOT data to the mapping of a soil erosion index. the case of the loamy plateau of northern France. *Soil Technology, 10*(2), 99-110.

Mathur, A., and Foody, G. M. (2008). Crop classification by support vector machine with intelligently selected training data for an operational application. *International Journal of Remote Sensing, 29*(8), 2227-2240.

Mati, B. M. and Veihe, A. (2008). Application of the USLE in a savannah environment: Comparative experiences from east and west Africa. *Singapore Journal of Tropical Geography, 22*(2), 138.

Meadows, M. E., and Hoffman, T. (2003). Land degradation and climate change in South Africa. *The Geographical Journal, 169*(7), 168-177.

Melgani, F., and Bruzzone, L. (2004). Classification of hyperspectral remote sensing images with support vector machines. *IEEE Transactions on Geoscience and Remote Sensing, 42*, 1778-1790.

Merrit, W. S., Letcher, R. A., and Jakeman, A. J. (2003). A review of erosion and sediment transport models. *Environmental Modeling and Software, 18*(8-9), 761-799.

Metternicht, G. I., and Fermont, A. (1998). Estimating erosion surface features by linear mixture modeling. *Remote Sensing of Environment, 64*(3), 254-265.

Metternicht, G. I., and Zinck, J. A. (1998). Evaluating the information content of JERS-1 SAR and landsat TM data for discrimination of soil erosion features. *ISPRS Journal of Photogrammetry and Remote Sensing, 53*(3), 143-153.

Millington, A. C., and Townshend, J. R. G. (1984). Remote sensing applications in African erosion and sedimentation studies. *Challenges in African Hydrology and Water Resources. Proc. Harare Symposium, 1984,* , 373-384.

Mills, A. J., and Fey, M. V. (2003). Declining soil quality in South Africa: Effects of land use on soil organic matter and surface crusting. *South Africa Journal of Science, 99*, 429-436.

Moore, T. R. (1979). Rainfall erosivity in east Africa. *Geographiska Annaler, 61A*, 136-147.

Morgan, R. P. C. (1986). *Soil erosion and conservation*. Essex: Longman Group.

Morgan, R. P. C., Rickson, R. J., McIntyre, K., Brewer, T. R. and Altshul, H. J. (1997). Soil erosion survey of the central part of the Swaziland middleveld. *Soil Technology, 11*, 263-289.

Mosley, M. P. (1972). Evolution of a discontinuous gully system. *Annals Association of American Geographer, 62*(4), 655-63.

Mountain, E. D. (1952). *Geology of the keiskammahoek*

Mpumalanga, D. (2002). *Mpumalanga province, state of environment report 2001*. KwaZulu-Natal: Mpumalanga Department of Agriculture, Conservation and Environment.

Mucina, L., and Rutherford, C. M. (2006). *The vegetation of South Africa, Lesotho's and Swaziland*. Pretoria: South African National Biodiversity Institute.

Nichol, J. E., Shaker, A., and Wong, M. S. (2006). Application of high-resolution stereo satellite images to detailed landslide hazard assessment. *Geomorphology, 76*, 68-75.

Nizeyimana, E., and Petersen, G. W. (1997). Remote sensing applications to soil degradation assessments. In R. Lal, W. H. Blum, C. Valentine and B. A. Stewart (Eds.), *Methods for assessment of soil degradation* (pp. 393). New York: CRC Press LLC.

Pal, M., and Mather, P. M. (2005). Support vector machines for classification in remote sensing. *International Journal of Remote Sensing, 26*(5), 1007-1011.

Patton, P. C., & Schumm, S. A. (1975). Gully erosion, NW Colorado: A threshold phenomenon. *Geology, 3*(2), 88-99.

Pickup, G., and Chewings, V. H. (1988). Forecasting patterns of soil erosion in arid lands from landsat MSS data. *International Journal of Remote Sensing, 9*(1), 69-84.

Pickup, G., and Nelson, D. J. (1984). Use of Landsat radiance parameters to distinguish soil erosion, stability and deposition in arid central Australia. *Remote Sensing of Environment, 16*(3), 195-209.

Poesen, J., Vandekerckhove, L., Nachtergaele, J., Oostwoud, W. D., Verstraeten, G. and van Wesemael, B. (2002). Gully erosion in Dryland environments. In Bull, L.J. Kirkby, M.J. (Ed.), *Dryland rivers: Hydrology and geomorphology of semi-arid channels* (pp. 62- 229). Chichester: John Wiley and Sons.

Pretorius, D. J. (1995). *The development of a soil degradation management support.* Unpublished manuscript.

Pretorius, D. J. and Bezuidenhout, C. J. (1994). *Report on the development of a methodology to determine the nature, rate and extent of soil erosion in South Africa* No. GW1A/94/7). Pretoria: National Department of Agriculture, Directorate Land and Resources Management.

Price, K. P. (1993). Detection of soil erosion within pinyon-juniper woodlands using thematic mapper (TM) data. *Remote Sensing of Environment, 45*(3), 233-248.

Richards, J. A., and Jia, X. (2006). *Remote sensing digital image analysis: An introduction* (4th ed.). Germany: Springer.

Richardson, A. J., and Wiegand, C. L. (1977). Distinguishing vegetation from soil background information. *Photogrammetric Engineering and Remote Sensing, 43*(12), 1541-1552.

Ritchie, J. C. (2000). Soil erosion. *Remote sensing in hydrology and water management* (Schultz GA, Engman ET ed., pp. 271). Berlin: Springer.

Robinovoe, C. J., Chavez Jr, P. S., and Dale, G. (1981). Arid land monitoring using Landsat albedo difference images. *Remote Sensing of Environment, 11*, 133-156.

Roli, F., and Fumera, G. (2001). Support vector machines for remote sensing image classification. *, 4170* 160-166.

Sabins, F. F. (1996). *Remote sensing: Principles and interpretation* (3rd ed.). United States of America: New York: W.H.Freeman and Company.

Sanchez-Hernandez, C., Boyd, D. S., and Foody, G. M. (2007a). Mapping specific habitats from remotely sensed imagery: Support vector machine and support vector data description based classification of coastal saltmarsh habitats. *Ecological Informatics, 2*(2), 83-88.

Sanchez-Hernandez, C., Boyd, D., and Foody, G. M. (2007b). One-class classification for mapping a specific land cover class: SVDD classification of fenland. *IEEE Transactions on Geoscience and Remote Sensing, 45*(4)

Schulze, R. E., Maharaj, M., Lynch, S. D., Howe, B. J., and Melvil-Thomson, B. (1997). *South African atlas of agrohydrology and climatology* (first ed.). Pretoria: Water Research Commission.

Scotney, D. (1978). *Soil erosion in natal. paper presented to the wildlife society of southern Africa symposium on agriculture and environmental conservation.* Unpublished manuscript.

Schowengerdt, R. A. (2007). *Remote sensing: Models and methods for image processing* (3rd ed.). United States of America: Elsevier Inc.

Servenay, A., and Prat, C. (2003). Erosion extension of indurated volcanic soils of Mexico by aerial photographs and remote sensing analysis. *Geoderma, 117*(3-4), 367-375.

Shonk, J. L., Gaultney, L. D., Schulze, D. G., and Van Scoyoc, G. E. (1991). Spectroscopic sensing of soil organic matter content. *ASAE,* (34)

Sidorchuk, A. (1999). Dynamic and static models of gully erosion. *CATENA, 37*(3-4), 401-414.

Singh, D., Herlin, I., Berroir, J. P., Silva, E. F., and Simoes, M. M. (2004). An approach to correlate NDVI with soil colour for erosion process using NOAA/AVHRR data. *Advances in Space Research, 33*(3), 328-332.

Soil Science Society of America. (1996). *Glossary of soil science terms*. USA: Madison.

Song, C., Woodcock, C. E., Seto, K. C., Lenney, M. P., and Macomber, S. A. (2001). Classification and change detection using Landsat TM data. *Remote Sensing of Environment, 75*(2), 230-244.

Sonneveld, M. P. W., Everson, T. M. and Veldkamp, A. (2005). Multi-scale analysis of soil erosion dynamics in Kwazulu-natal, South Africa. *Land Degradation and Development, 16*(3), 287-301.

Story, M., and Congalton, R. G. (1986). Accuracy assessment: A user's perspective. *Photogrammetric Engineering and Remote Sensing,* (52)

Sujatha, G., Dwivedi, R. S., Sreenivas, K., and Venkataratnam, L. (2000). Mapping and monitoring of degraded lands in part of jaunpur district of uttar pradesh using temporal spaceborne multispectral data. *International Journal of Remote Sensing, 21*(3), 519-531.

Summer, P. D. and Meiklejohn, I. (2000). Landscape evolution in a changing environment. In R. Fox and K. Rowntree (Eds.), *The geography of South Africa in a changing world* (). Cape Town: Oxford University Press Southern Africa.

Symeonakis, E., and Drake, N. (2004). Monitoring desertification and land degradation over sub-Saharan Africa. *International Journal of Remote Sensing, 25*(3), 573-592.

Tax, D. M. J., and Duin, R. P. W. (2004). Support vector data description. *Machine Learning, 54*, 45-66.

Teng, W. L., Loew, E. R., Ross, D. I., Zsilinszky, V. G., Lo, C. P., Philipson, W. R., et al. (1997). Fundamentals of photographic interpretation. In W. R. Philipson (Ed.), *Manual of photographic interpretation* (pp. 49-113). American Society of Photogrammetry and Remote Sensing: Bethesda.

Terrence, J., Foster, G. and Renard, G. K. (Eds.). (2002). *Soil erosion: Processes, predictions, measurement and control*. New York: John Wiley and Sons.

Thiam, A. K. (2003). The causes and spatial pattern of land degradation risk in southern Mauritania using multitemporal AVHRR-NDVI imagery and field data. *Land Degradation and Development, 14*(1), 133-142.

Thwaites, R. N. (1986). A technique for local soil erosion survey. *South African Geographical Journal, 68*(1), 67-76.

Twidale, C. R. (2004). River pattern and their meaning. *Earth Science Review, 67*, 159-218.

Vaidyanathan, N. S., Sharama, G., Sinha, R., and Dikshit, O. (2002). Mapping of erosion intensity in the Garhwali Himalaya. *International Journal of Remote Sensing, 23*(20), 4125-4129.

van der Eyck, J.J., MacVicar, C. N. and de Villiers, J. M. (1969). *Soils of the Tugela basin - a study in sub-tropical Africa* No. 15) Natal Town and Regional Planning Report.

Van Dijk, A., Bruijnzeel, L. and Rosewell, C. (2002). Rainfall intensity-kinetic energy relationships: A critical literature appraisal. *Journal of Hydrology, 261*, 1-23.

Van Zuidam, R. E. (1985). *Terrain analysis and classification using aerial photographs* (2nd ed.). Enschede: International Institute for Aerospace Survey and Earth Science.

Vapnik, V. N. (1995). *The nature of statistical learning theory*. New York: Springer-Verlag.

Vapnik, V. N. (1998). *Statistical learning theory*. New York: Wiley.

Vrieling, A. (2006). Satellite remote sensing for water erosion assessment: A review. *Catena, 65*, 2-18.

Vrieling, A., de Jong, S. M., Sterk, G., and Rodrigues, S. C. (2008). Timing of erosion and satellite data: A multi-resolution approach to soil erosion risk mapping. *International Journal of Applied Earth Observation and Geoinformation, 10*(3), 267-281.

Wang, G., Wente, S., Gertner, G. Z., and Anderson, A. (2002). Improvement in mapping vegetation cover factor for the universal soil loss equation by geostatistical methods with Landsat thematic mapper images. *International Journal of Remote Sensing, 23*(18), 3649-3667.

Watson, H. K. (1997). Geology as an indicator of land capability in the mfolozi area, KwaZulu-natal. *South African Journal of Science, 93*, 39-44.

Weaver, A. v. (1988). Factors affecting the spatial variation in soil erosion in Ciskei: An initial assessment at the macroscale. In G. F. Dardis, and B. P. Moon (Eds.), *Geomorphological studies in southern Africa* (pp. 215). Rotterdam, Netherlands: Balkema.

Weaver, A. v. (1991). The distribution of soil erosion as a function of slope aspect and parent material in ciskei, South Africa. *South Africa GeoJournal,* (23), 29-34.

Wessels, K. J., Prince, S. D., Frost, P. E., and van Zyl, D. (2004). Assessing the effects of human-induced land degradation in the former homelands of northern South Africa with a 1 km AVHRR NDVI time-series. *Remote Sensing of Environment, 91*(1), 47-67.

Wilkie, D. S., and Finn, T. J. (1996). *Remote sensing imagery for natural resources monitoring*. New York: Columbia University Press.

Whitmore, G., Meth, D. and Uken, R. (2006). *Geological science: Geology of KwaZulu-natal.* Retrieved October, 2008, from http://www.geology.ukzn.ac.za/GEM/kzngeol/kzngeol.htm

Wu, D., and Linders, J. (2000). Comparison of three different methods to select feature for discriminating forest cover types using SAR imagery. *International Journal of Remote Sensing, 21*(10), 2089-2099.

Zhang, J. and Goodchild, M. F. (Eds.). (2002). *Uncertainty in geographical information*. New York: Taylor and Francis

Appendix A

Erosion Controlling Factors

Factor	Author	Findings/Comments
Soil	Weaver (1991)	Soils with a high clay content as well as a structured A-horizon tend to exhibit relatively low degrees of erosion. Duplex soils with restrictive horizons and shallow soils with a low permeability exhibit higher levels of erosion.
	Watson (1997)	Unconsolidated sediments and several of the weaker, particularly shale formations are susceptible to both gully and sheet erosion
	Berjack et al. (1986) and Liggit (1988)	Soils underlain by Dwyka Tillite were the worst affected by gulling.
Colluvial or Sediments	Garland, (2000); Botha, (1994); Watson, (1997)	In KwaZulu-Natal most gullies form on transported colluvial or alluvial sediments.
Climate	Moore (1979); Van Dijk (2002)	Affect soil erosion directly, through precipitation, temperature, evapotranspiration; indirectly, through the conditions that influence the soil moisture and vegetation cover (biomass). Rainfall, in particular, is a major driving force of many erosional processes and the amount of soil that is detached is related to rainfall intensity.
Topography	Morgan (1986)	Important topographical properties regarding degradation processes are slope steepness, slope length and slope shape
	De Jong (1994)	Erosion normally increases with increasing slope steepness and slope length because of the increase of velocity and volume of surface runoff
	Liggitt (1988)	Gradient less than 10° was a critical slope value, where gullies occur most frequent in part of KZN.
	Weaver (1991)	North-facing slopes tend to be more heavily eroded than south-facing slopes because natural forests tend to concentrate on the cool, moist south-facing slops, hence restricting erosion.
Bedrock	Botha, (1996)	Strong direct relationship between gully erosion and specific bedrock types
	Weaver (1991); Berjak (1986); Mountain (1952);Bader 1962	Soil erosion is more severe on soils underlain by dolerite than on those underlain by sedimentary rocks.
	Mountain (1952); Berjak (1986)	Soils underlain by shale's and mudstone of the Beaufort Group were more heavily erodable than those underlain by dolerite

Appendix B

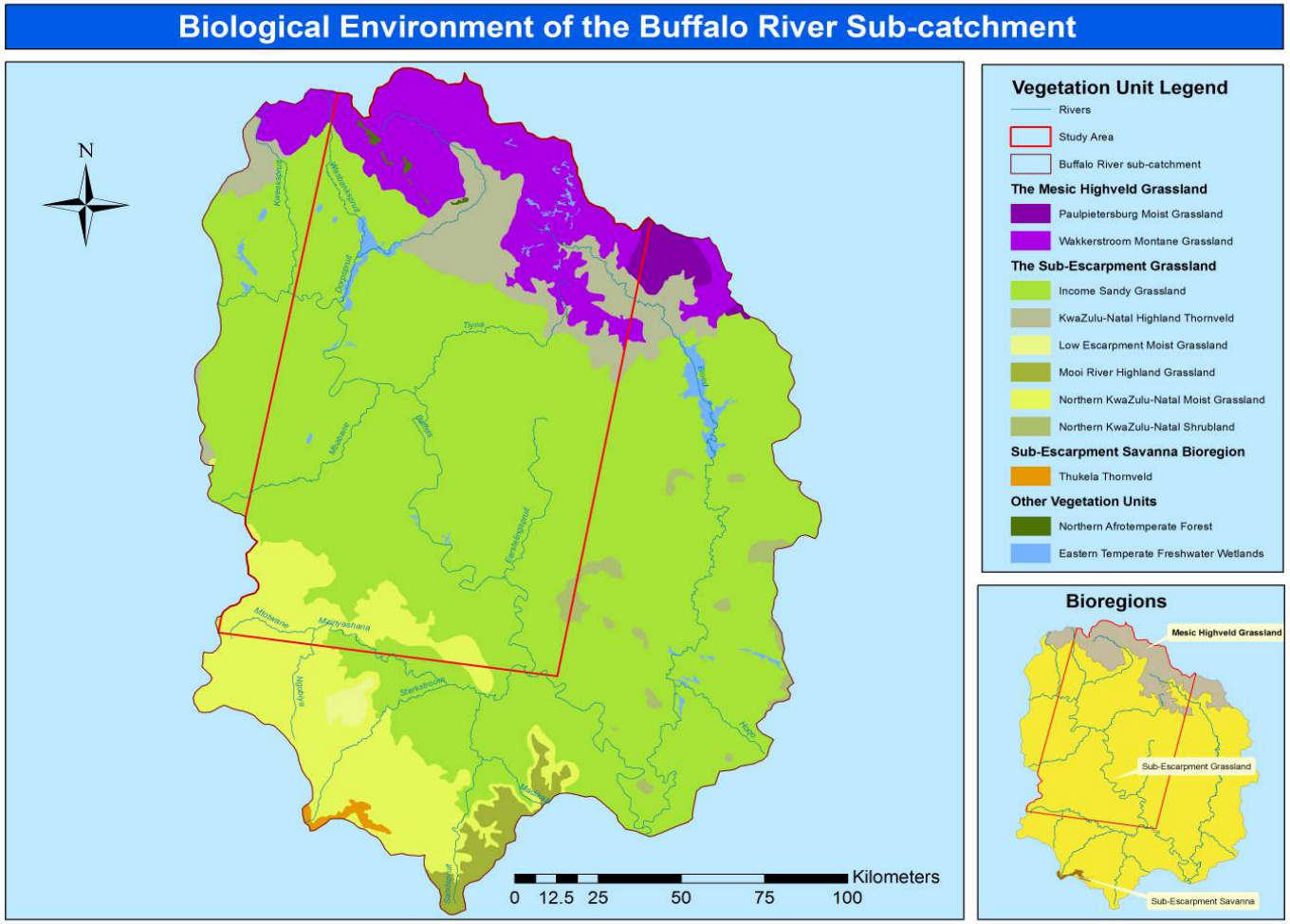

Bioregion and vegetation unit map of the Buffalo river sub-catchment (Spatial data source: (Mucina and Rutherford, 2006))

Appendix C

Summary of the Biological Environment

1.0 Grassland Biome: The topography of this biome is mainly flat to rolling, but also includes mountainous regions and the escarpment. This biome experiences large temperature differences from winter to summer with high frequency of frost.	
	1.1 Mesic Highveld Grassland
	1.1.1 Wakkerstrom Montane Grassland (Gm14) • Short montane grassland found on the plateaus and flat areas, with short forest and thickets occurring along steep, mainly east facing slops and drainage areas. • Occurs on shallow soils
	1.1.2 Paulpietersburg Moist Grassland (Gm15) • Underlain by Archaean granite and gneiss • Vulnerable vegetation unit because of its usefulness for cultivation
	1.2 Sub Escarpment Grassland
	1.2.1 Low escarpment Moist Grassland (Gs3) • Found on complex mountain topography and on mudstone or shale
	1.2.2 Northern KwaZulu-Natal Moist Grassland (Gs4) • Geology is similar to Gs3 and is considered vulnerable as more than a quarter has already been transformed either for cultivation, plantation and urban sprawl or by building dams
	1.2.3 Northern KwaZulu-Natal Shrubland (Gs5) • Widely scattered group of patches embedded within Gs4, Gs6 and Gs7. • Small dolerite koppies and steeper slopes of ridges with sparse grass cover and scattered shrubland pockets.
	1.2.4 KwaZulu-Natal Highland Thorn Shrubland(Gs6) • Occurs in both dry valleys and moist upland
**	*1.2.5 Income Sandy Grassland (Gs7)* • Landscape includes very flat with generally shallow, poorly drained, sandy soils • Found on sandstones and shale supporting poorly drained sand soils.
	1.2.6 Mooi River Highland (Gs8) • Soils are derived from sedimentary rock and are generally shallow and poor
2.0 Savanna Biome It is the most widespread biome in Africa. The temperatures in this biome are slightly higher than the surrounding grasslands mostly due to the lower elevation.	
	2.1 Sub-escarpment
	• *2.1.1 Thukela Thornveld (Sv2)* • Landscape includes valley slopes and undulating hills
3.0 Other Vegetation Units	
	3.1 Northern Afrotemperate Forest (FOz2) • Represents the indigenous forest scattered within the study region
	3.2 Eastern Temperate Freshwater Wetland (AZf3) • Found around stagnant water bodies and is embedded within the grassland

(Table modified from Munica and Rutherford (2006)

Appendix D

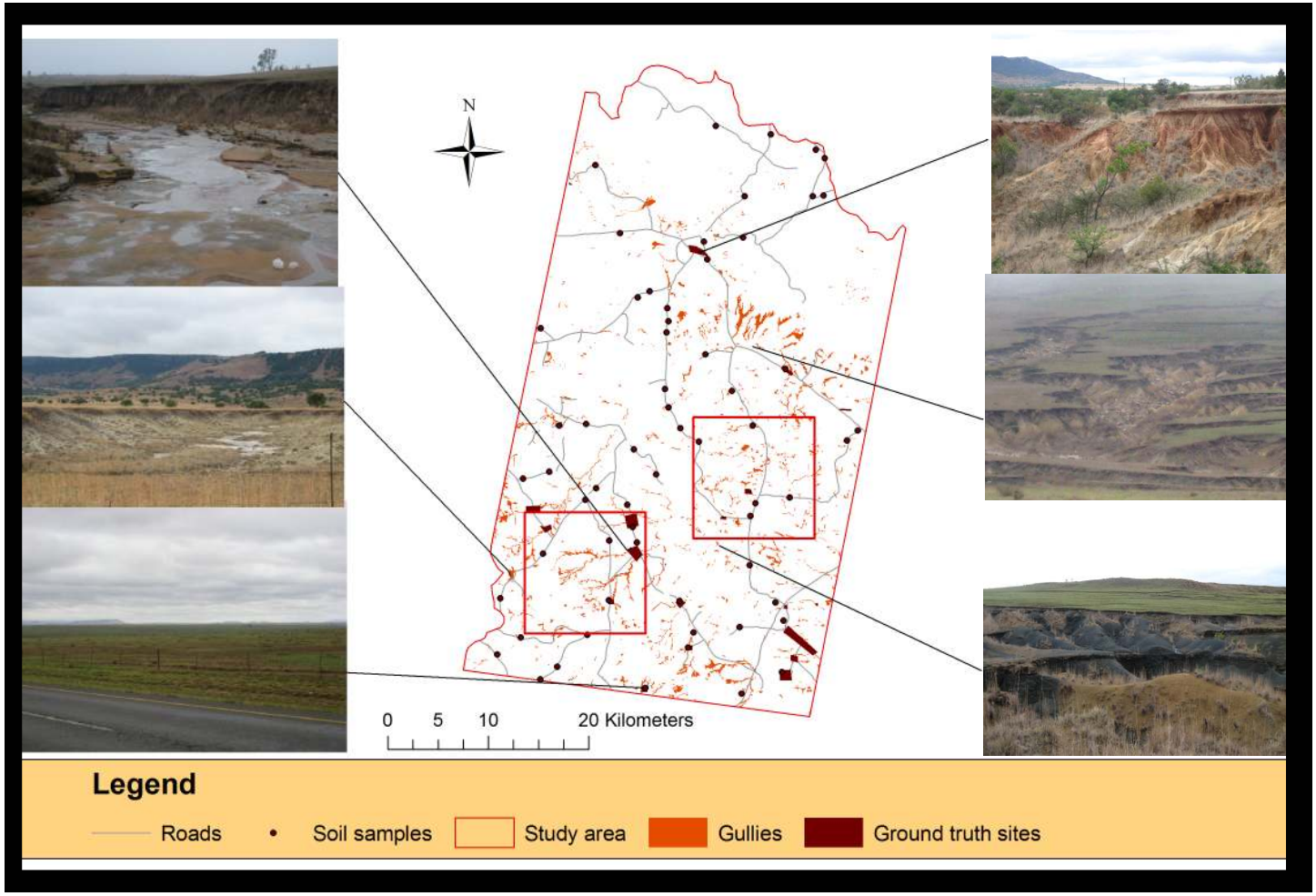

Ground truth study sites (Photographs were taken in October 2007)

Appendix E

Support Vector Parameter Test Results

Kernel	Kappa statistic	Comments
Linear	0.5735	Long processing time
Polynomial	0.5766	
Sigmoid	0.5685	
Radial Basis Function (RBF)	0.5794	

C parameter	Kappa statistic	Comments
0.1	0.3	Visually unimpressive gullies appeared wider than normal
50	0.5933	Reduced accuracy and slow
500	0.6002	Faster processing time
1000	0.601	Faster processing time and improved accuracy

Gamma (γ)	Kappa statistic	Comments
0	-	took too long to process results, computer crashed
0.167	0.601	Default value
0.0039	59.79	
5	0.5979	
60	0.5888	